MagLIF simulations with Gorgon

Jeremy Chittenden, James Pecover,
Marcus Weinwurm, Brian Appelbe
Imperial College

Simon Vickers
AWE Aldermaston

Chris Jennings
Sandia National Lab.

Work supported by SNL, ISP, AWE & EPSRC

Liner workshop, Albuquerque Feb. 2012

MagLIF simulations with Gorgon

Dynamics
Preheat
Perturbation
Instability
Stagnation
Ignition
Pulse Shaping

Liner workshop, Albuquerque Feb. 2012

1st generation MagLIF, Be liner, DT gas fill, 27MA, B_z 30 T

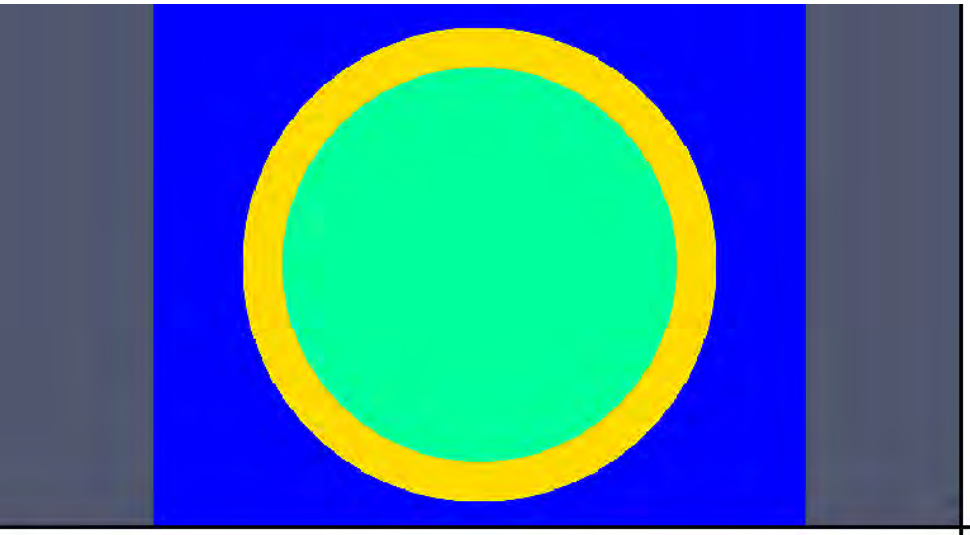

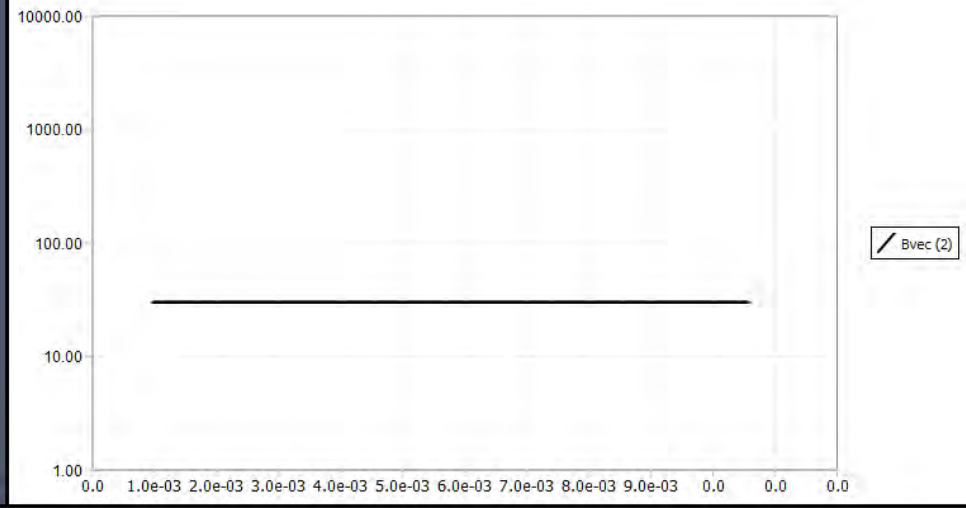

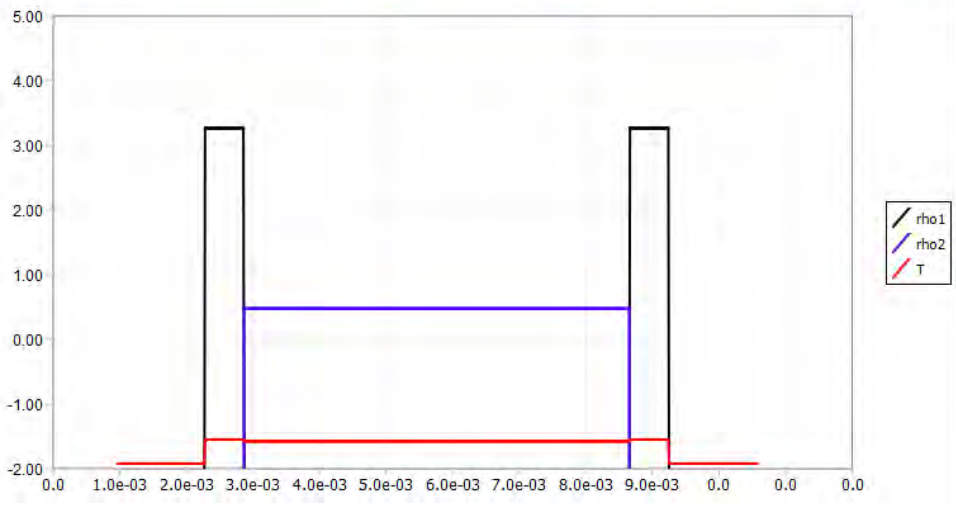

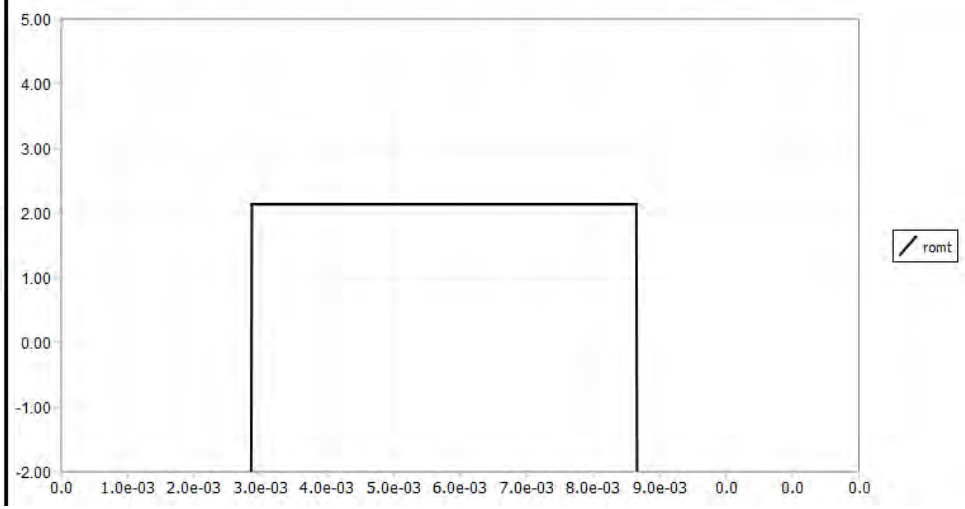

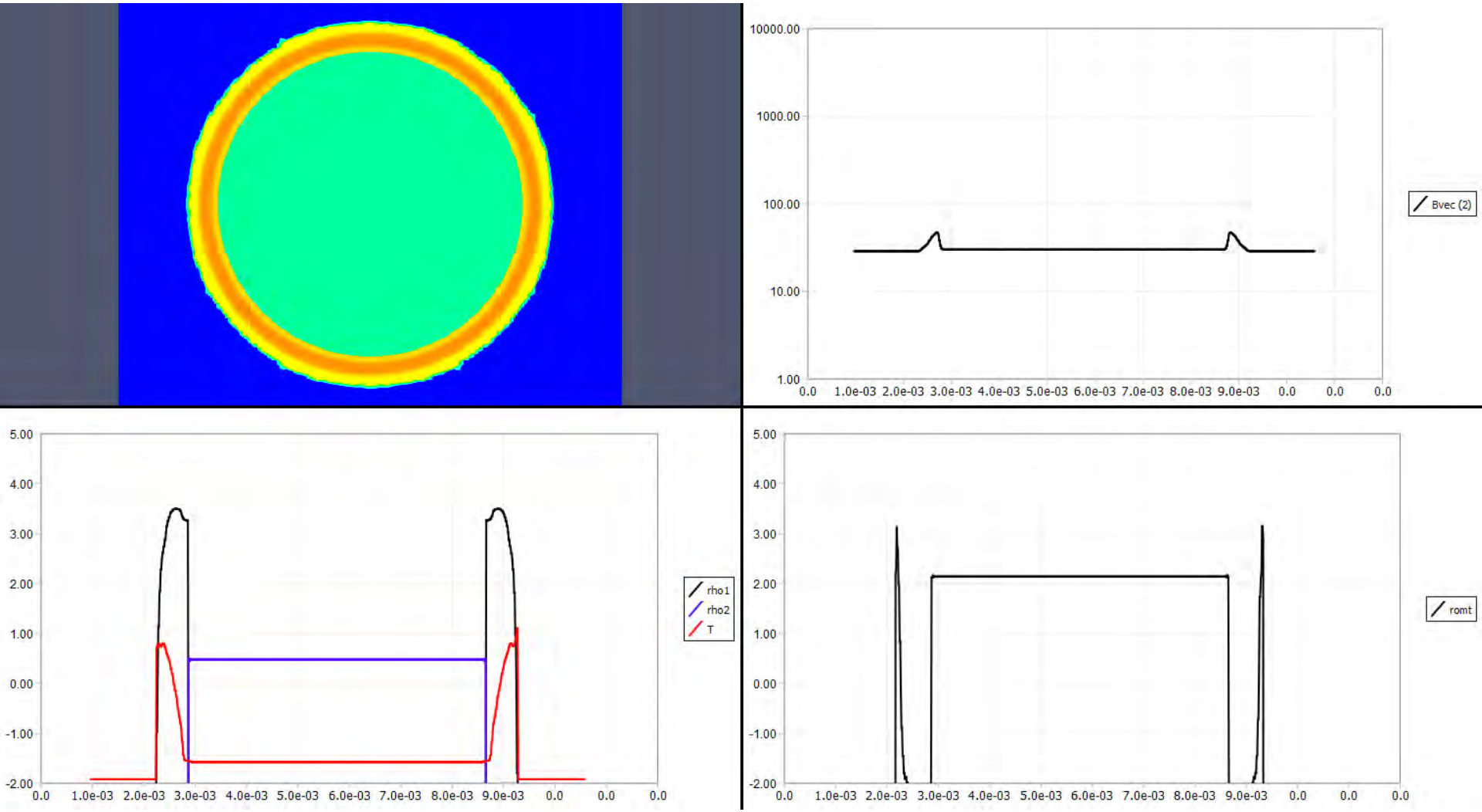

Here with instantaneous and uniform preheat

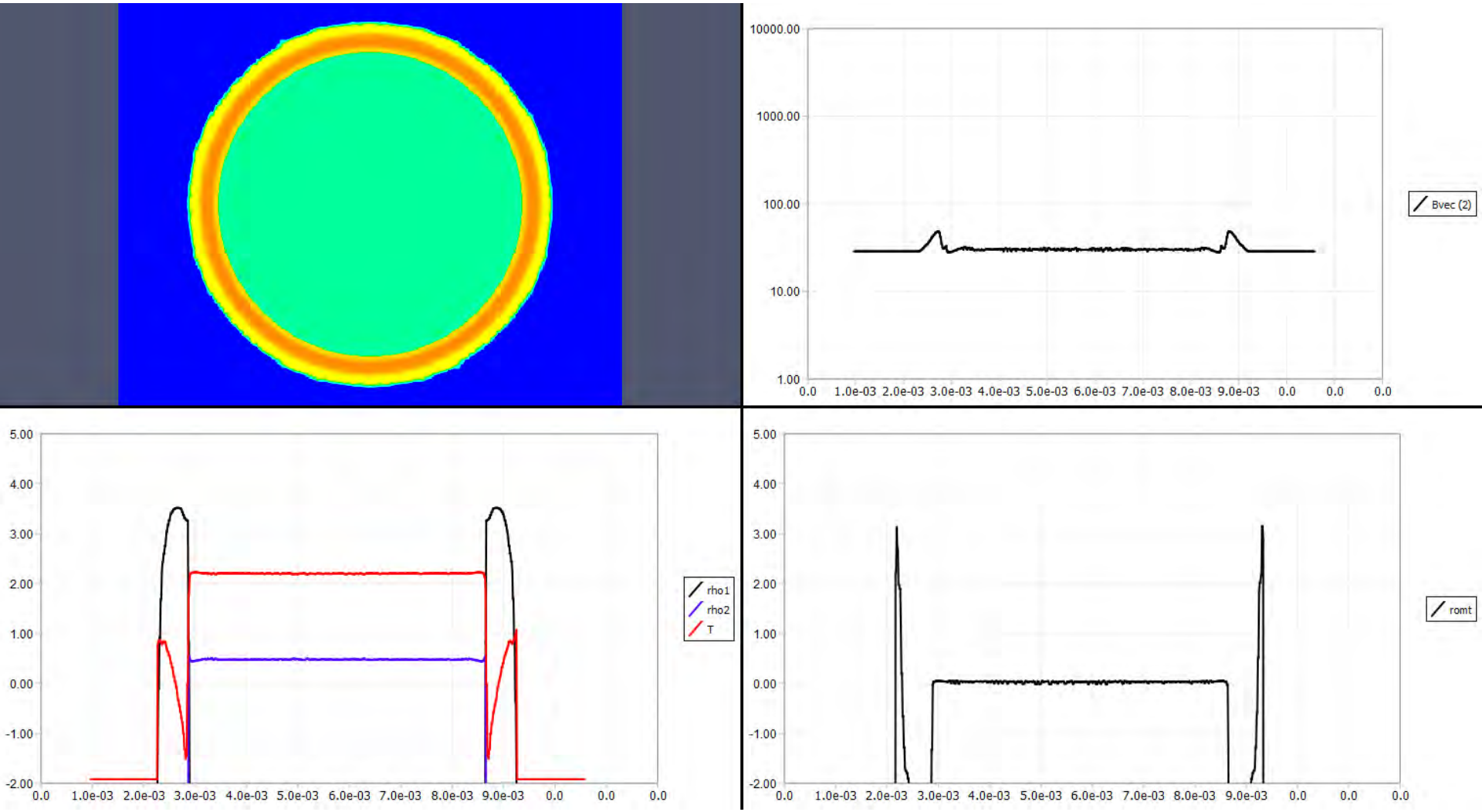

Here with instantaneous and uniform preheat

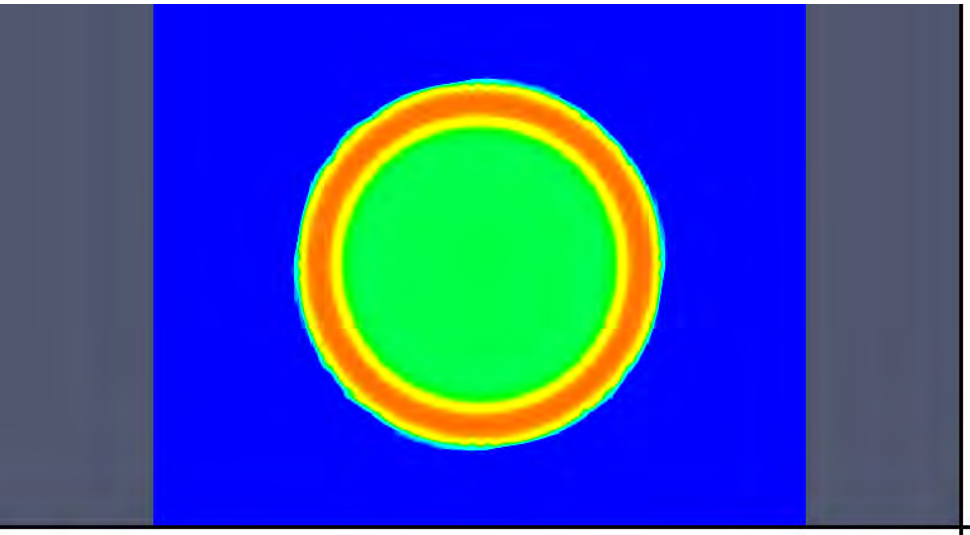

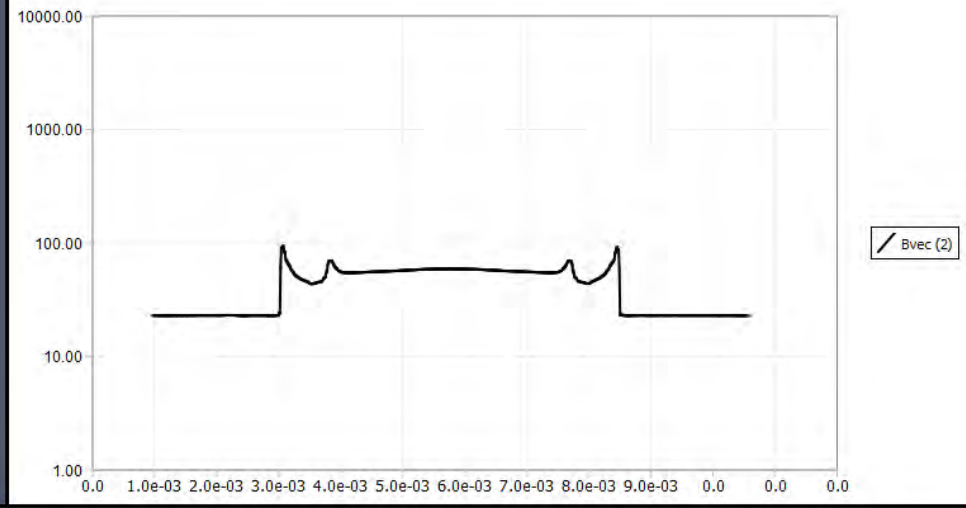
10000.00
1000.00
100.00
10.00
1.00
0.0
1.0e-03
2.0e-03
3.0e-03
4.0e-03
5.0e-03
6.0e-03
7.0e-03
8.0e-03
9.0e-03
0.0
0.0
0.0
Bvec (2)

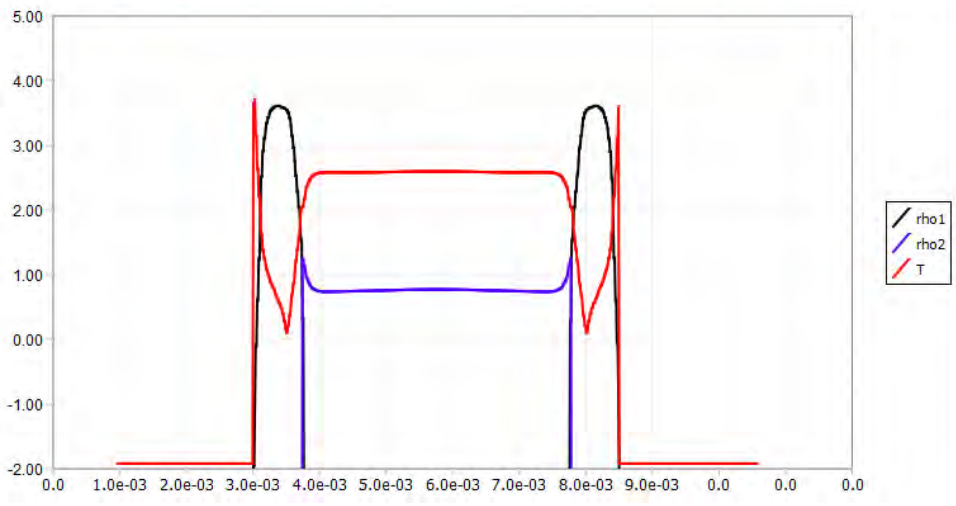
5.00
4.00
3.00
2.00
1.00
0.00
-1.00
-2.00
0.0
1.0e-03
2.0e-03
3.0e-03
4.0e-03
5.0e-03
6.0e-03
7.0e-03
8.0e-03
9.0e-03
0.0
0.0
0.0
rho1
rho2
T

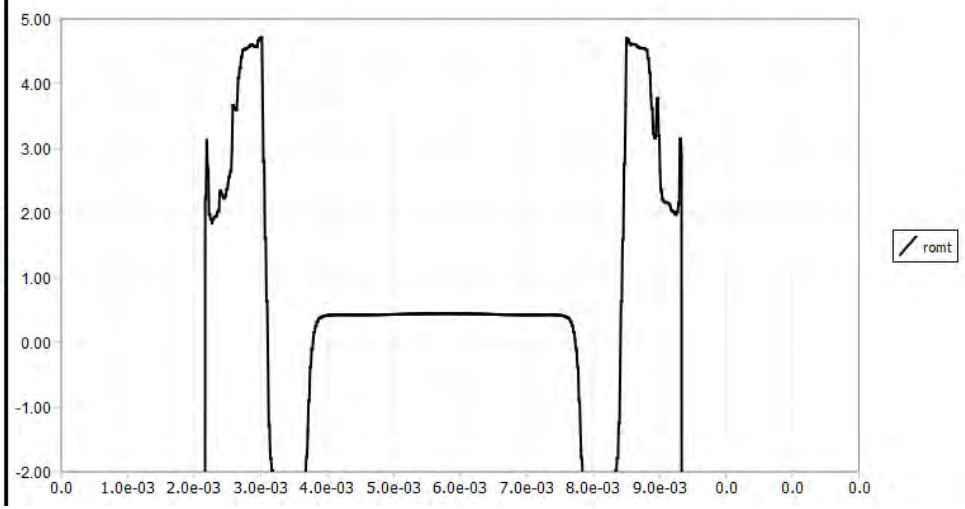
5.00
4.00
3.00
2.00
1.00
0.00
-1.00
-2.00
0.0
1.0e-03
2.0e-03
3.0e-03
4.0e-03
5.0e-03
6.0e-03
7.0e-03
8.0e-03
9.0e-03
0.0
0.0
0.0
romt

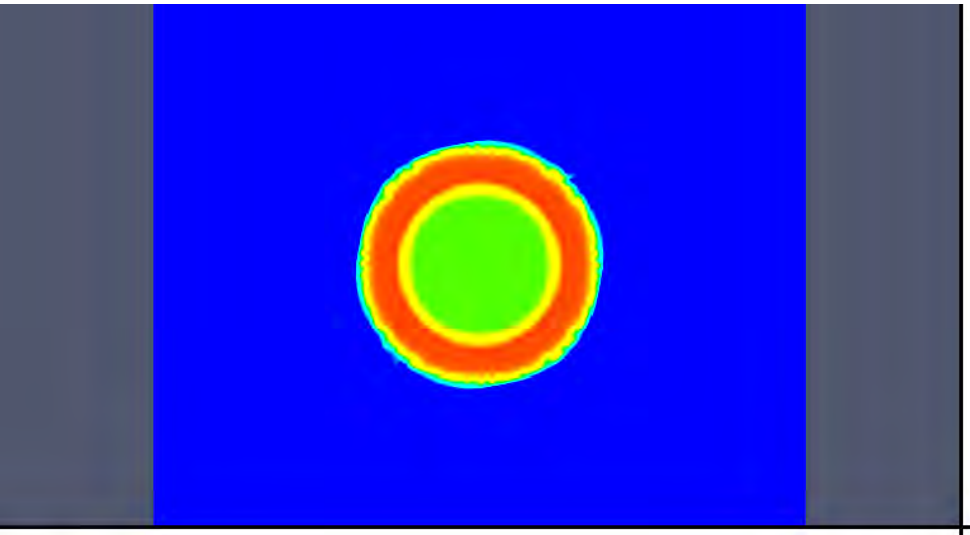

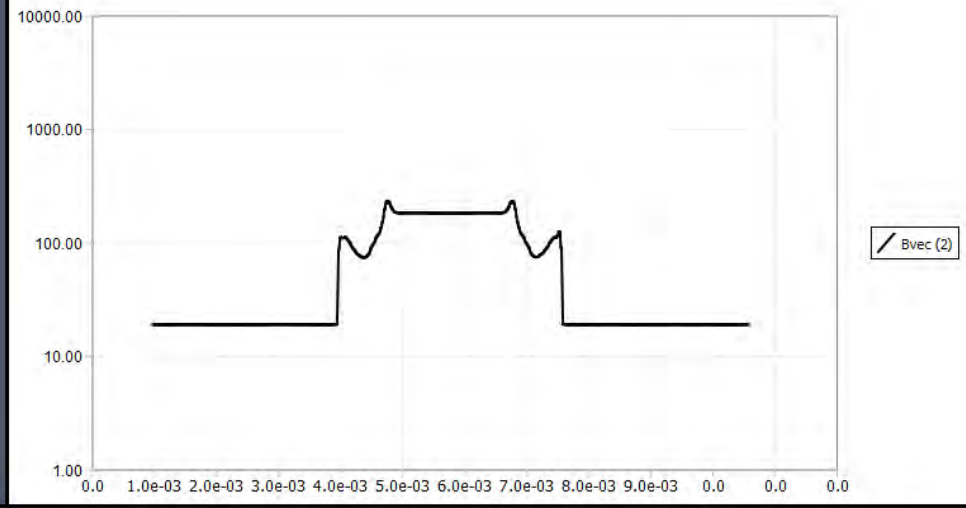
10000.00
1000.00
100.00
10.00
1.00
0.0
1.0e-03
2.0e-03
3.0e-03
4.0e-03
5.0e-03
6.0e-03
7.0e-03
8.0e-03
9.0e-03
0.0
0.0
0.0
Bvec (2)

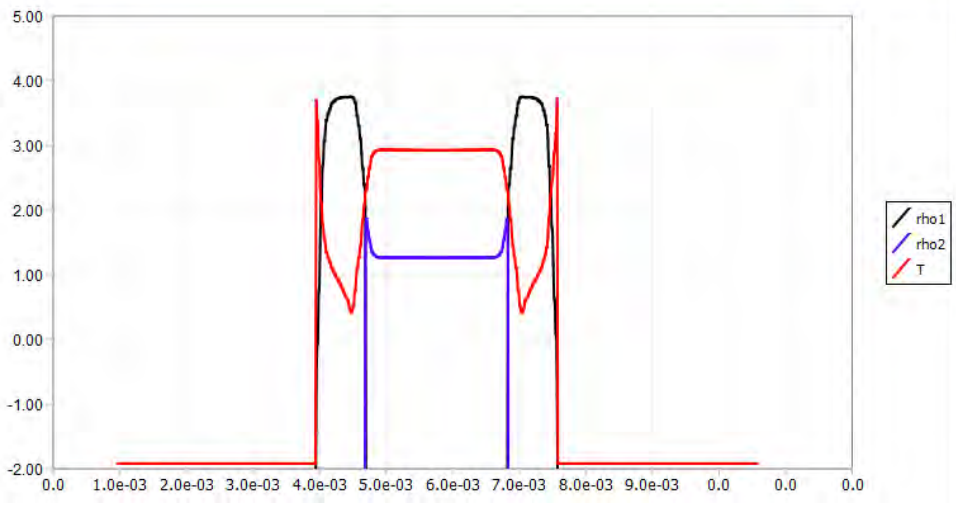
5.00
4.00
3.00
2.00
1.00
0.00
-1.00
-2.00
0.0
1.0e-03
2.0e-03
3.0e-03
4.0e-03
5.0e-03
6.0e-03
7.0e-03
8.0e-03
9.0e-03
0.0
0.0
0.0
rho1
rho2
T

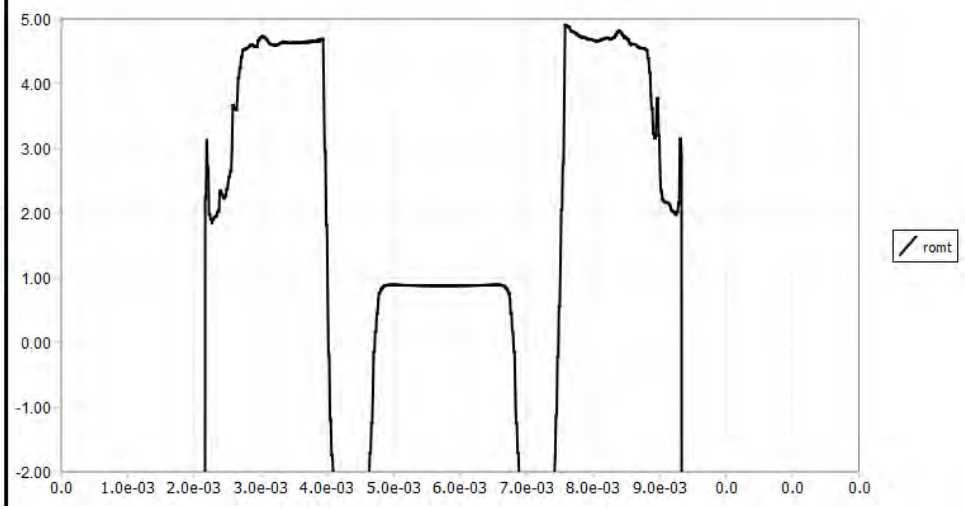
5.00
4.00
3.00
2.00
1.00
0.00
-1.00
-2.00
0.0
1.0e-03
2.0e-03
3.0e-03
4.0e-03
5.0e-03
6.0e-03
7.0e-03
8.0e-03
9.0e-03
0.0
0.0
0.0
romt

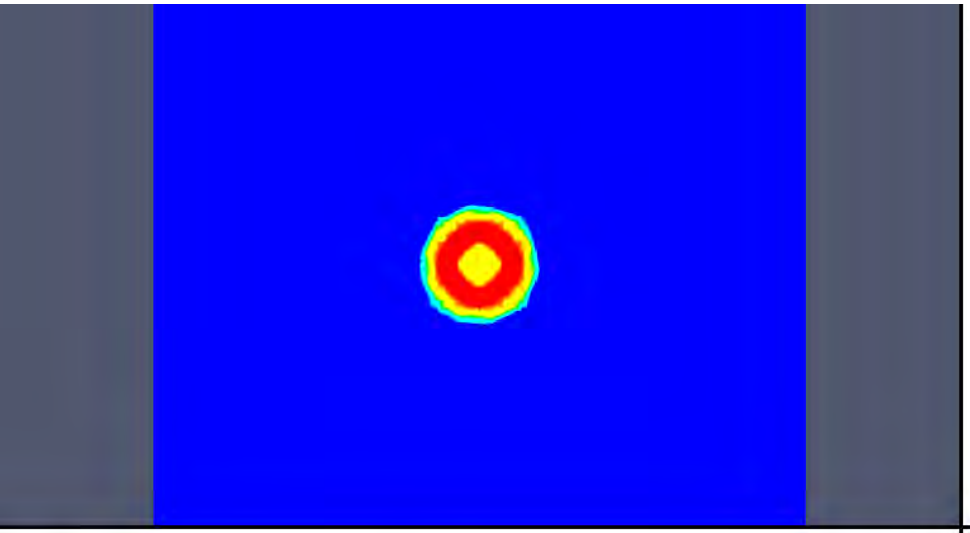

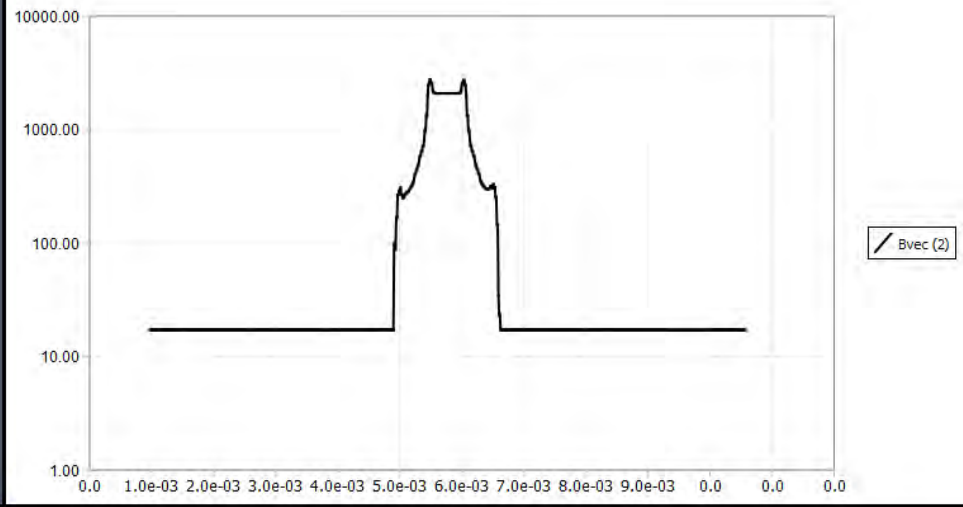
10000.00
1000.00
100.00
10.00
1.00
0.0
1.0e-03
2.0e-03
3.0e-03
4.0e-03
5.0e-03
6.0e-03
7.0e-03
8.0e-03
9.0e-03
0.0
0.0
0.0
Bvec (2)

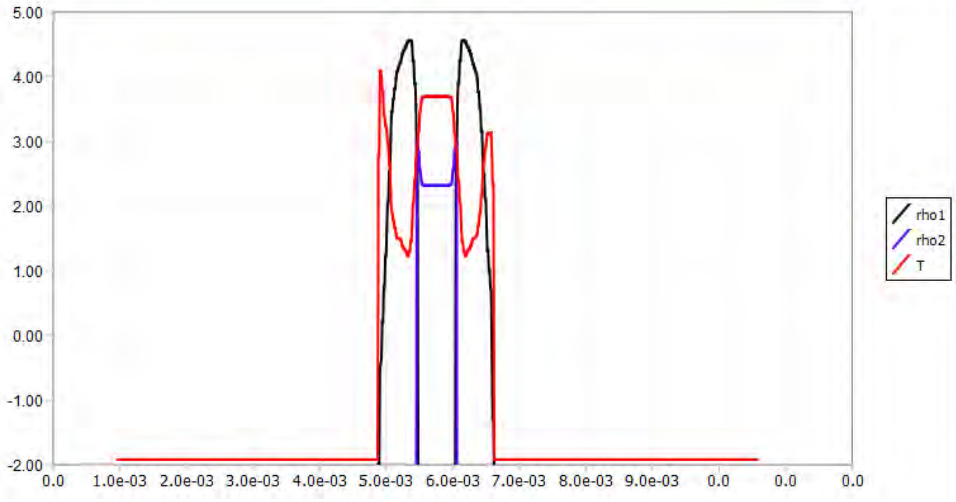
5.00
4.00
3.00
2.00
1.00
0.00
-1.00
-2.00
0.0
1.0e-03
2.0e-03
3.0e-03
4.0e-03
5.0e-03
6.0e-03
7.0e-03
8.0e-03
9.0e-03
0.0
0.0
0.0
rho1
rho2
T

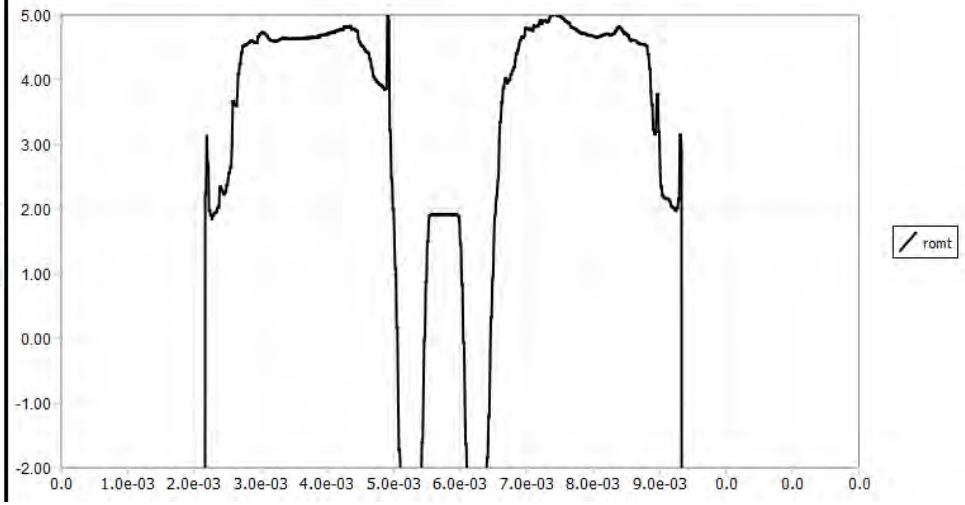
5.00
4.00
3.00
2.00
1.00
0.00
-1.00
-2.00
0.0
1.0e-03
2.0e-03
3.0e-03
4.0e-03
5.0e-03
6.0e-03
7.0e-03
8.0e-03
9.0e-03
0.0
0.0
0.0
romt

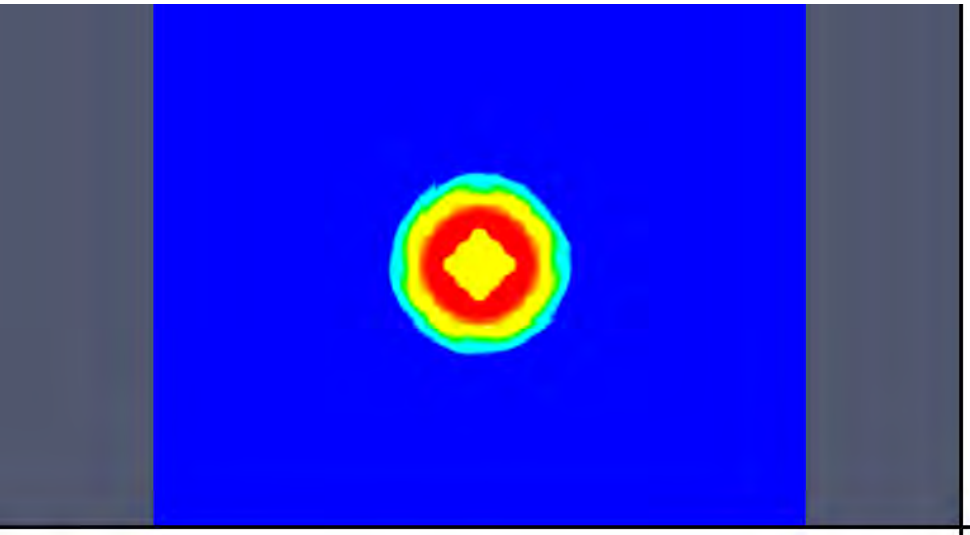

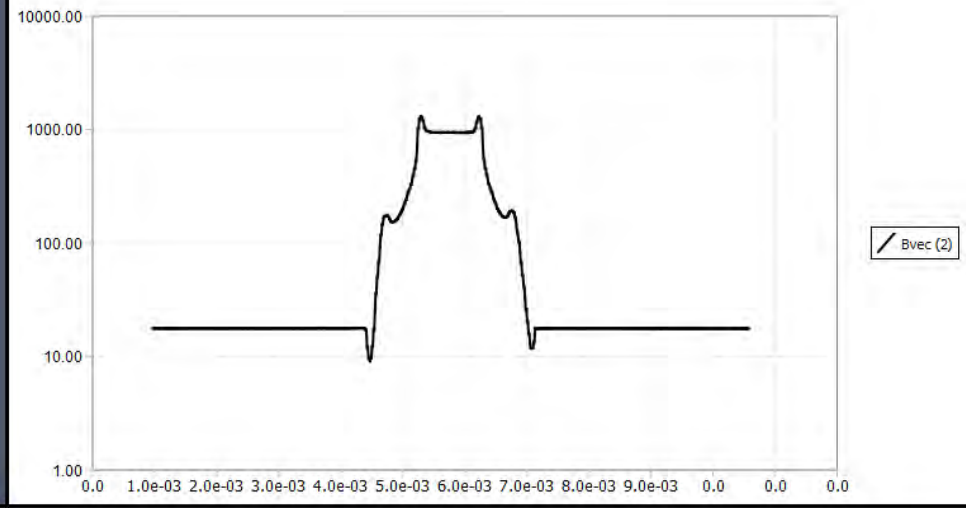
10000.00
1000.00
100.00
10.00
1.00
0.0
1.0e-03
2.0e-03
3.0e-03
4.0e-03
5.0e-03
6.0e-03
7.0e-03
8.0e-03
9.0e-03
0.0
0.0
0.0
Bvec (2)

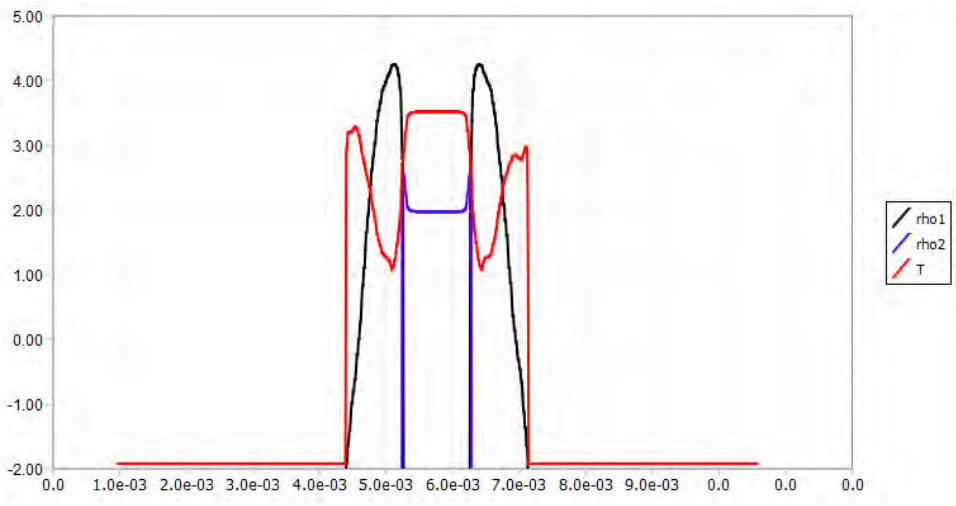
5.00
4.00
3.00
2.00
1.00
0.00
-1.00
-2.00
0.0
1.0e-03
2.0e-03
3.0e-03
4.0e-03
5.0e-03
6.0e-03
7.0e-03
8.0e-03
9.0e-03
0.0
0.0
0.0
rho1
rho2
T

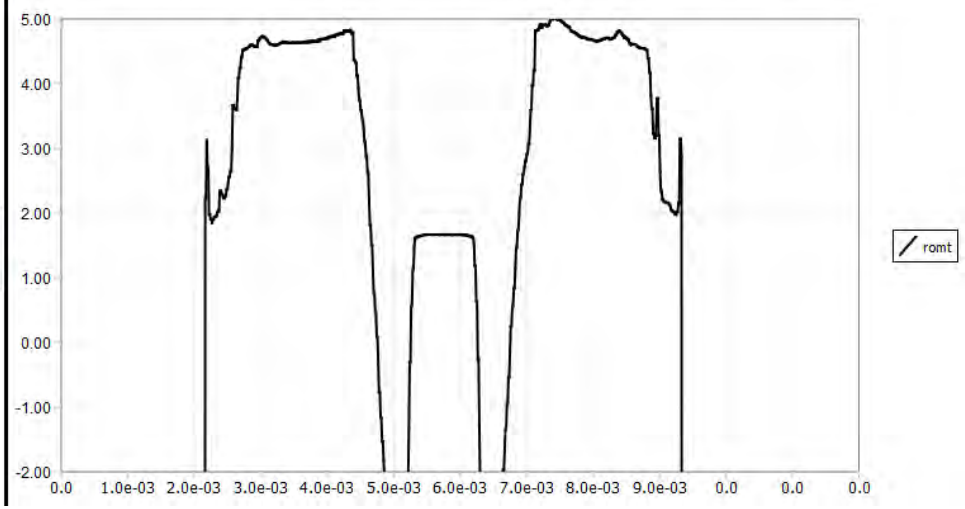
5.00
4.00
3.00
2.00
1.00
0.00
-1.00
-2.00
0.0
1.0e-03
2.0e-03
3.0e-03
4.0e-03
5.0e-03
6.0e-03
7.0e-03
8.0e-03
9.0e-03
0.0
0.0
0.0
romt

Yields sensitive to heating method and radiation cooling

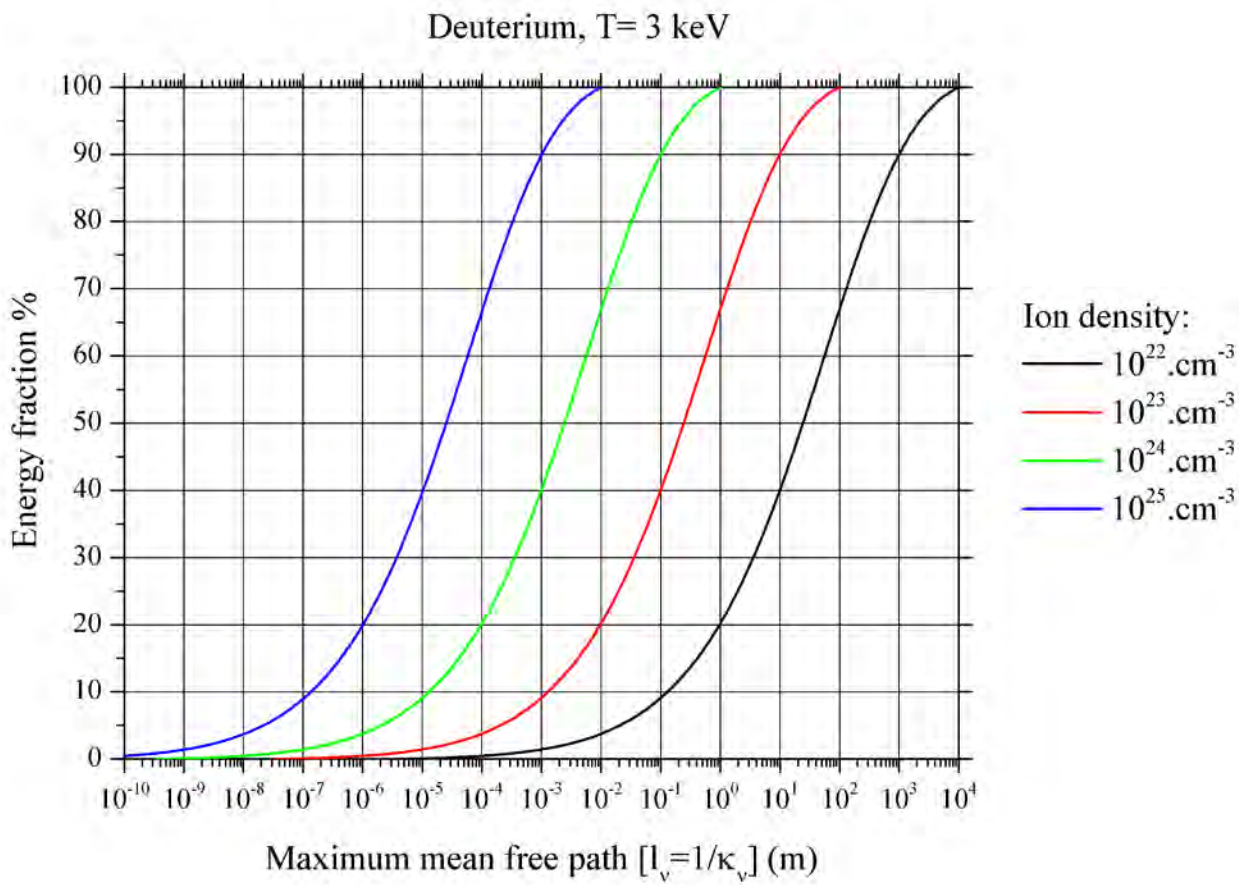

1st generation MagLIF, Be liner, DT gas fill, 27MA, B_z 30 T

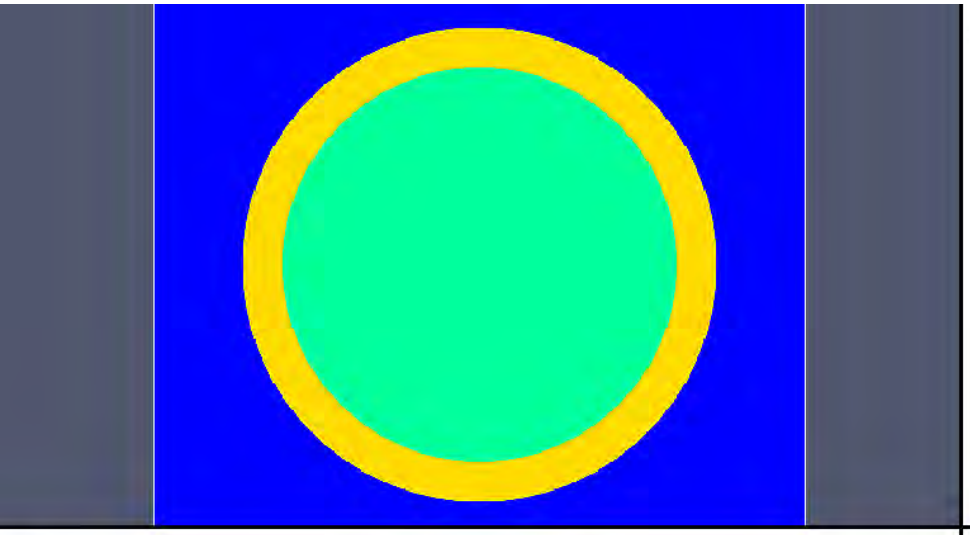

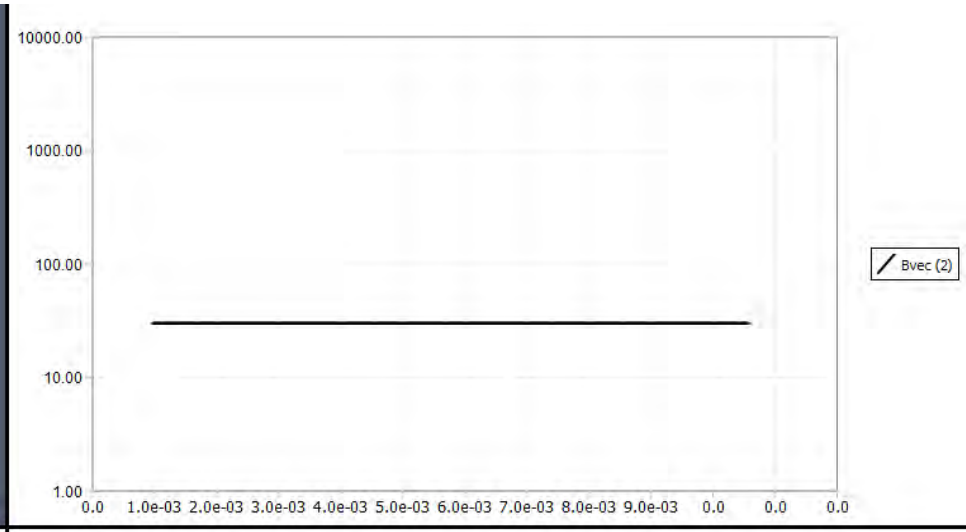

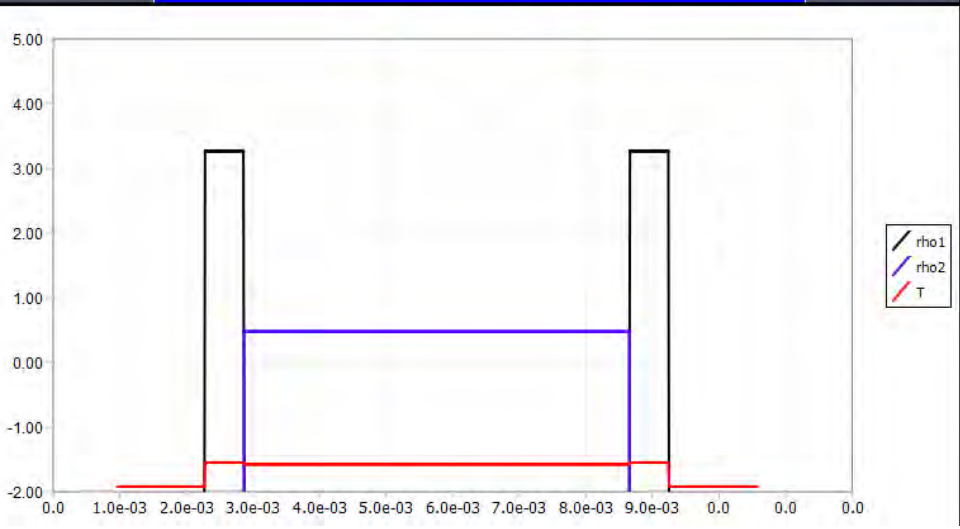

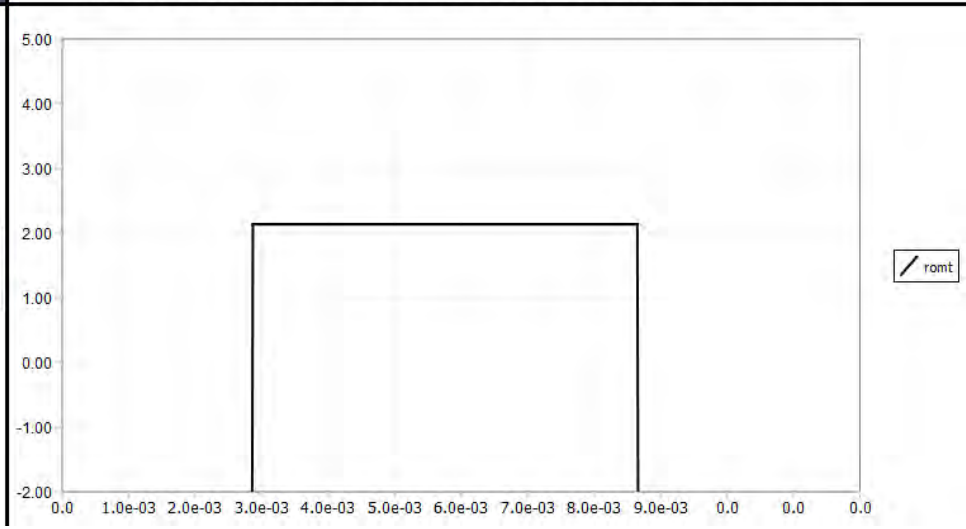

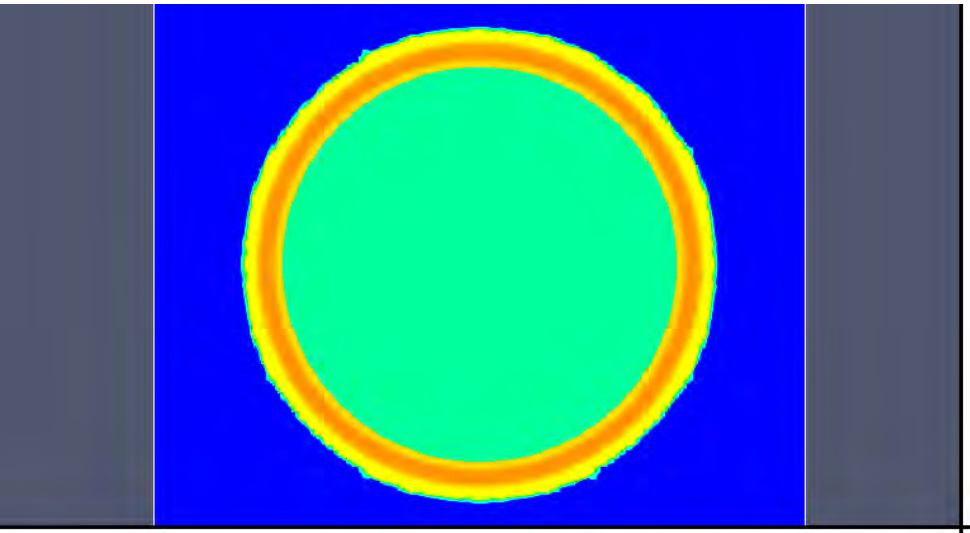

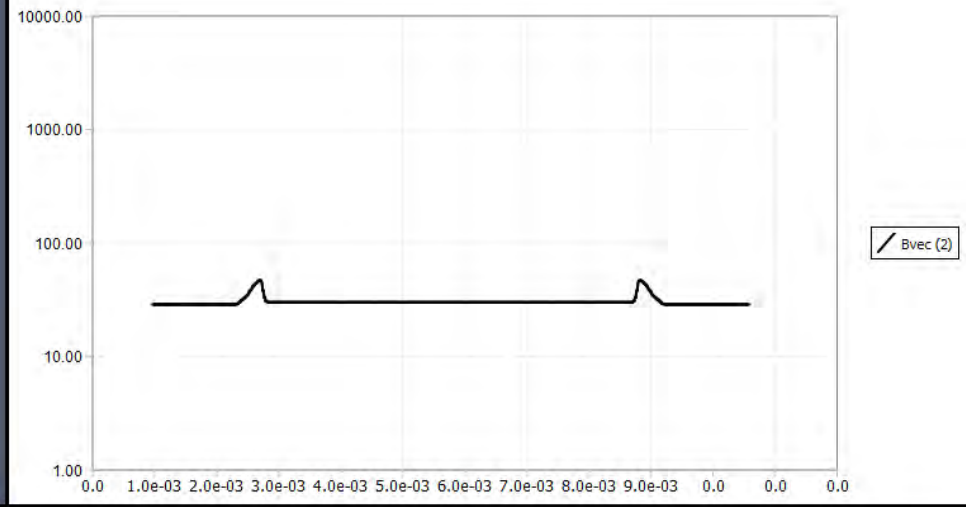
10000.00
1000.00
100.00
10.00
1.00
0.0 1.0e-03 2.0e-03 3.0e-03 4.0e-03 5.0e-03 6.0e-03 7.0e-03 8.0e-03 9.0e-03 0.0 0.0 0.0
Bvec (2)

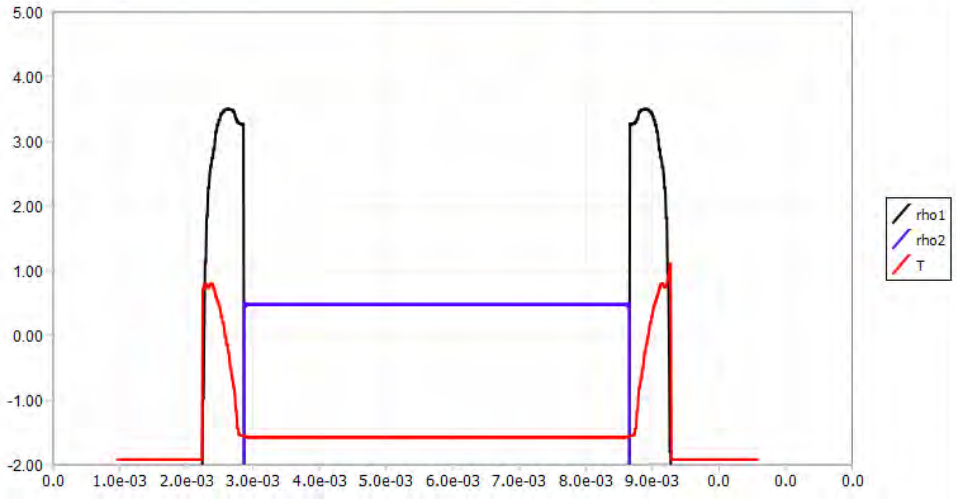
5.00
4.00
3.00
2.00
1.00
0.00
-1.00
-2.00
0.0 1.0e-03 2.0e-03 3.0e-03 4.0e-03 5.0e-03 6.0e-03 7.0e-03 8.0e-03 9.0e-03 0.0 0.0 0.0
rho1
rho2
T

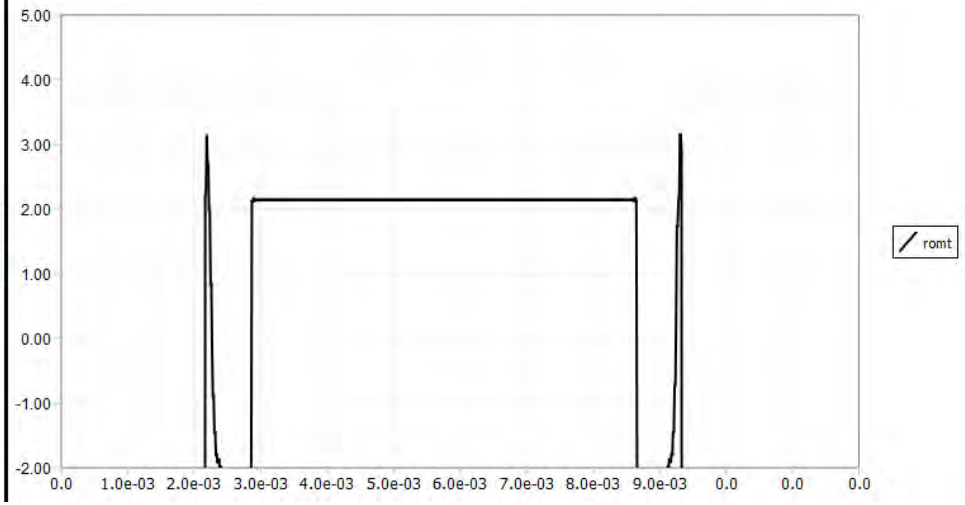
5.00
4.00
3.00
2.00
1.00
0.00
-1.00
-2.00
0.0 1.0e-03 2.0e-03 3.0e-03 4.0e-03 5.0e-03 6.0e-03 7.0e-03 8.0e-03 9.0e-03 0.0 0.0 0.0
romt

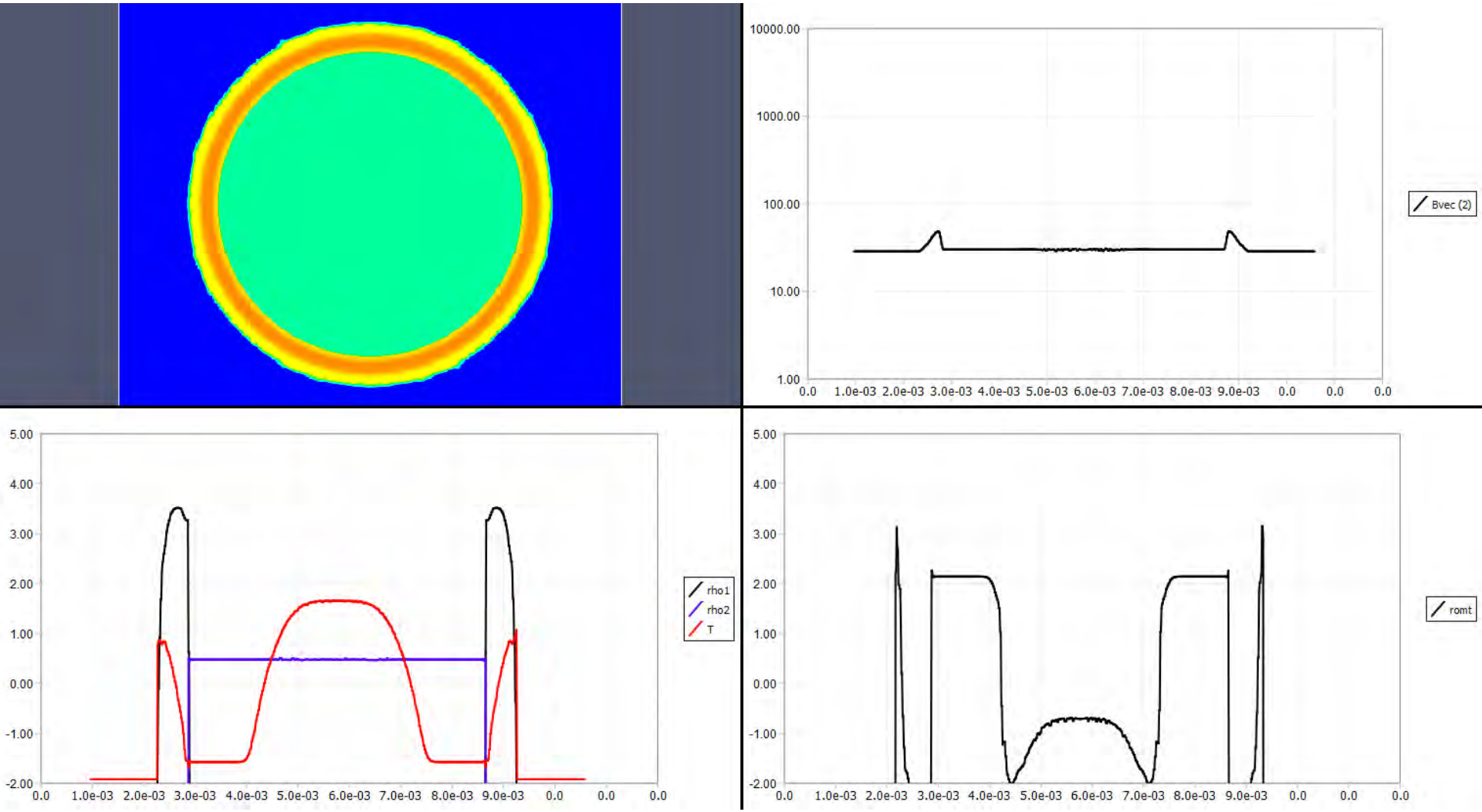

Here with Gaussian laser profile and density dependent preheat

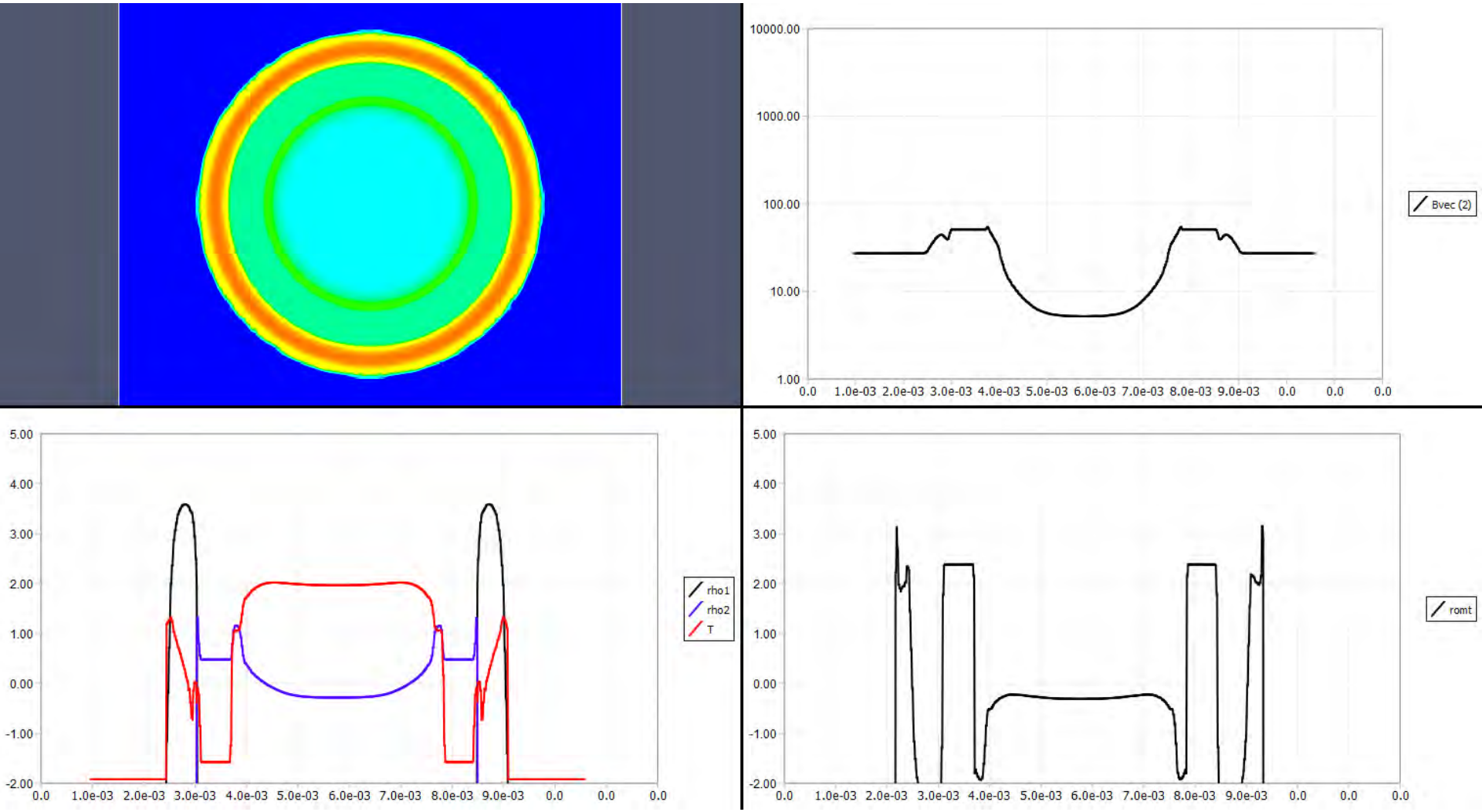

Here with Gaussian laser profile and density dependent preheat

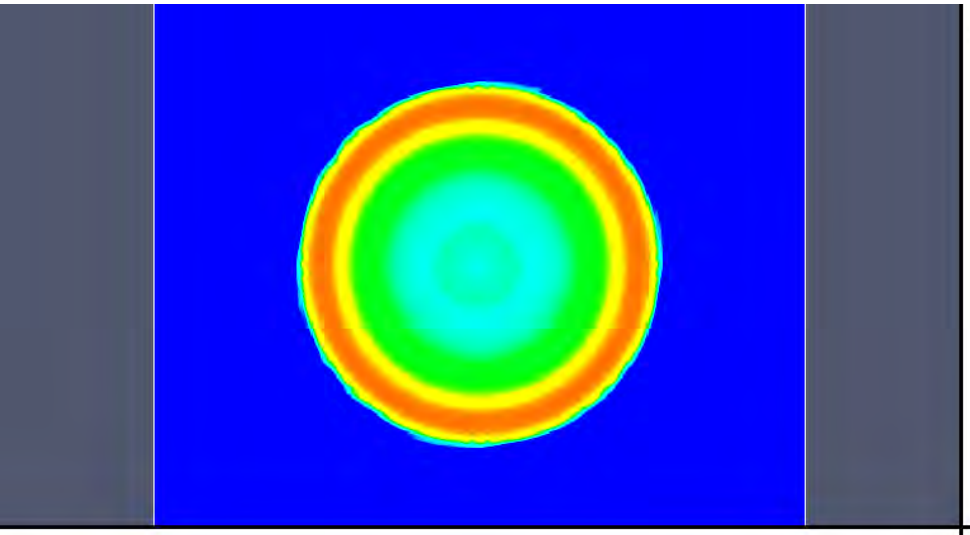

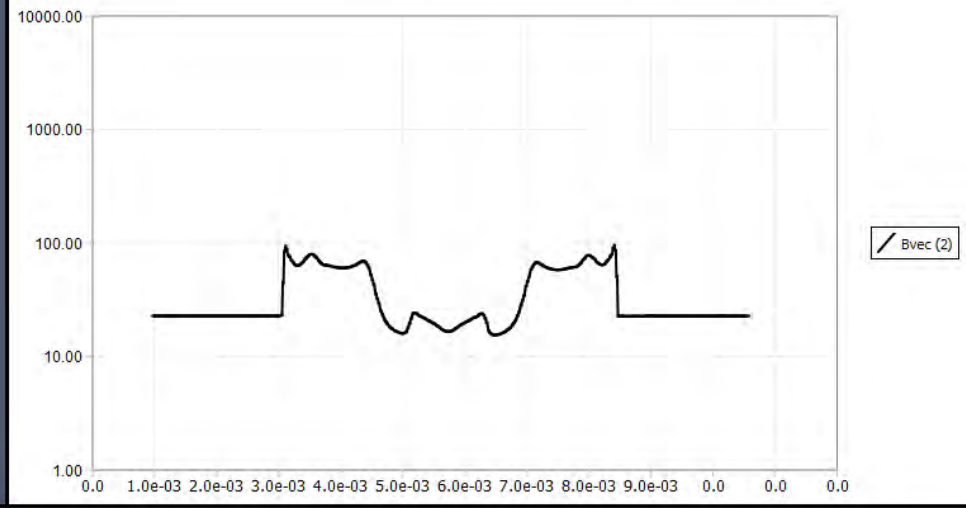
10000.00
1000.00
100.00
10.00
1.00
0.0
1.0e-03
2.0e-03
3.0e-03
4.0e-03
5.0e-03
6.0e-03
7.0e-03
8.0e-03
9.0e-03
0.0
0.0
0.0
Bvec (2)

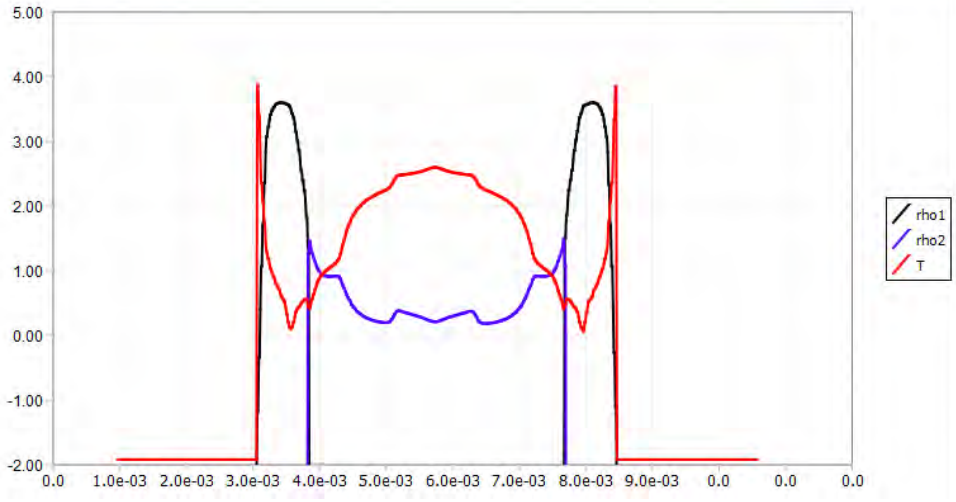
5.00
4.00
3.00
2.00
1.00
0.00
-1.00
-2.00
0.0
1.0e-03
2.0e-03
3.0e-03
4.0e-03
5.0e-03
6.0e-03
7.0e-03
8.0e-03
9.0e-03
0.0
0.0
0.0
rho1
rho2
T

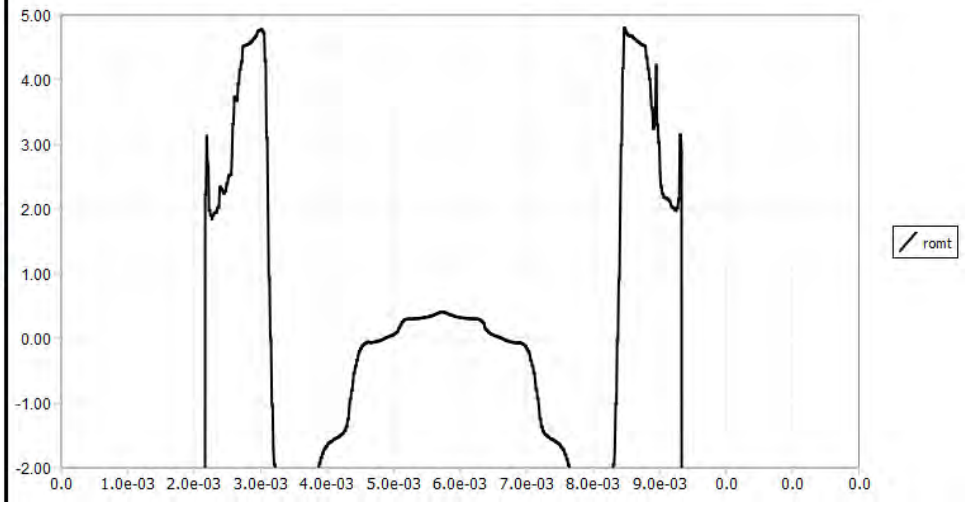
5.00
4.00
3.00
2.00
1.00
0.00
-1.00
-2.00
0.0
1.0e-03
2.0e-03
3.0e-03
4.0e-03
5.0e-03
6.0e-03
7.0e-03
8.0e-03
9.0e-03
0.0
0.0
0.0
romt

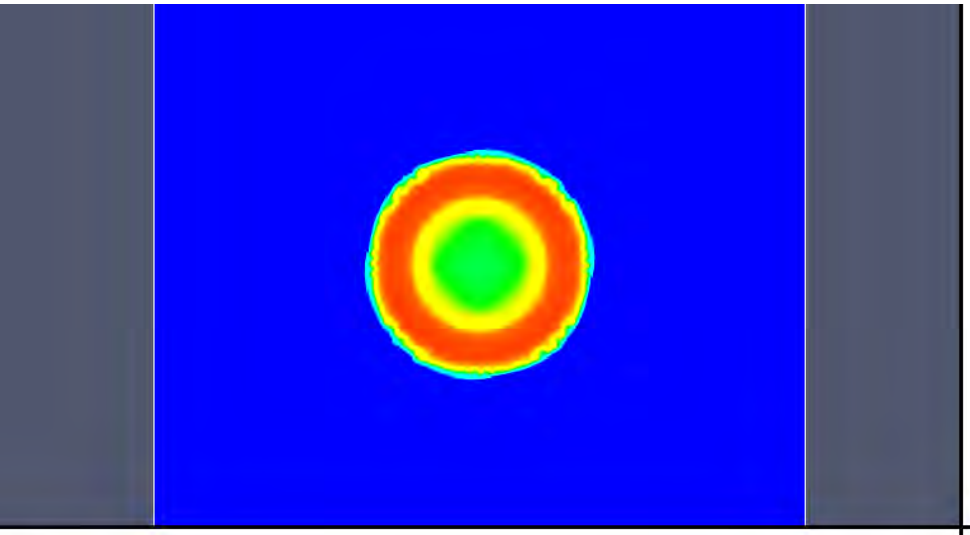

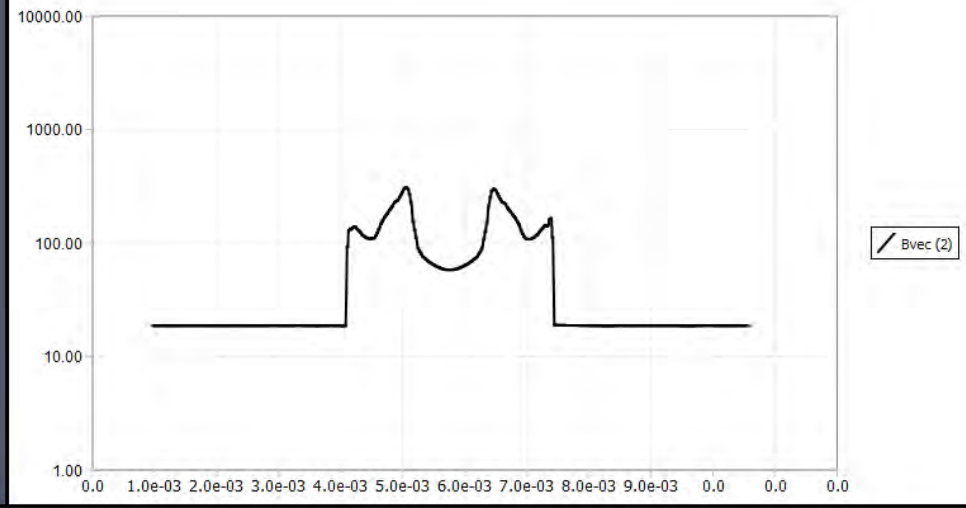
10000.00
1000.00
100.00
10.00
1.00
0.0
1.0e-03
2.0e-03
3.0e-03
4.0e-03
5.0e-03
6.0e-03
7.0e-03
8.0e-03
9.0e-03
0.0
0.0
0.0
Bvec (2)

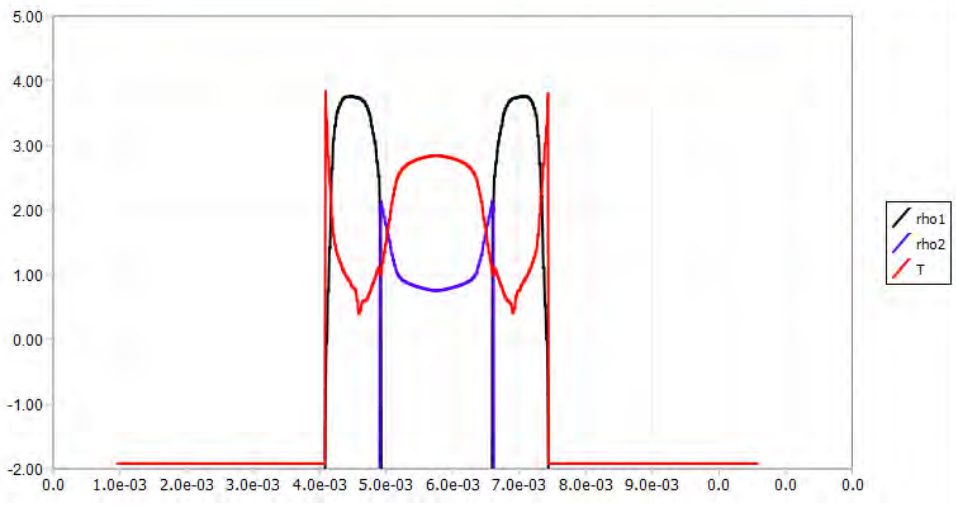
5.00
4.00
3.00
2.00
1.00
0.00
-1.00
-2.00
0.0
1.0e-03
2.0e-03
3.0e-03
4.0e-03
5.0e-03
6.0e-03
7.0e-03
8.0e-03
9.0e-03
0.0
0.0
0.0
rho1
rho2
T

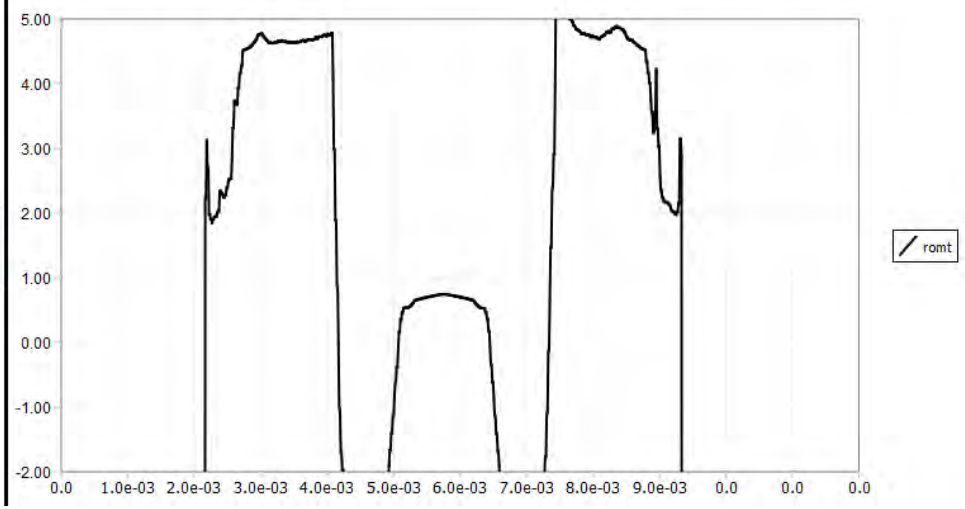
5.00
4.00
3.00
2.00
1.00
0.00
-1.00
-2.00
0.0
1.0e-03
2.0e-03
3.0e-03
4.0e-03
5.0e-03
6.0e-03
7.0e-03
8.0e-03
9.0e-03
0.0
0.0
0.0
romt

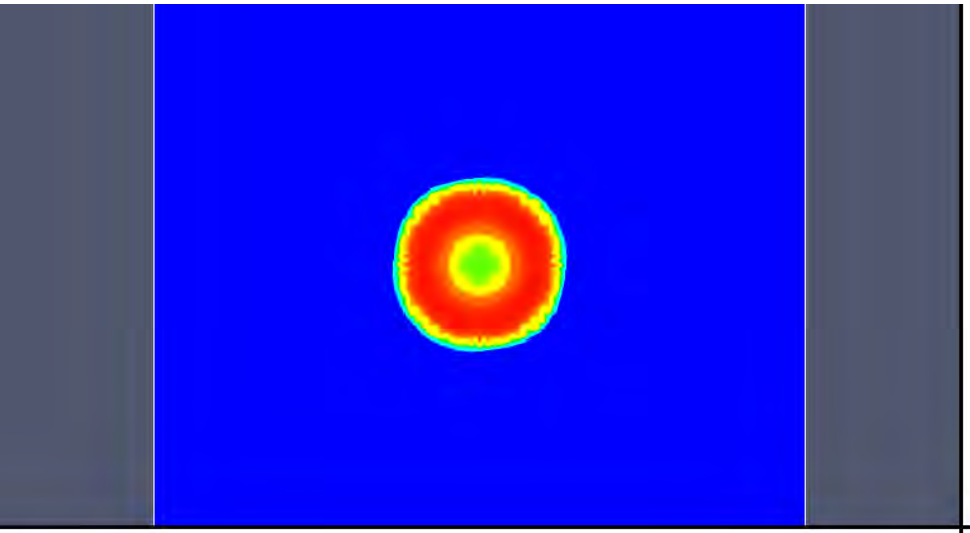

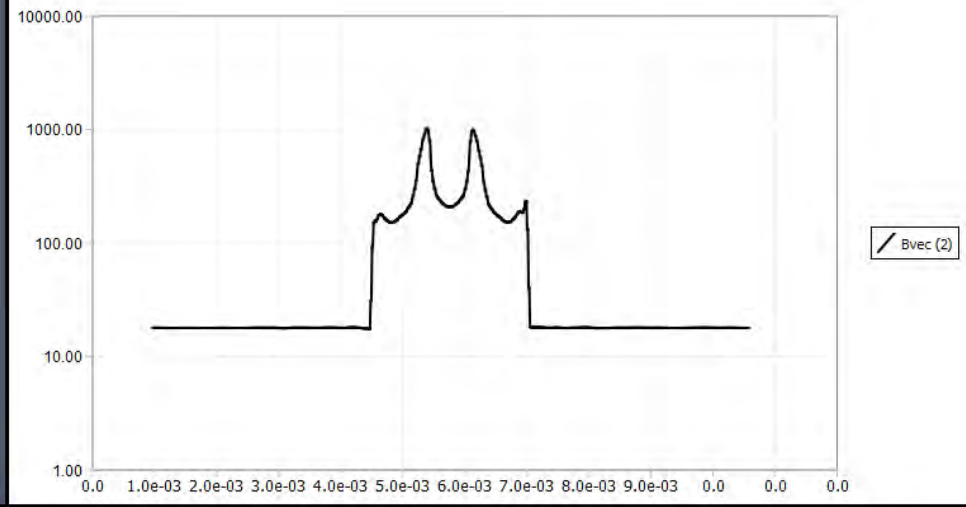
10000.00
1000.00
100.00
10.00
1.00
0.0
1.0e-03
2.0e-03
3.0e-03
4.0e-03
5.0e-03
6.0e-03
7.0e-03
8.0e-03
9.0e-03
0.0
0.0
0.0
Bvec (2)

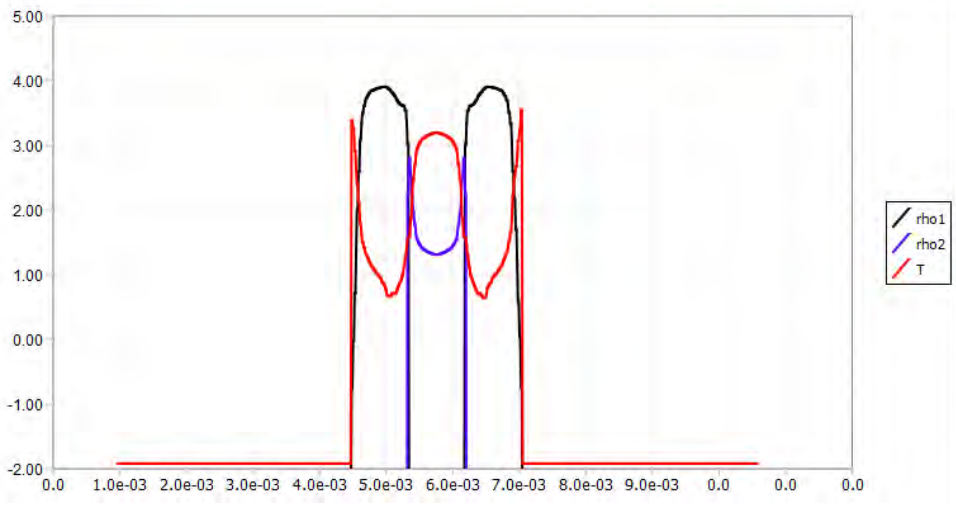
5.00
4.00
3.00
2.00
1.00
0.00
-1.00
-2.00
0.0
1.0e-03
2.0e-03
3.0e-03
4.0e-03
5.0e-03
6.0e-03
7.0e-03
8.0e-03
9.0e-03
0.0
0.0
0.0
rho1
rho2
T

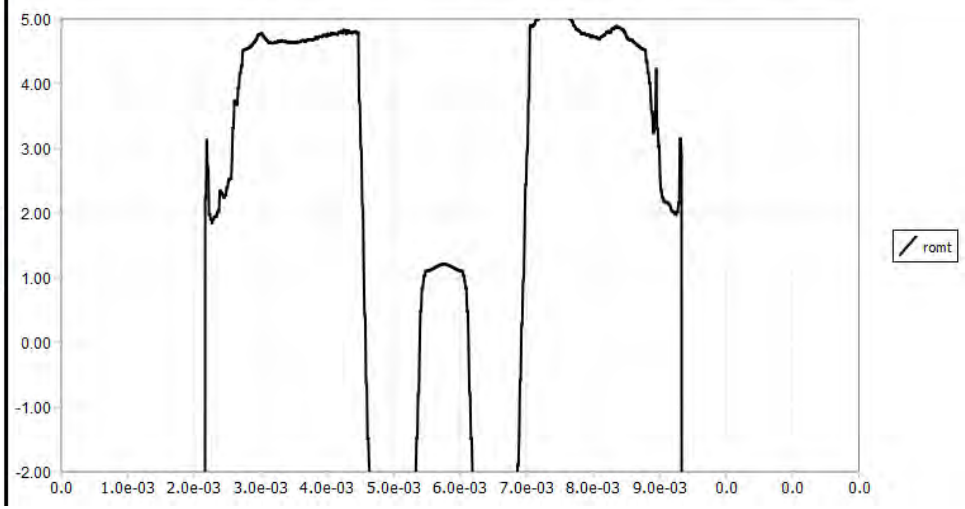
5.00
4.00
3.00
2.00
1.00
0.00
-1.00
-2.00
0.0
1.0e-03
2.0e-03
3.0e-03
4.0e-03
5.0e-03
6.0e-03
7.0e-03
8.0e-03
9.0e-03
0.0
0.0
0.0
romt

Density dependence of resistivity dominates early development of instability

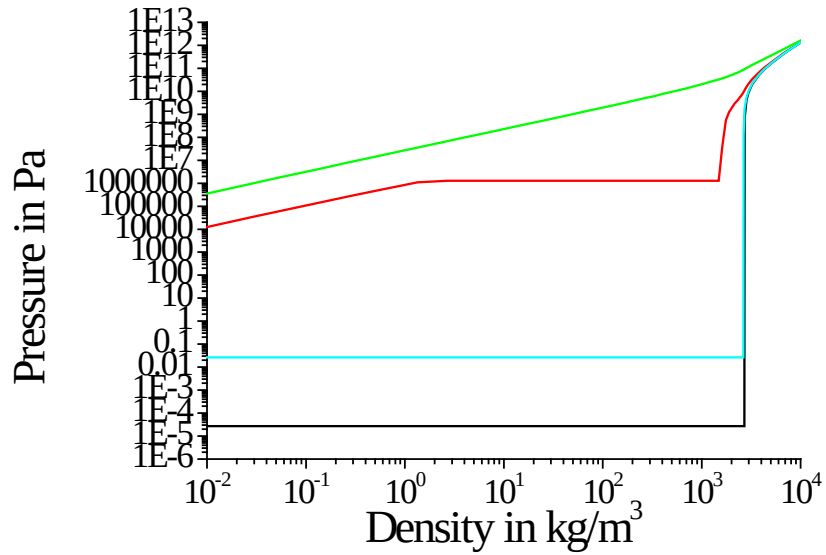

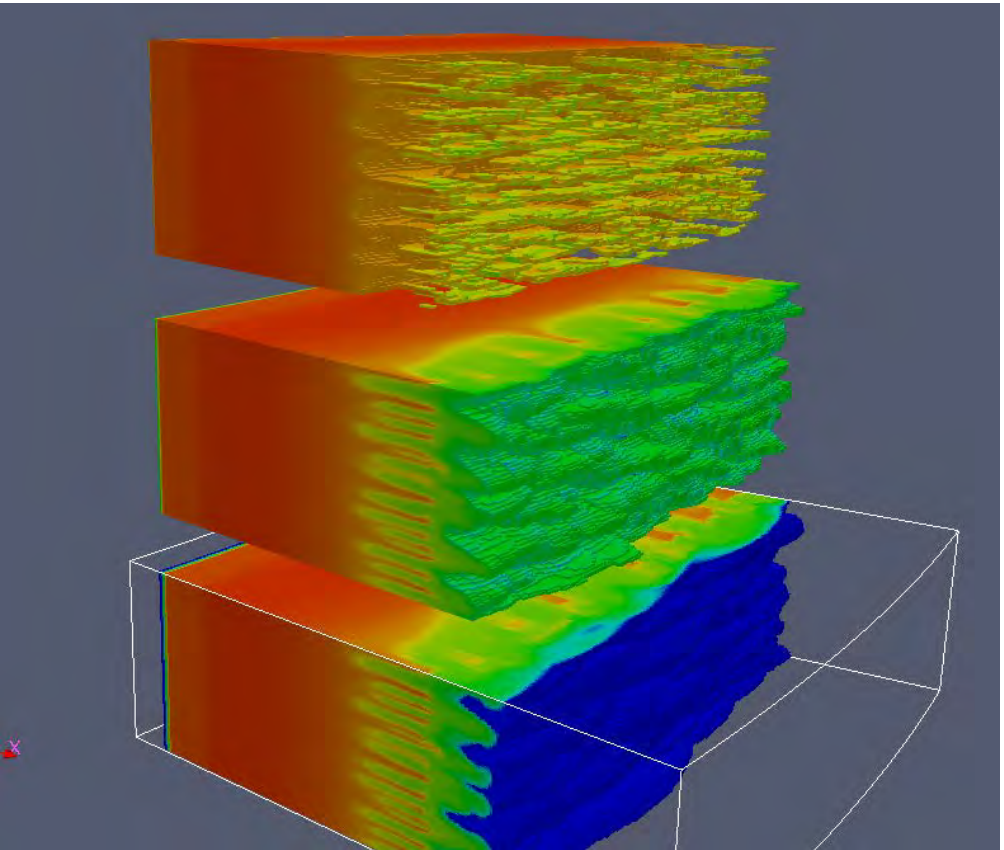

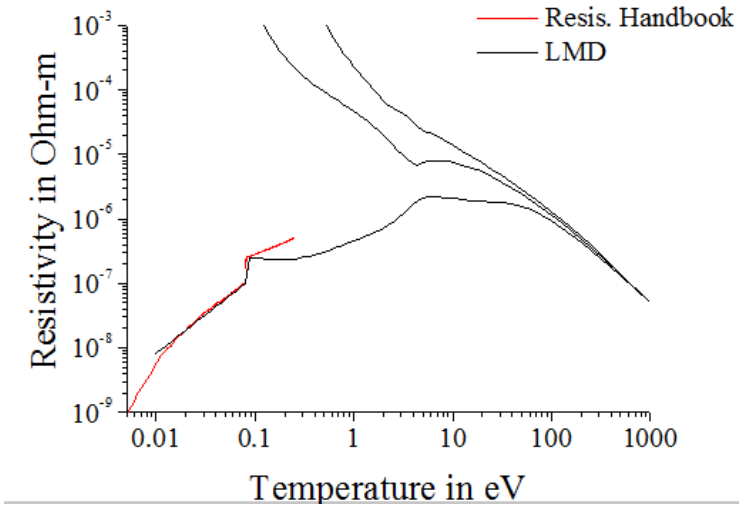

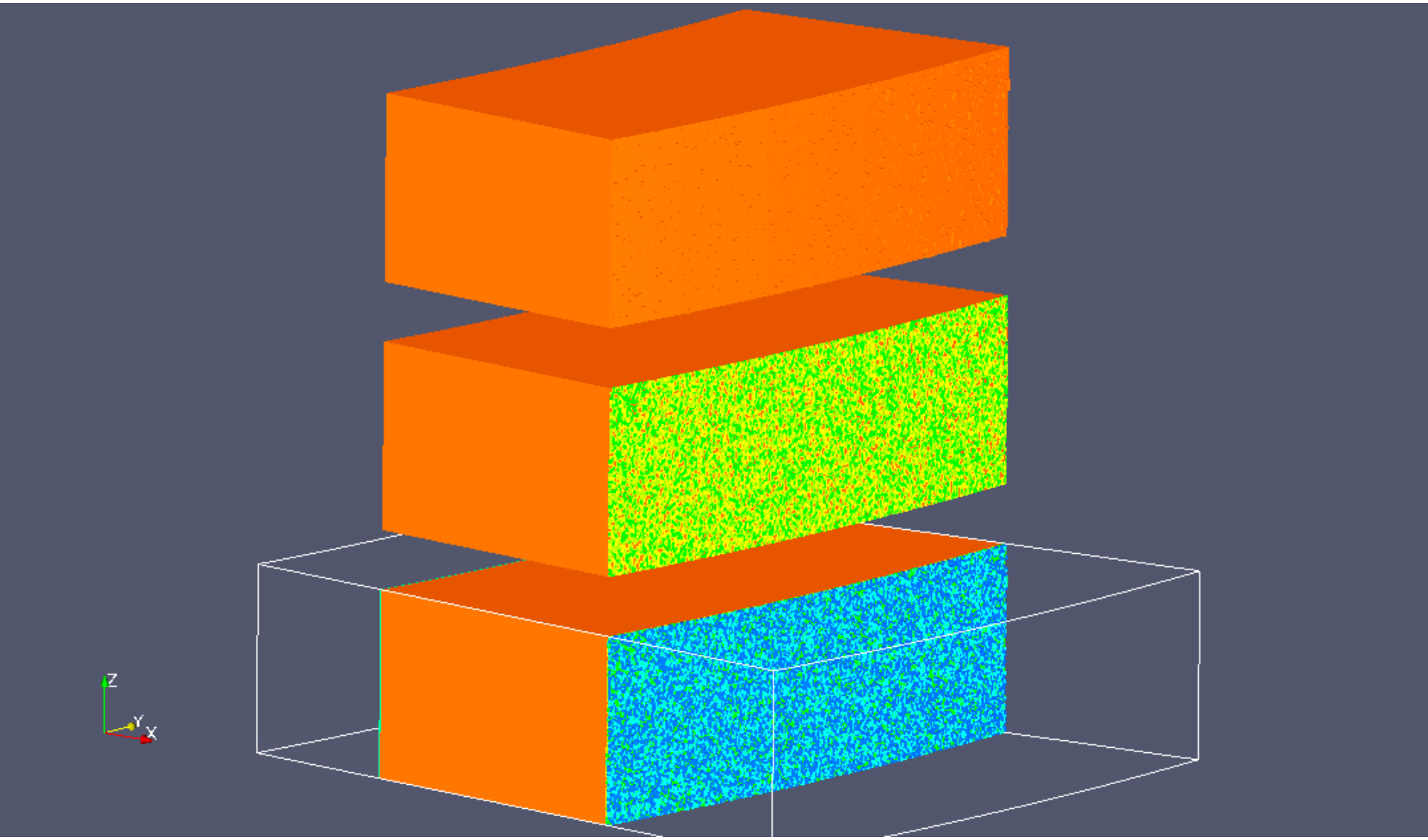
Z
Y
X

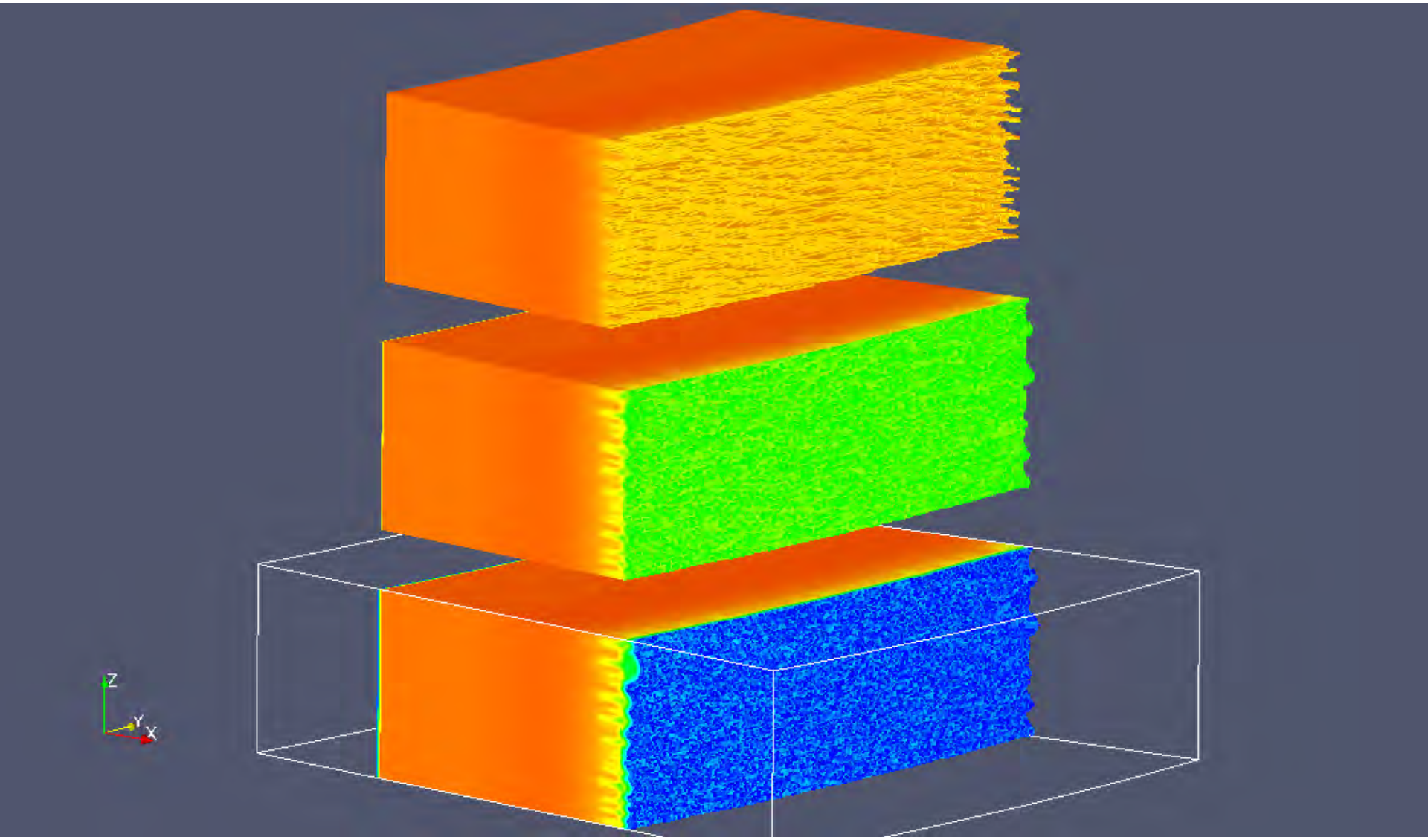
Z
Y
X

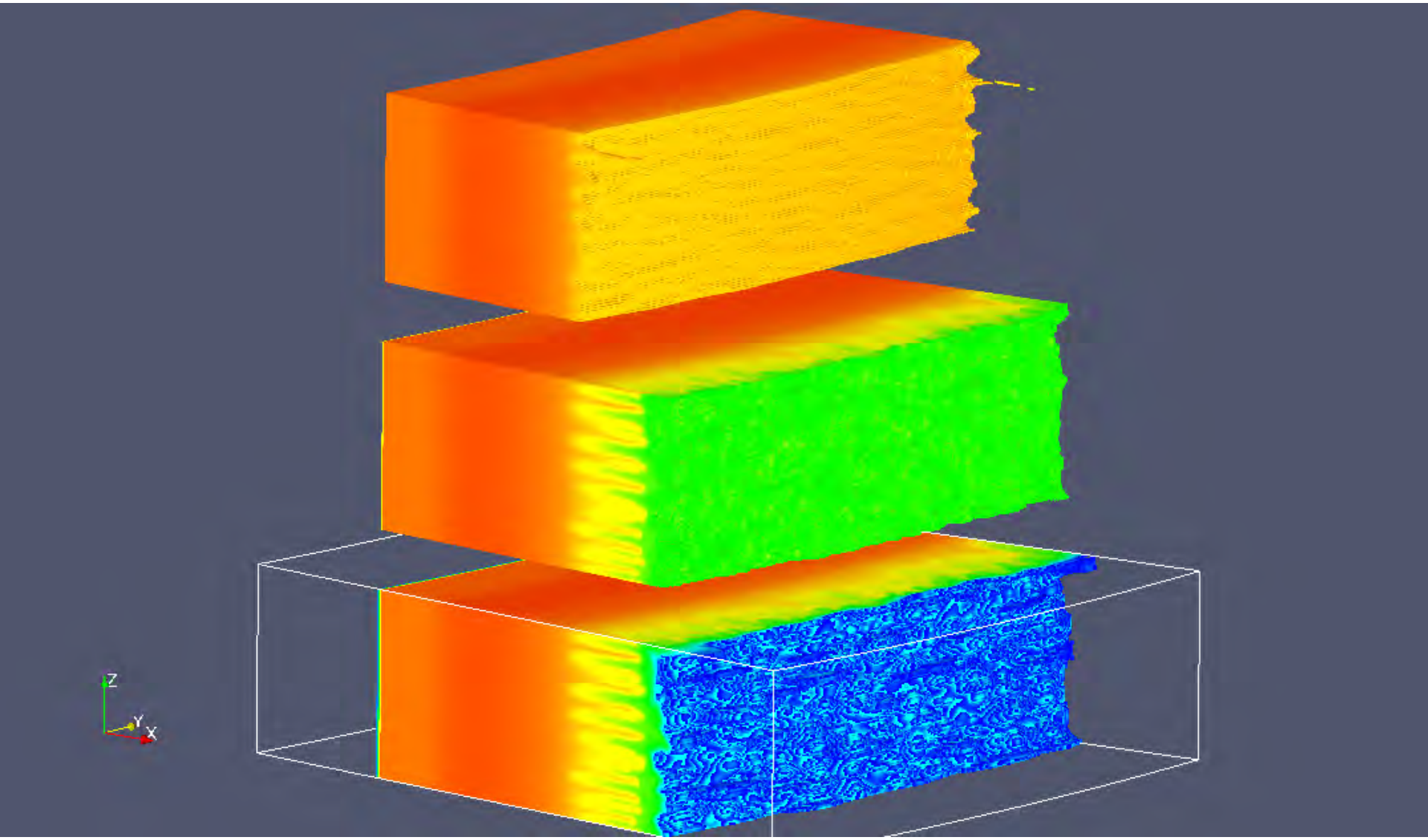
Z
Y
X

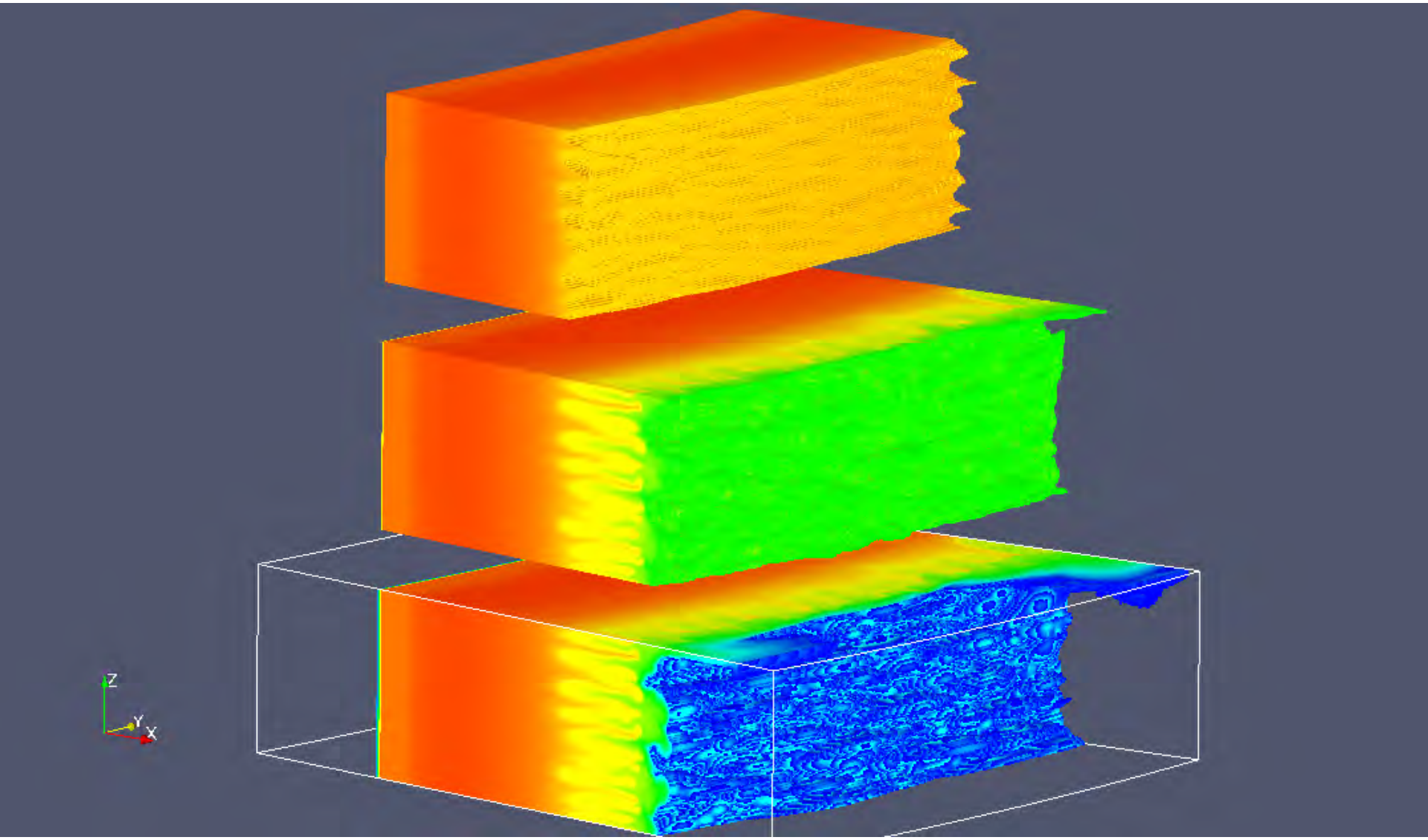
Z
Y
X

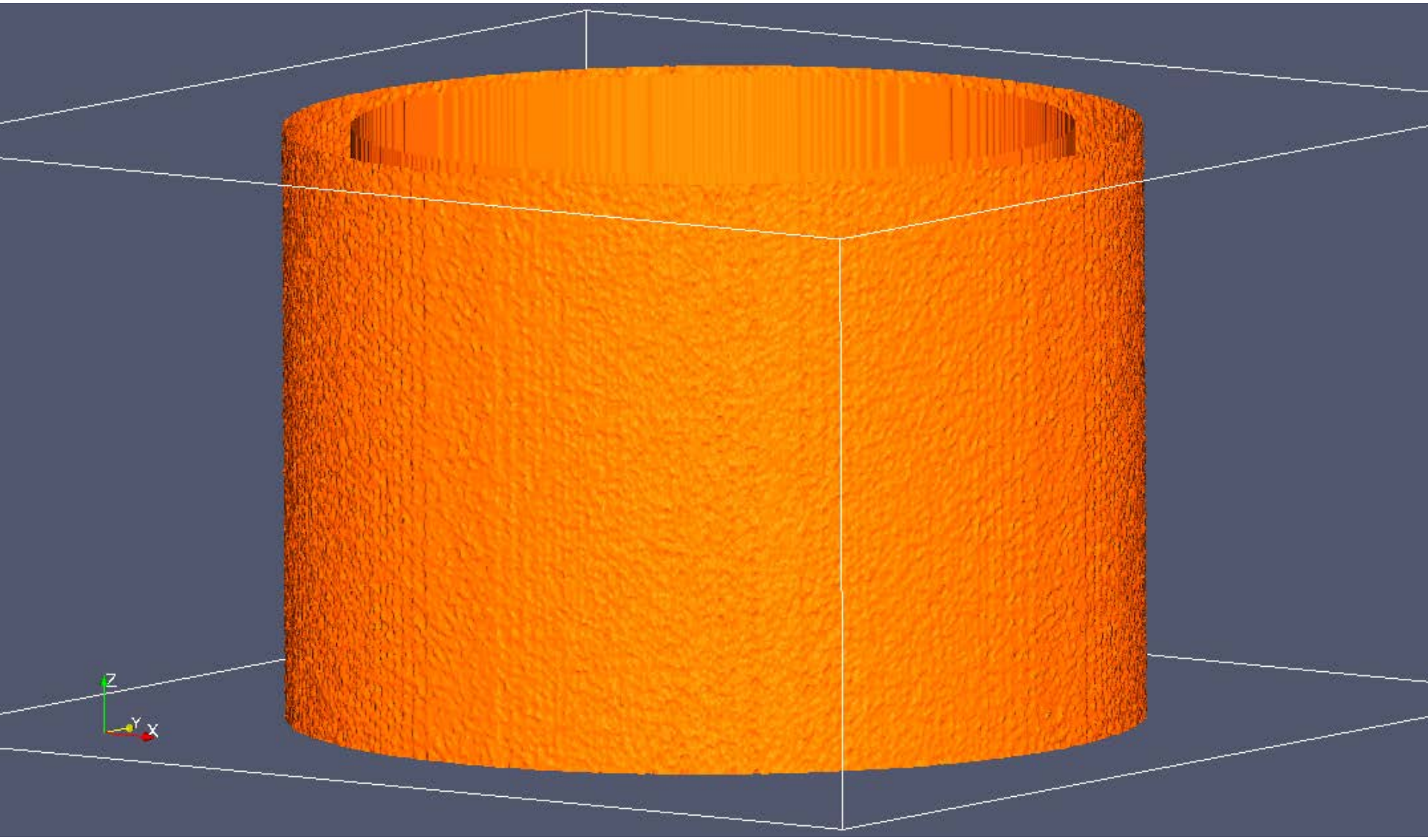
Z
Y
X

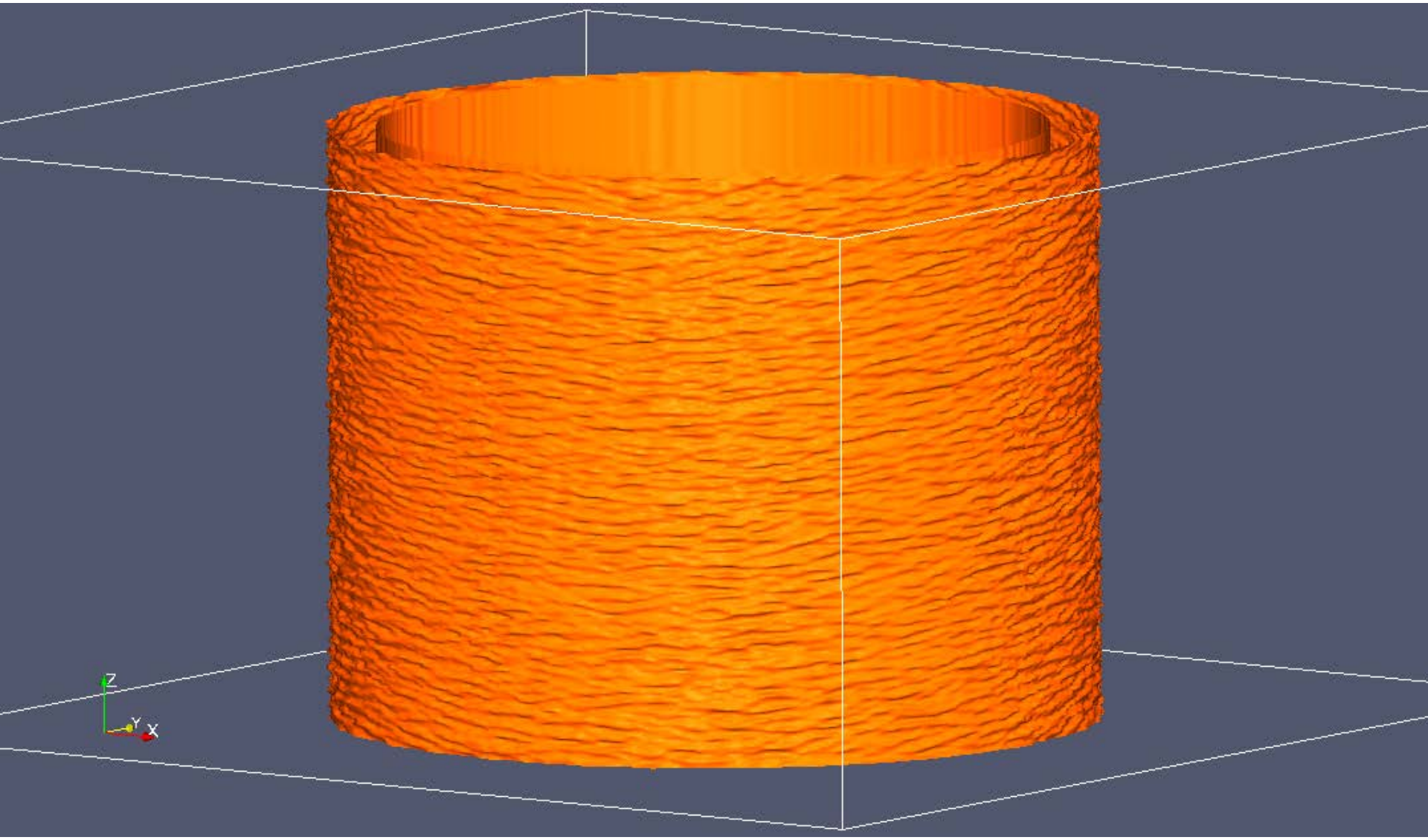
Z
Y
X

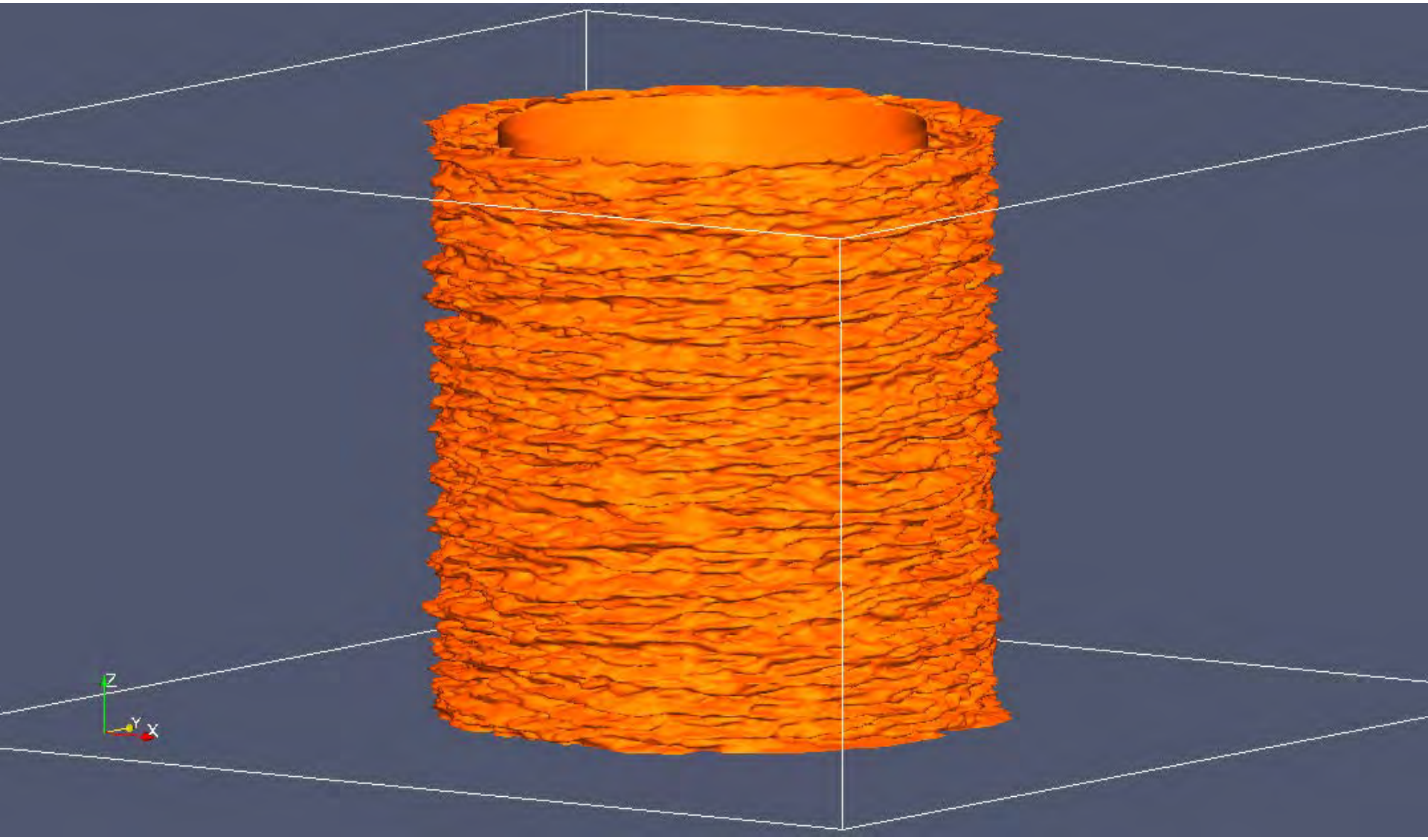
Z
Y
X

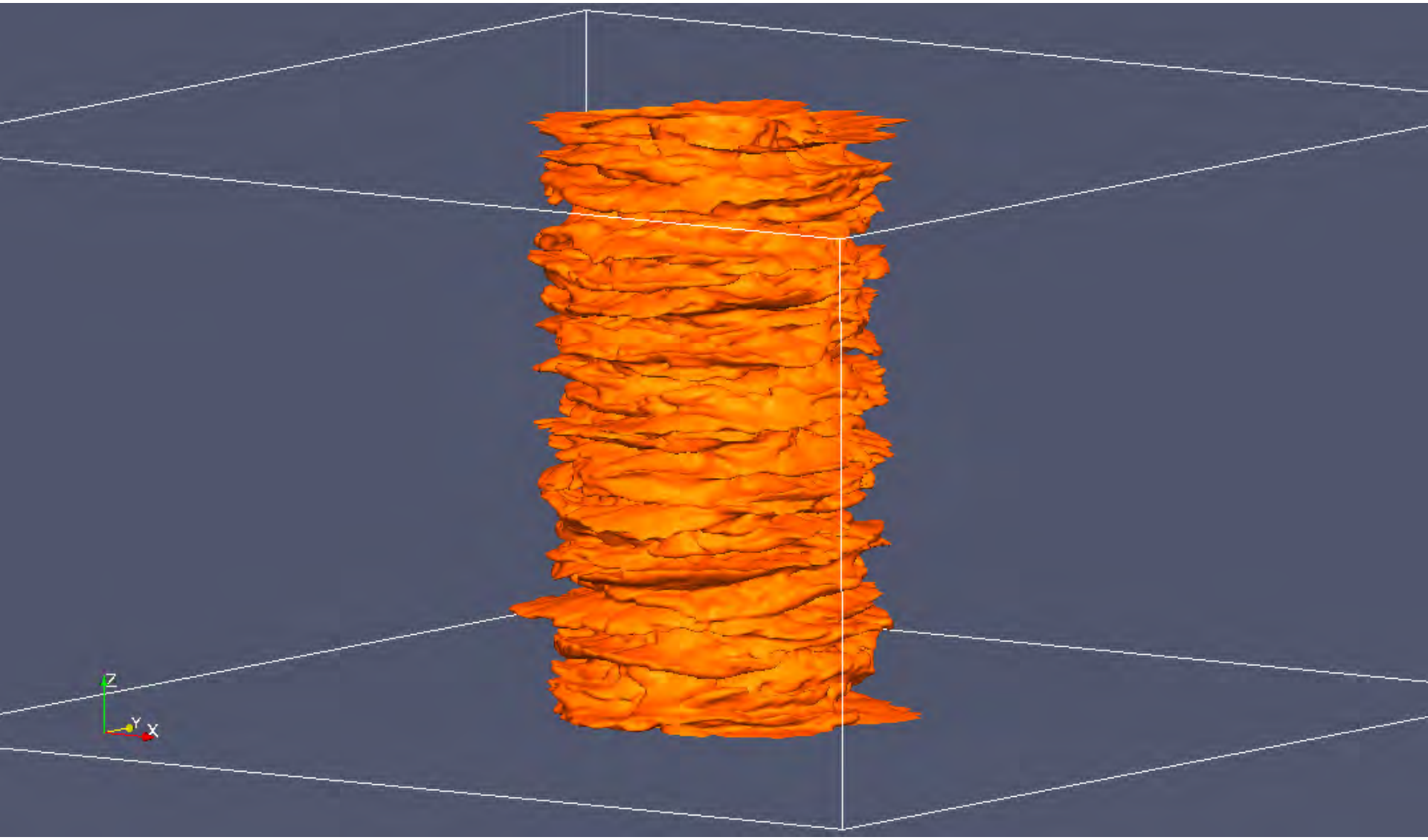
Z
Y
X

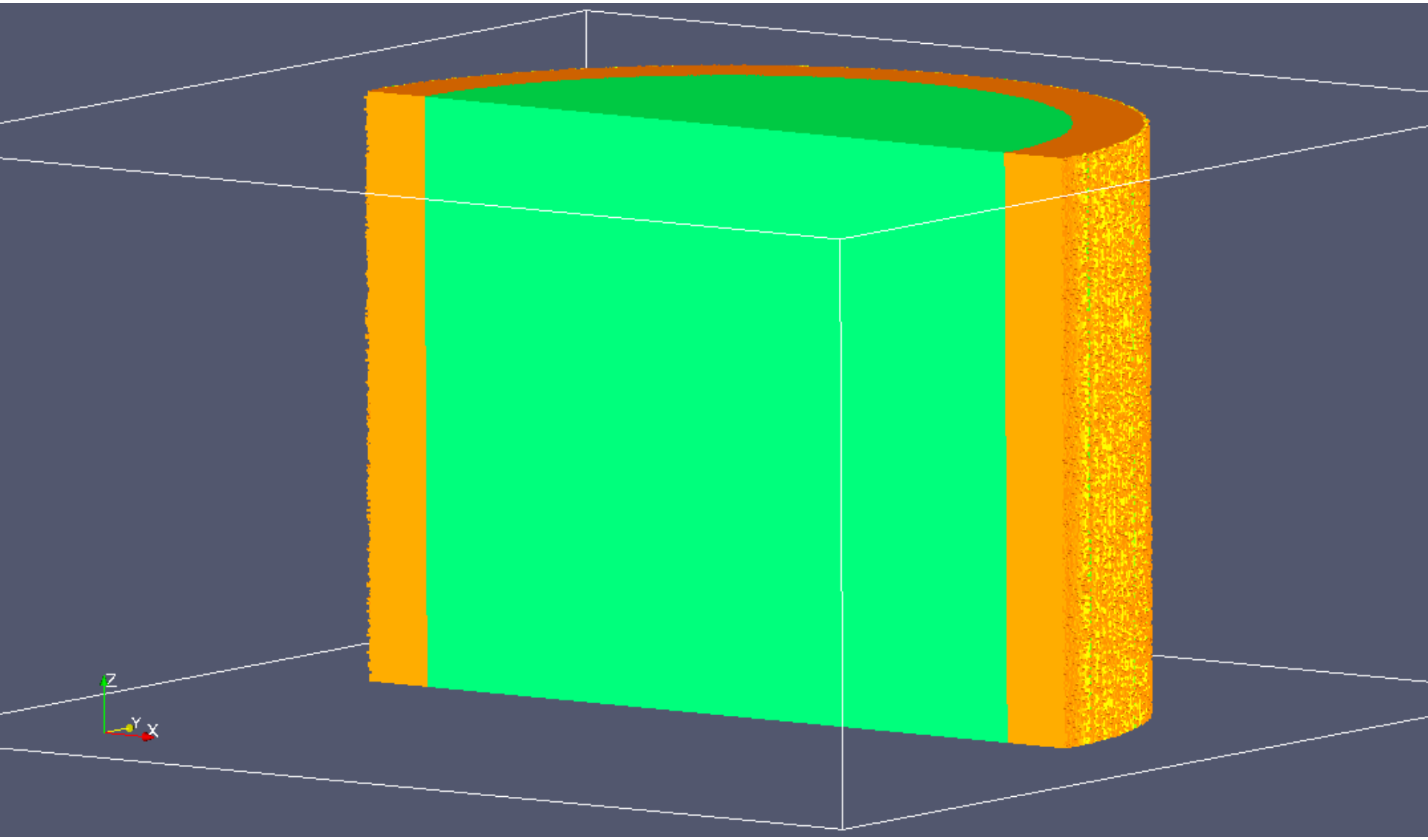
Z
Y
X

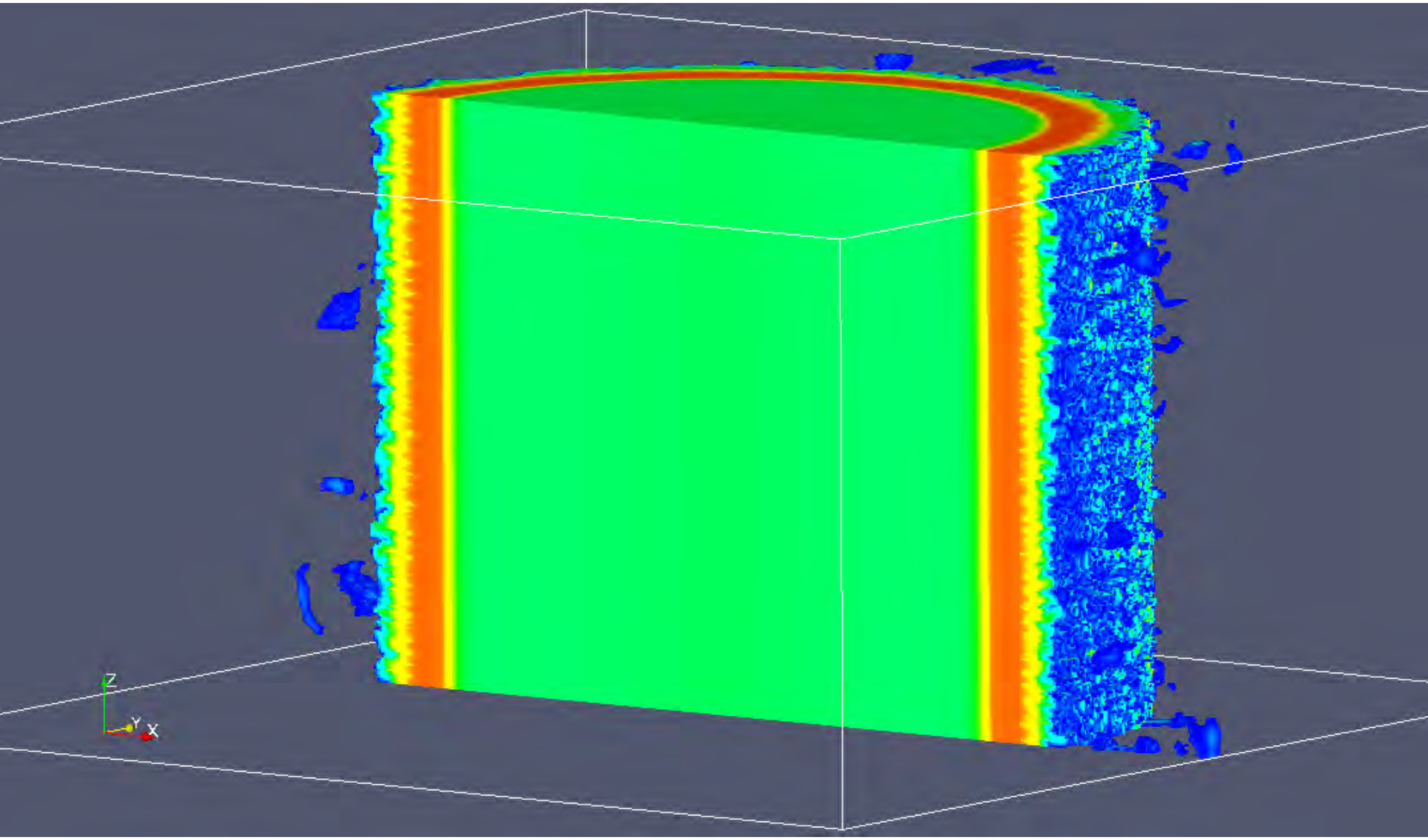
Z
Y
X

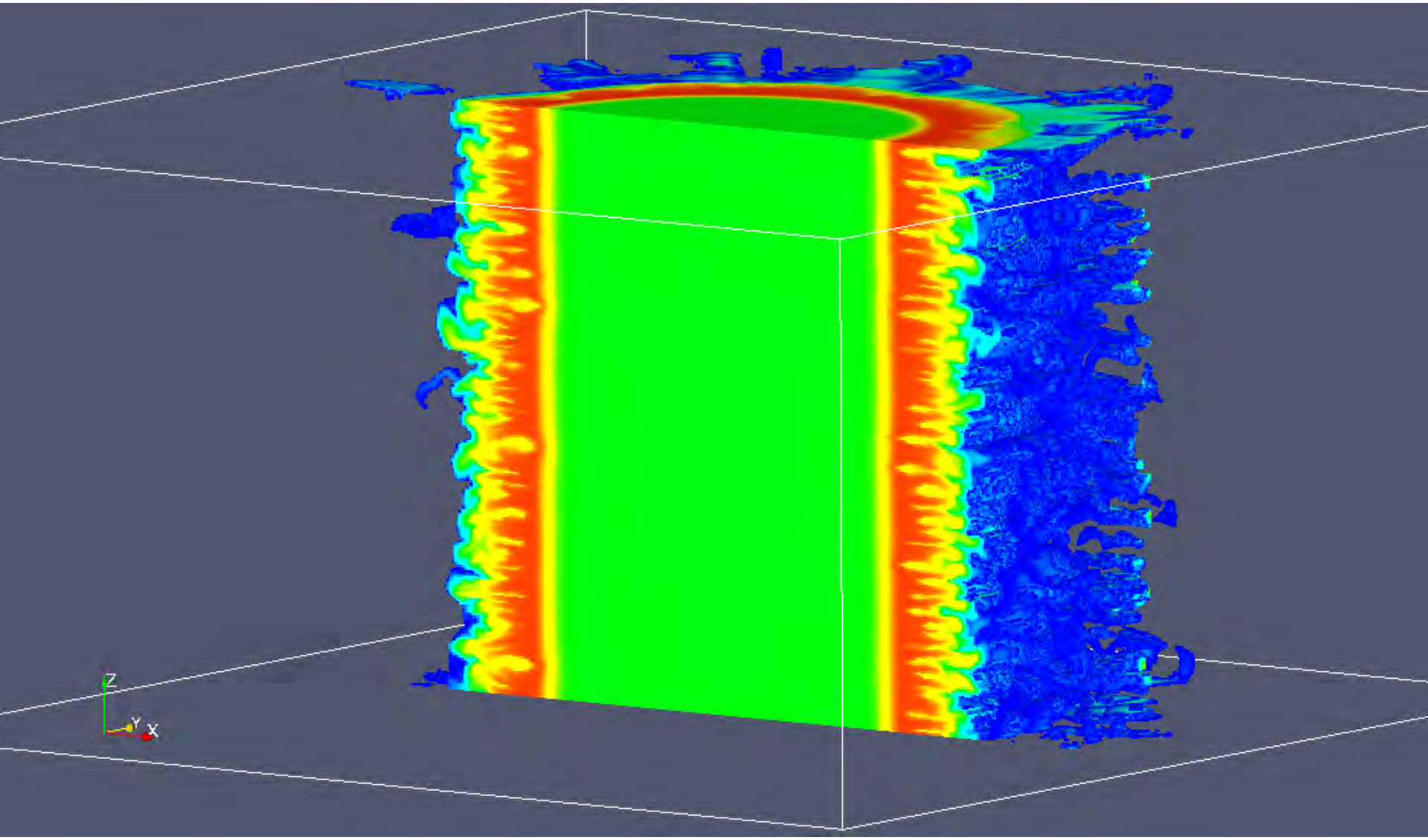
Z
Y
X

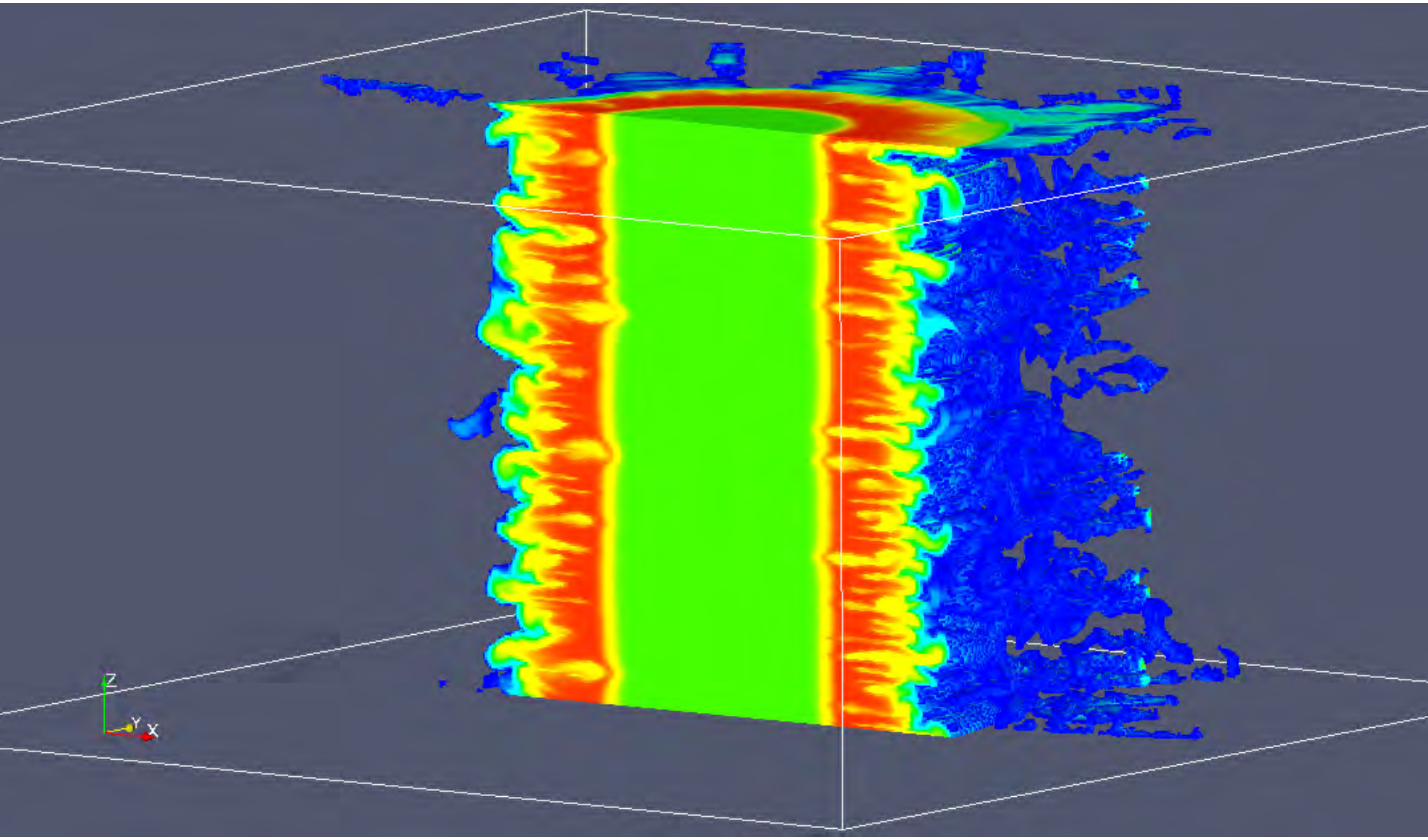
Z
Y
X

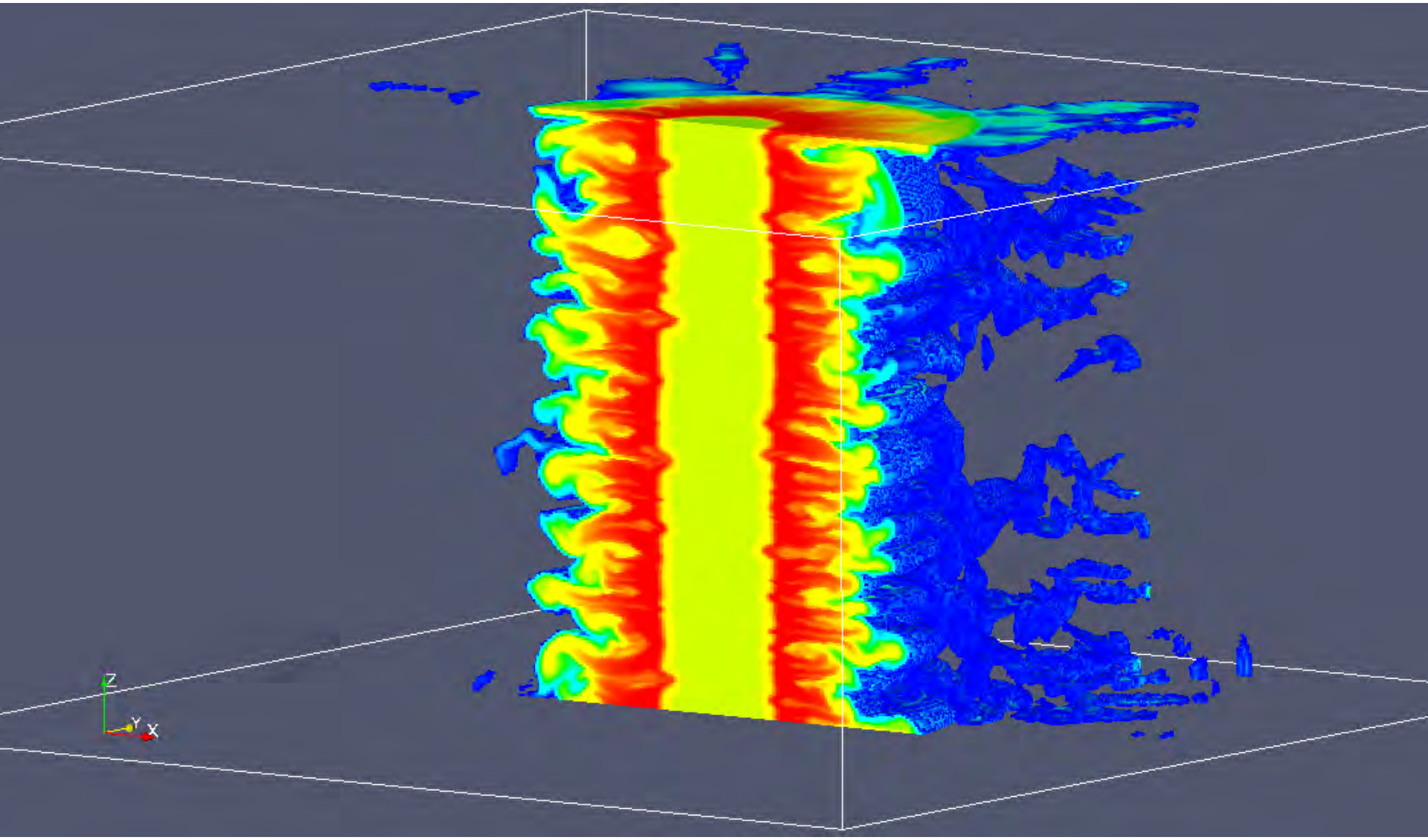
Z
Y
X

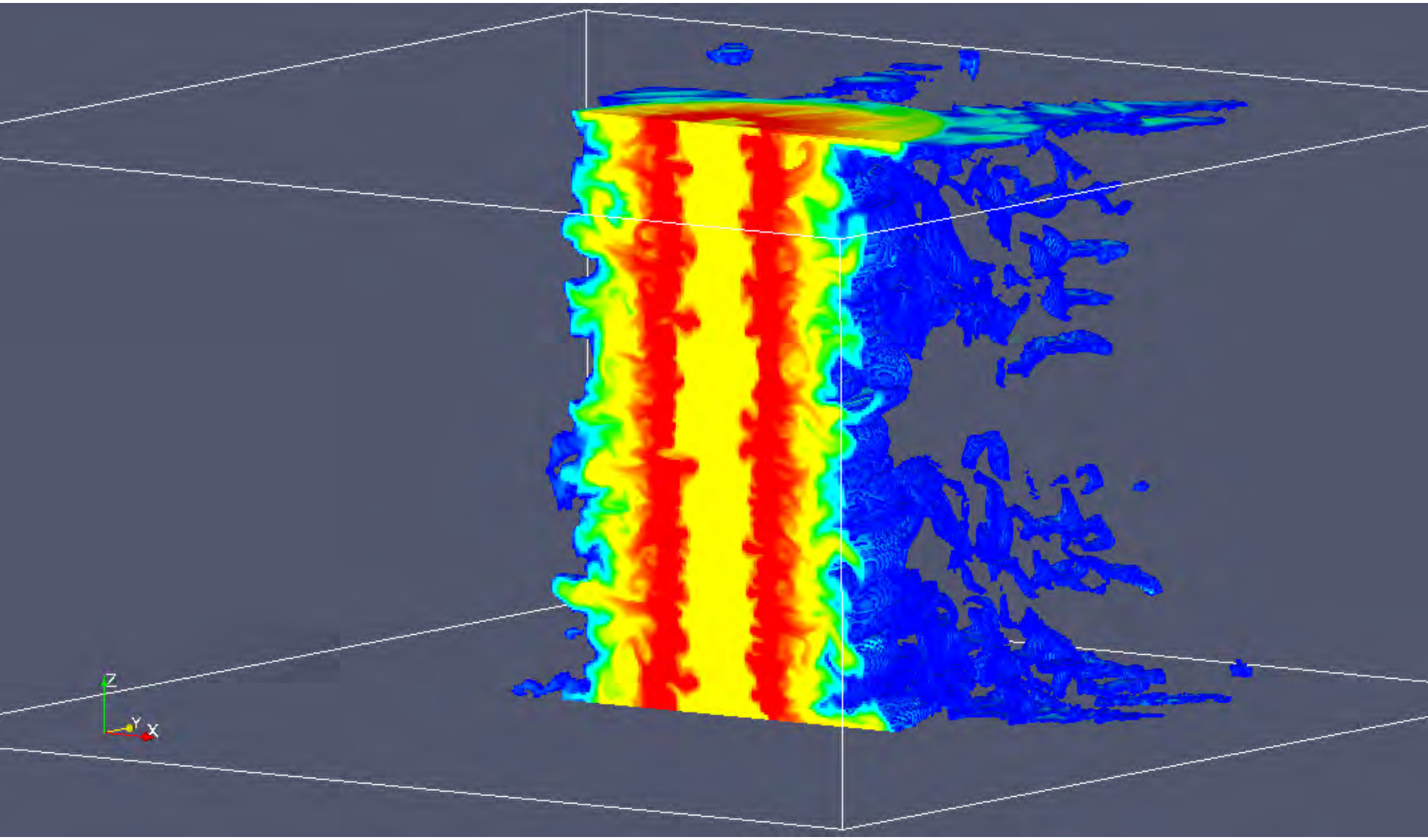
Z
Y
X

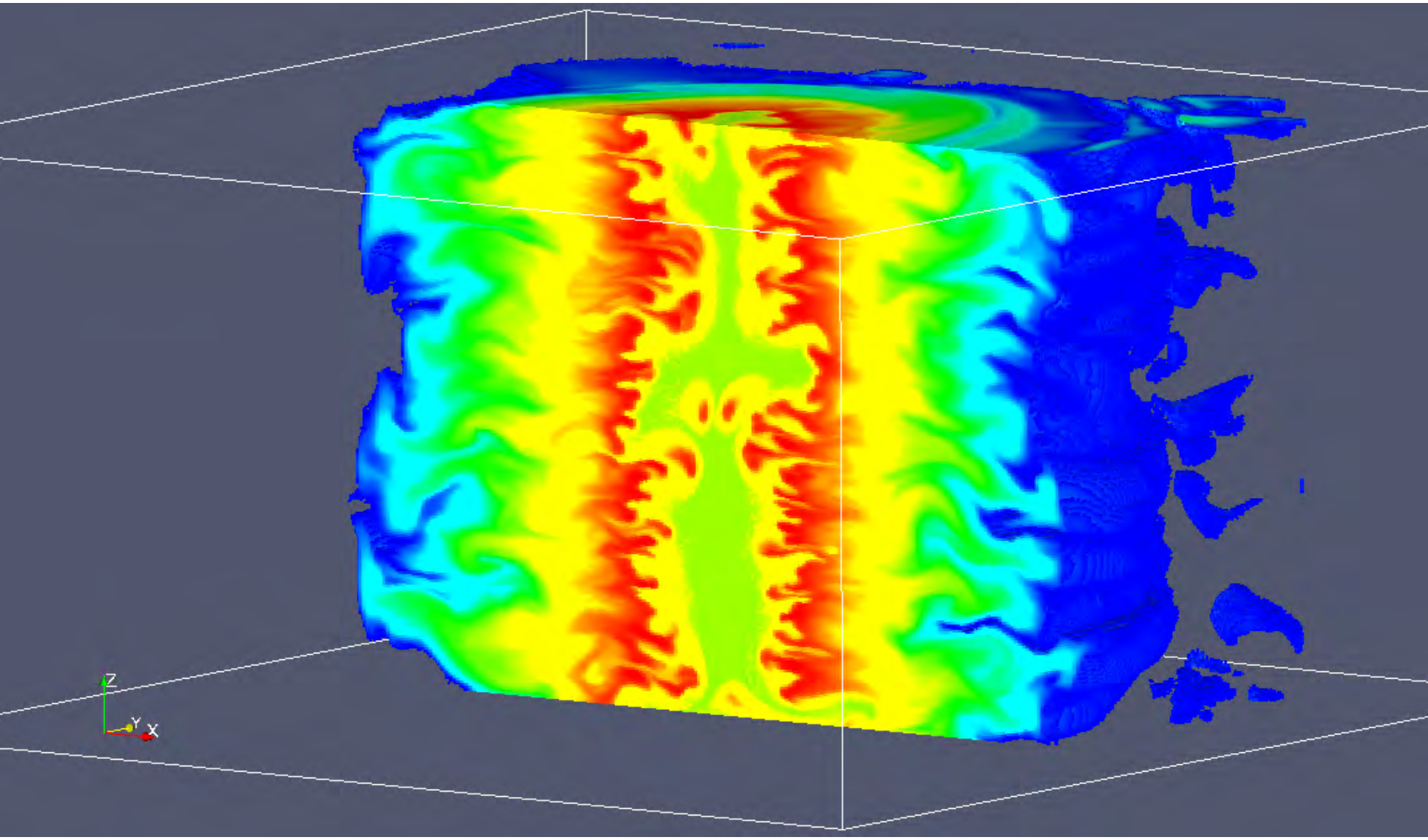
Z
Y
X

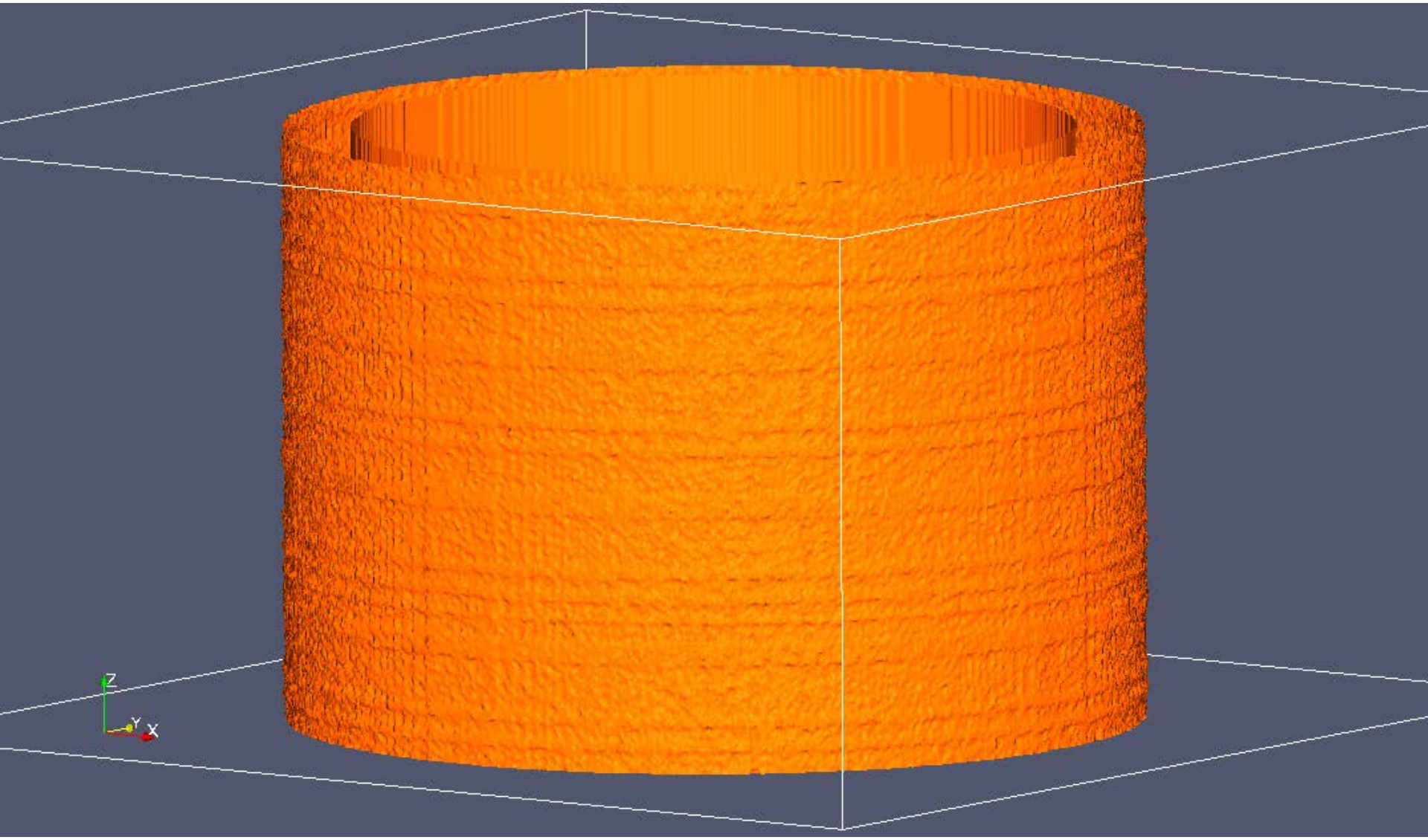
Z
Y
X

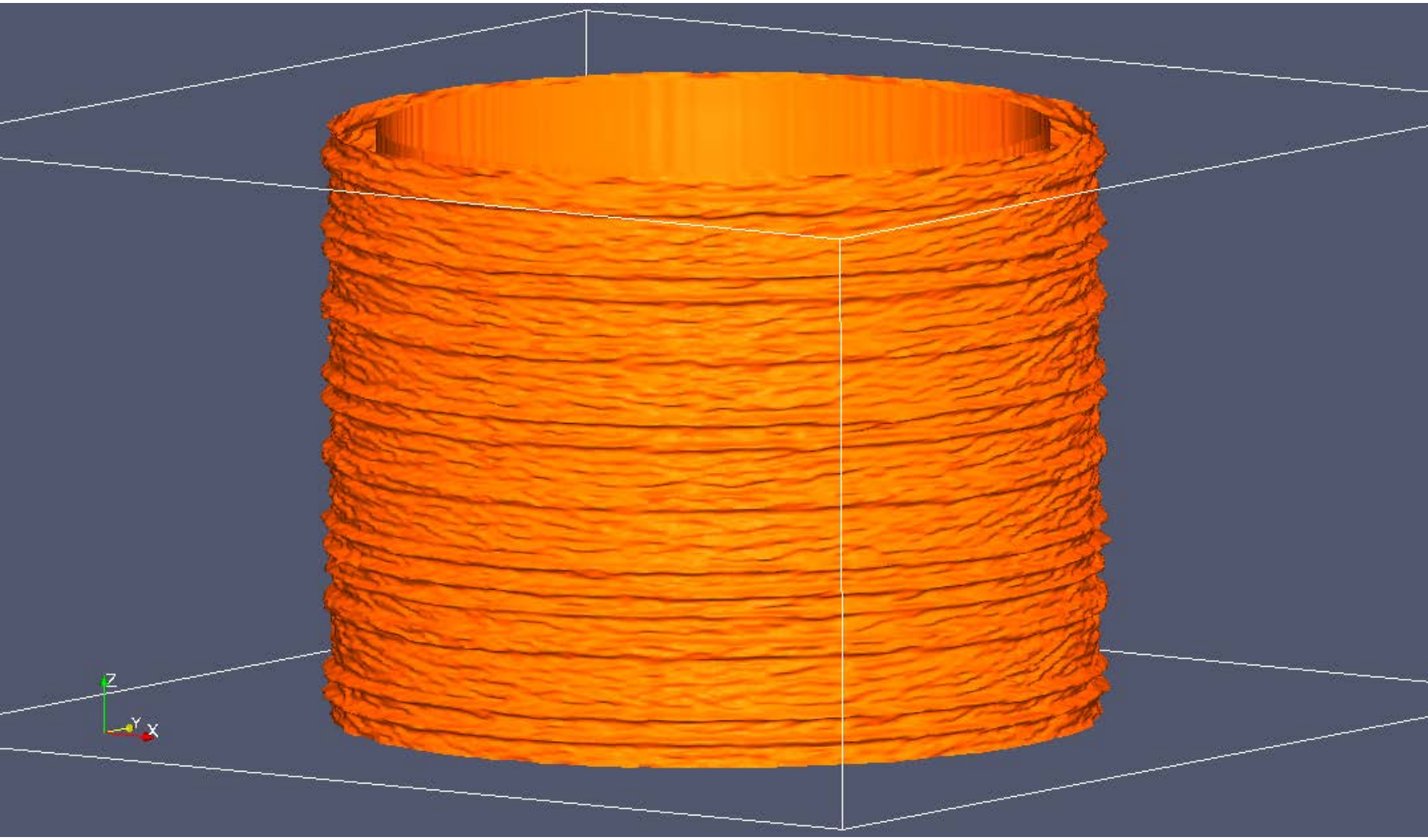
Z
Y
X

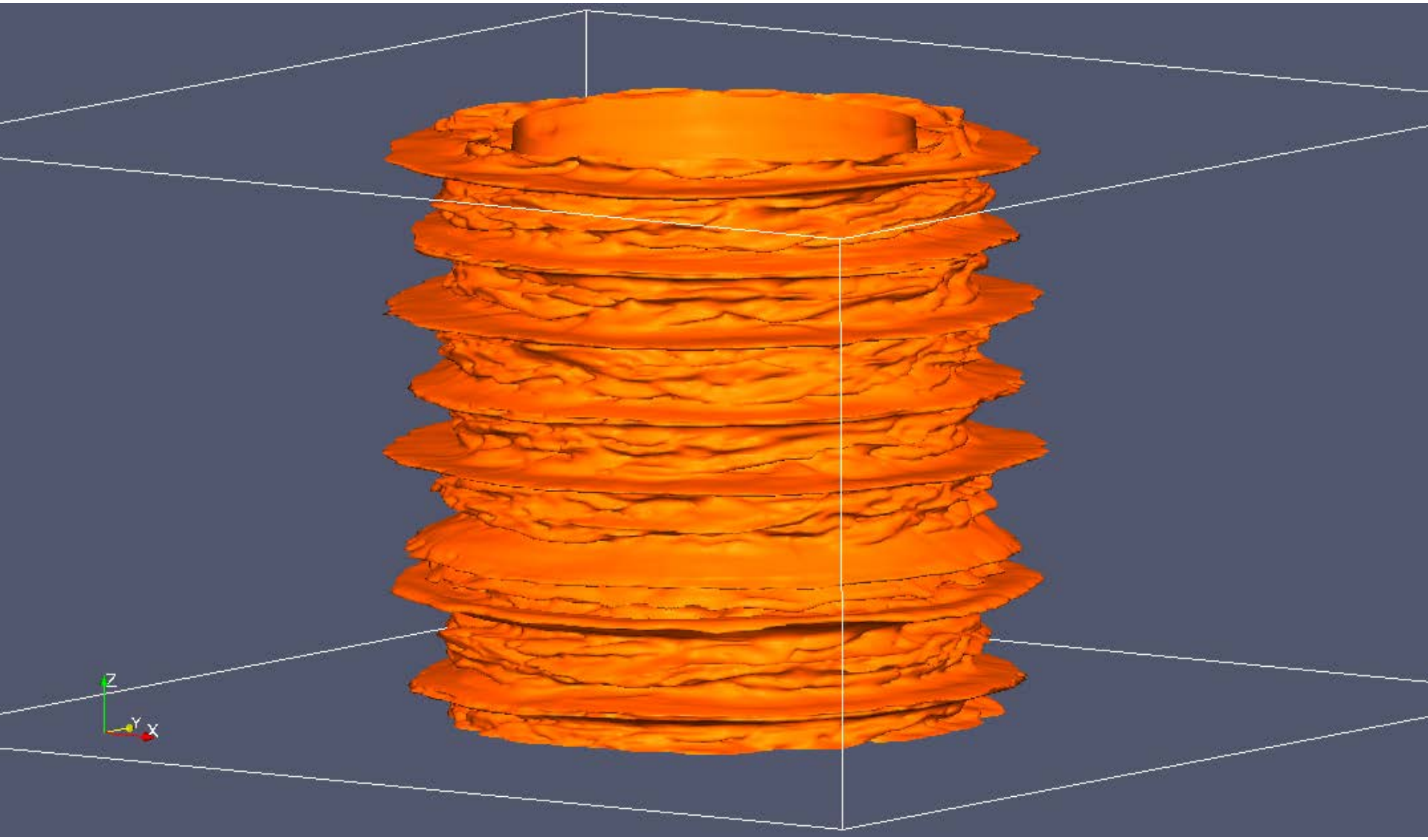
Z
Y
X

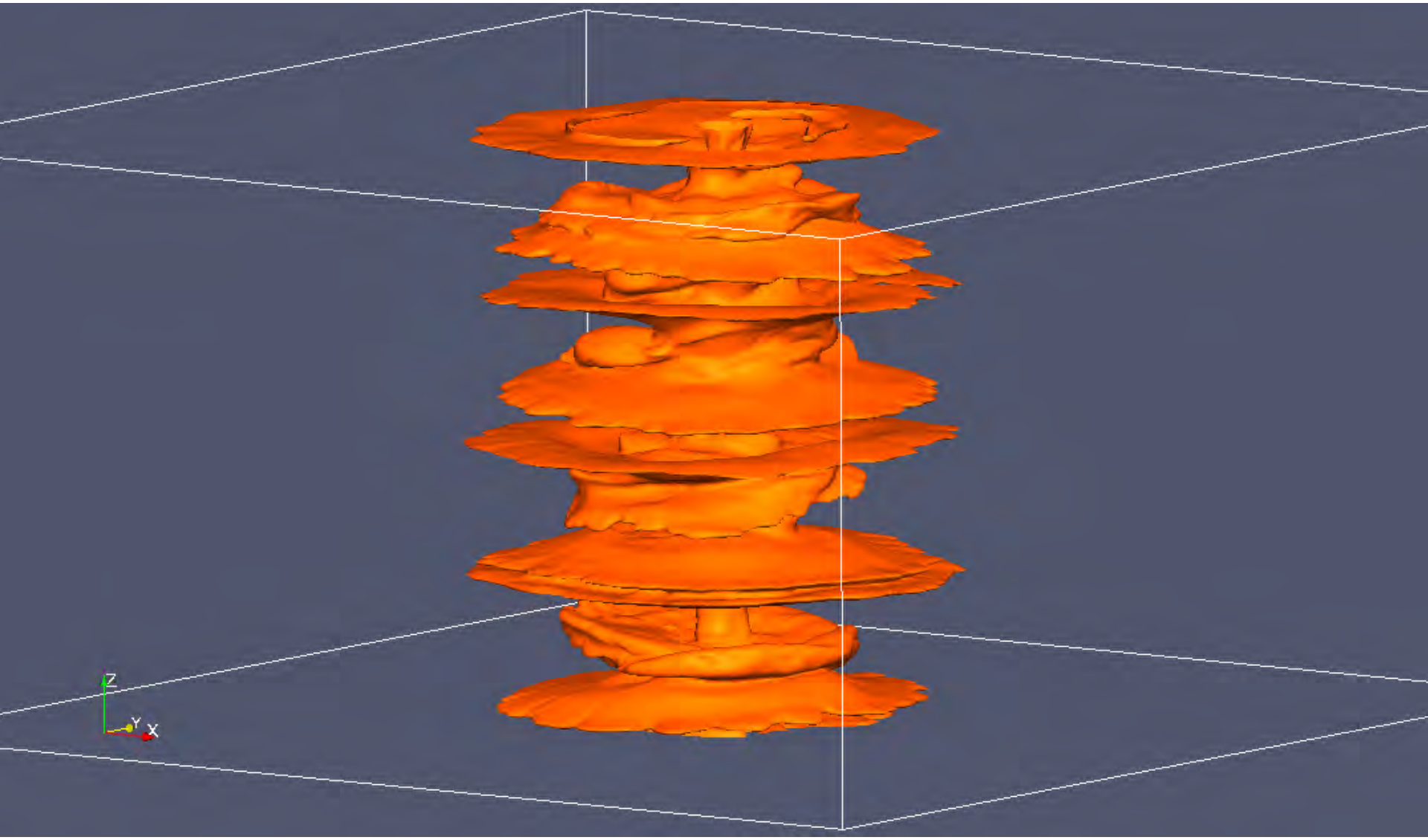
Z
Y
X

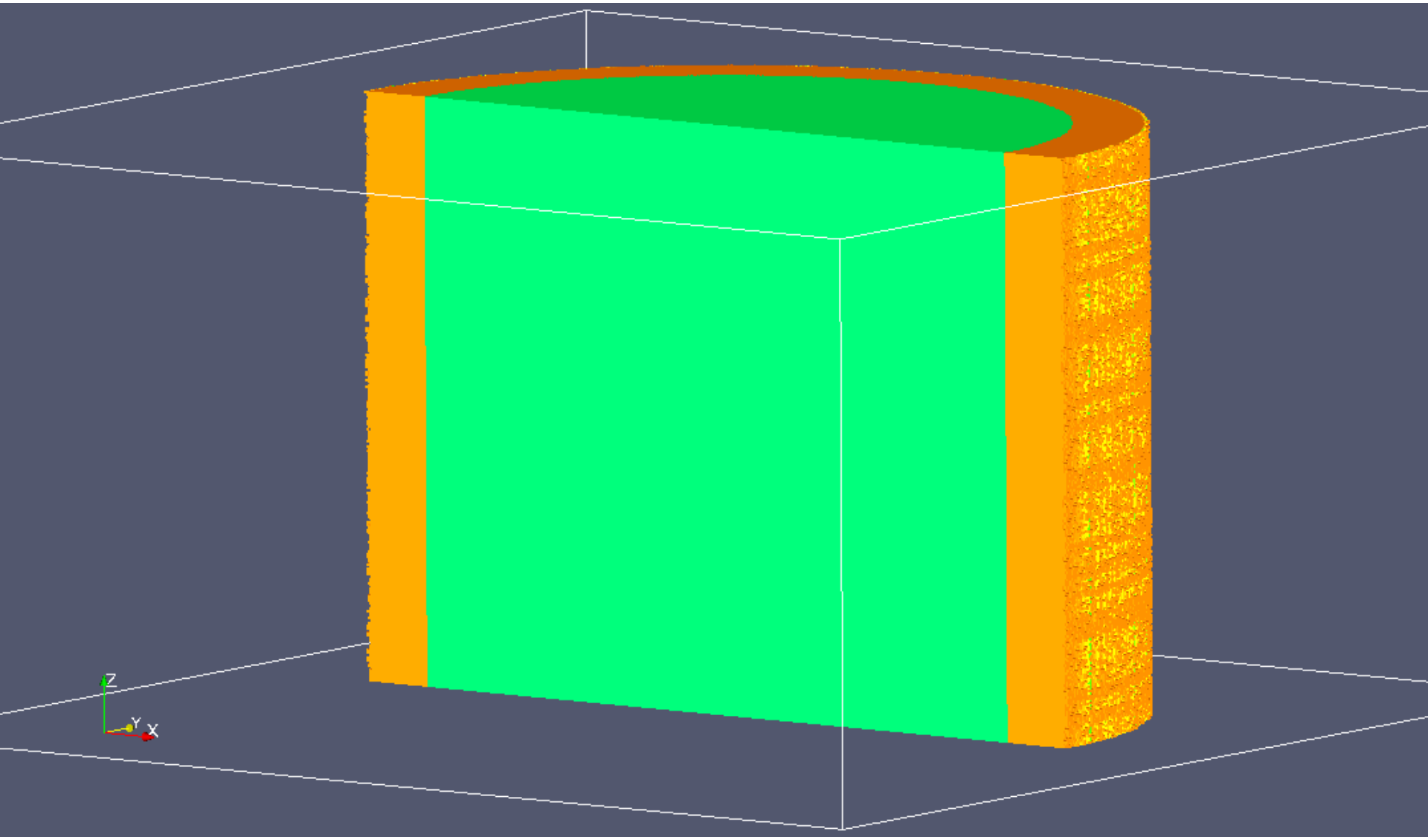
Z
Y
X

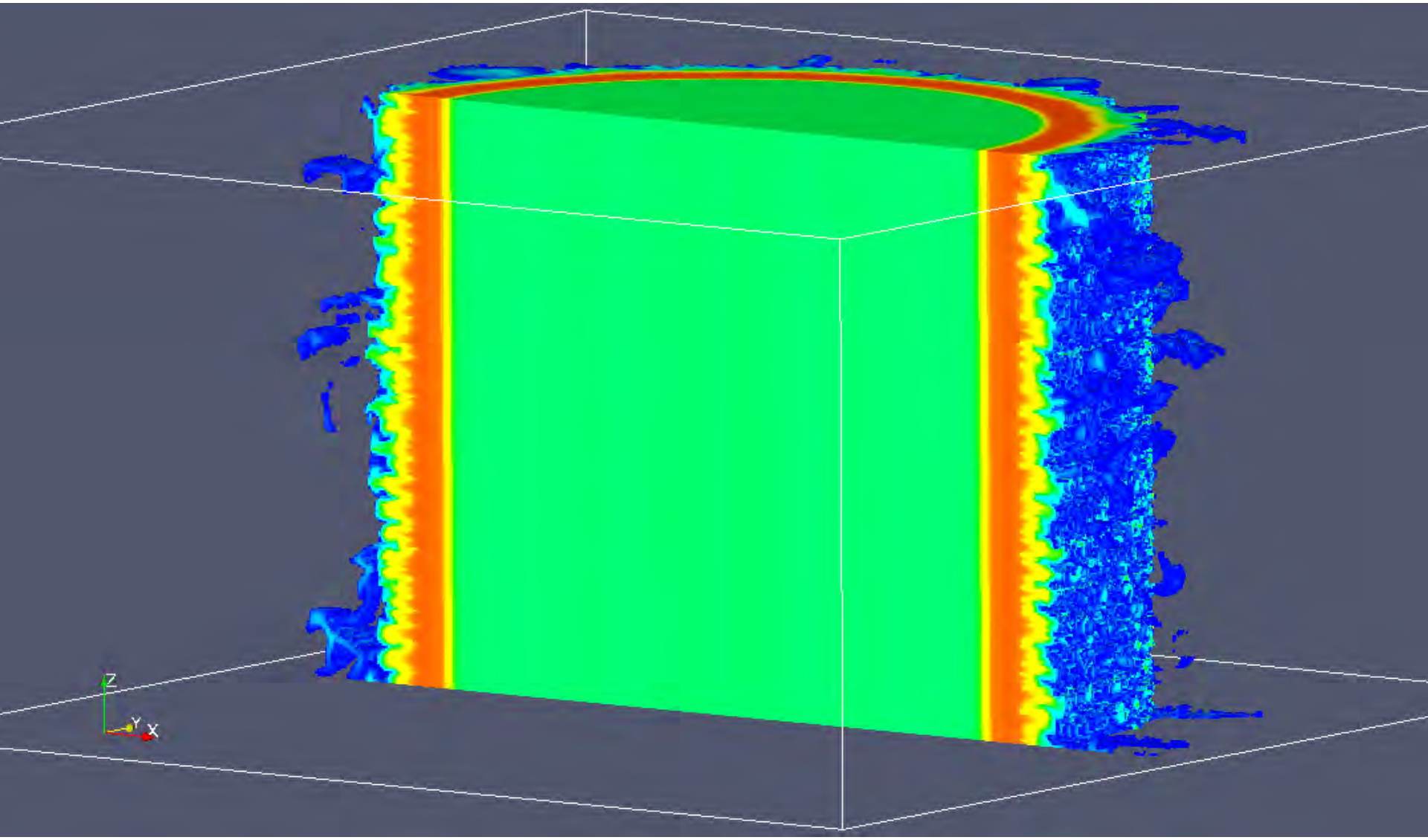
Z
Y
X

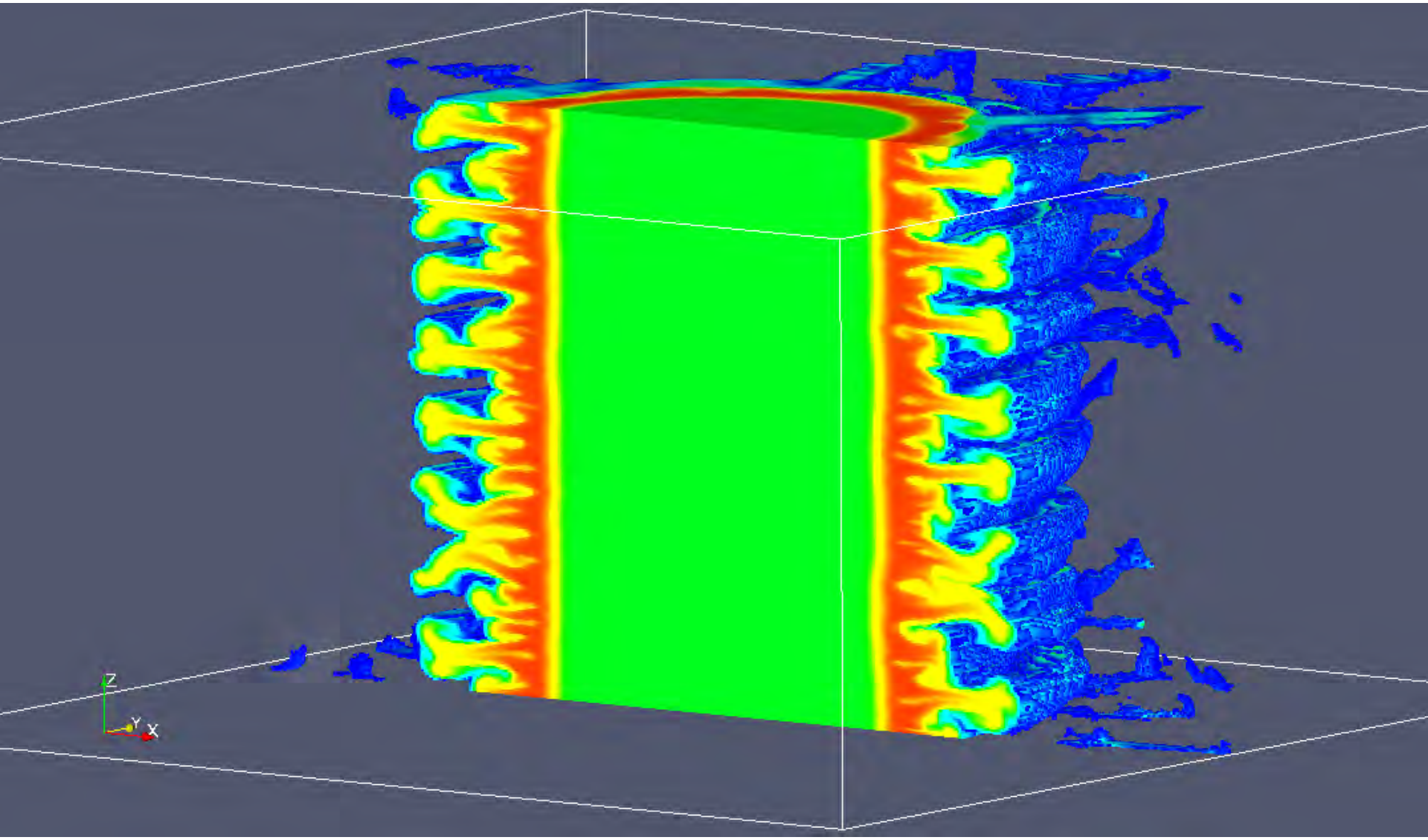
Z
Y
X

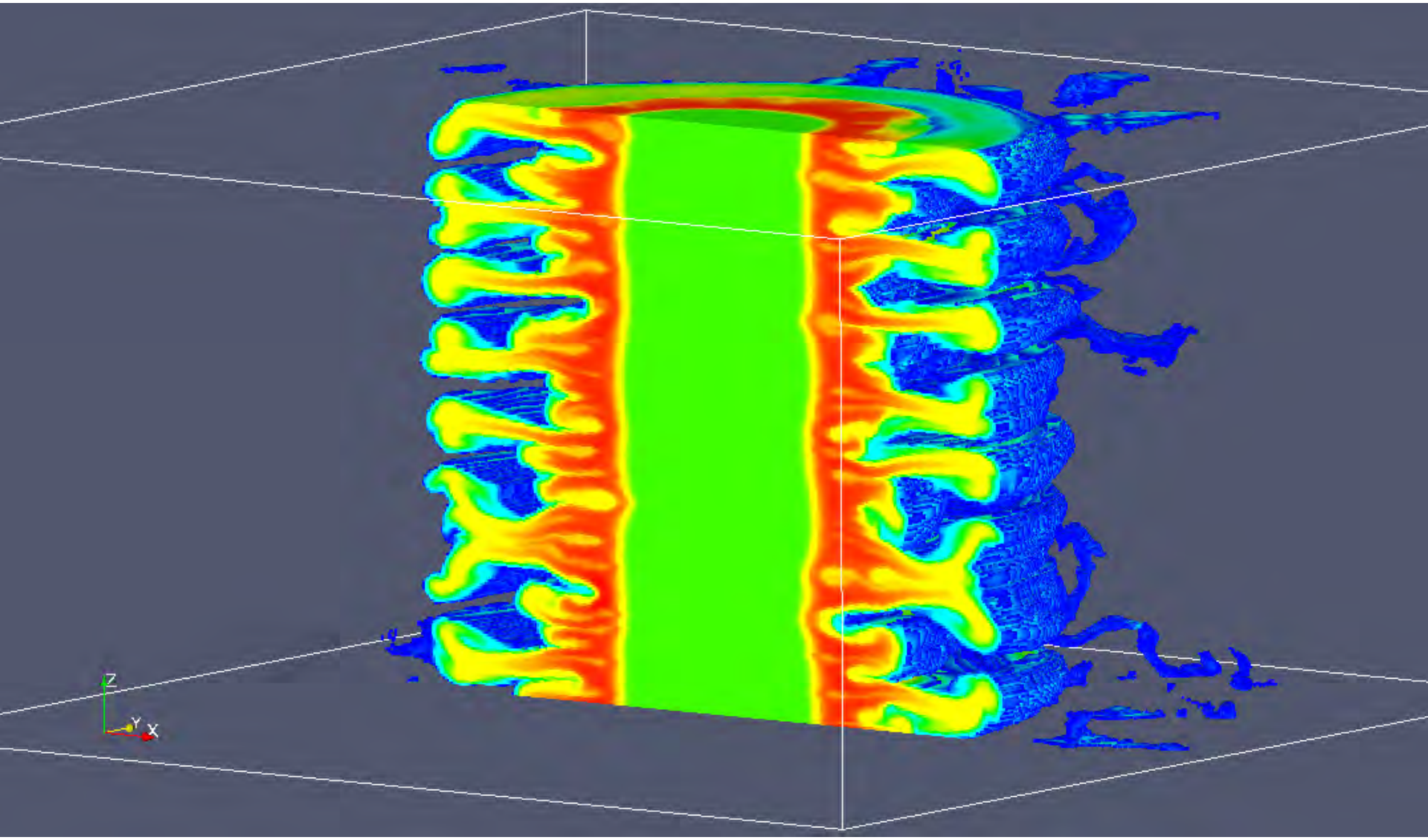
Z
Y
X

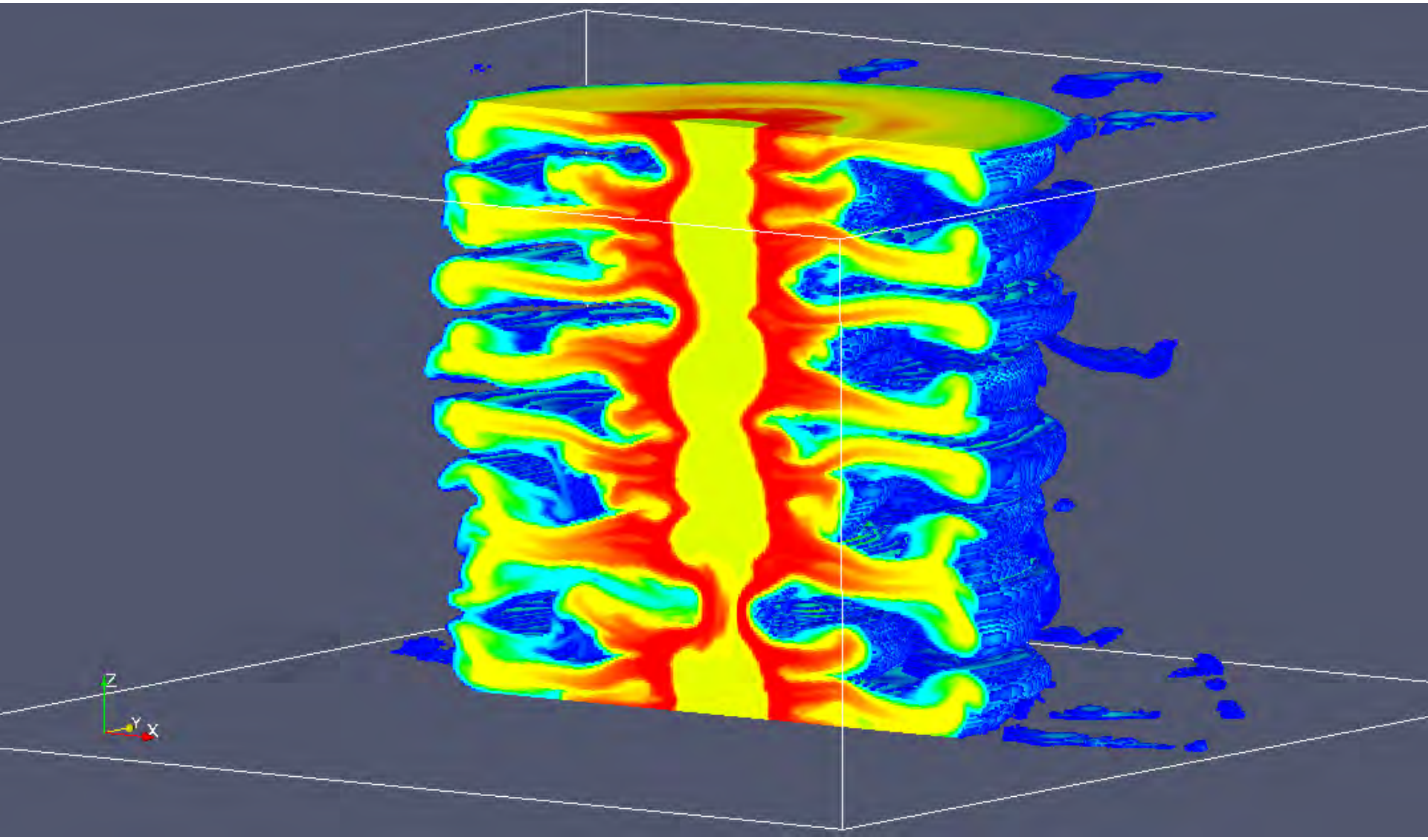
Z
Y
X

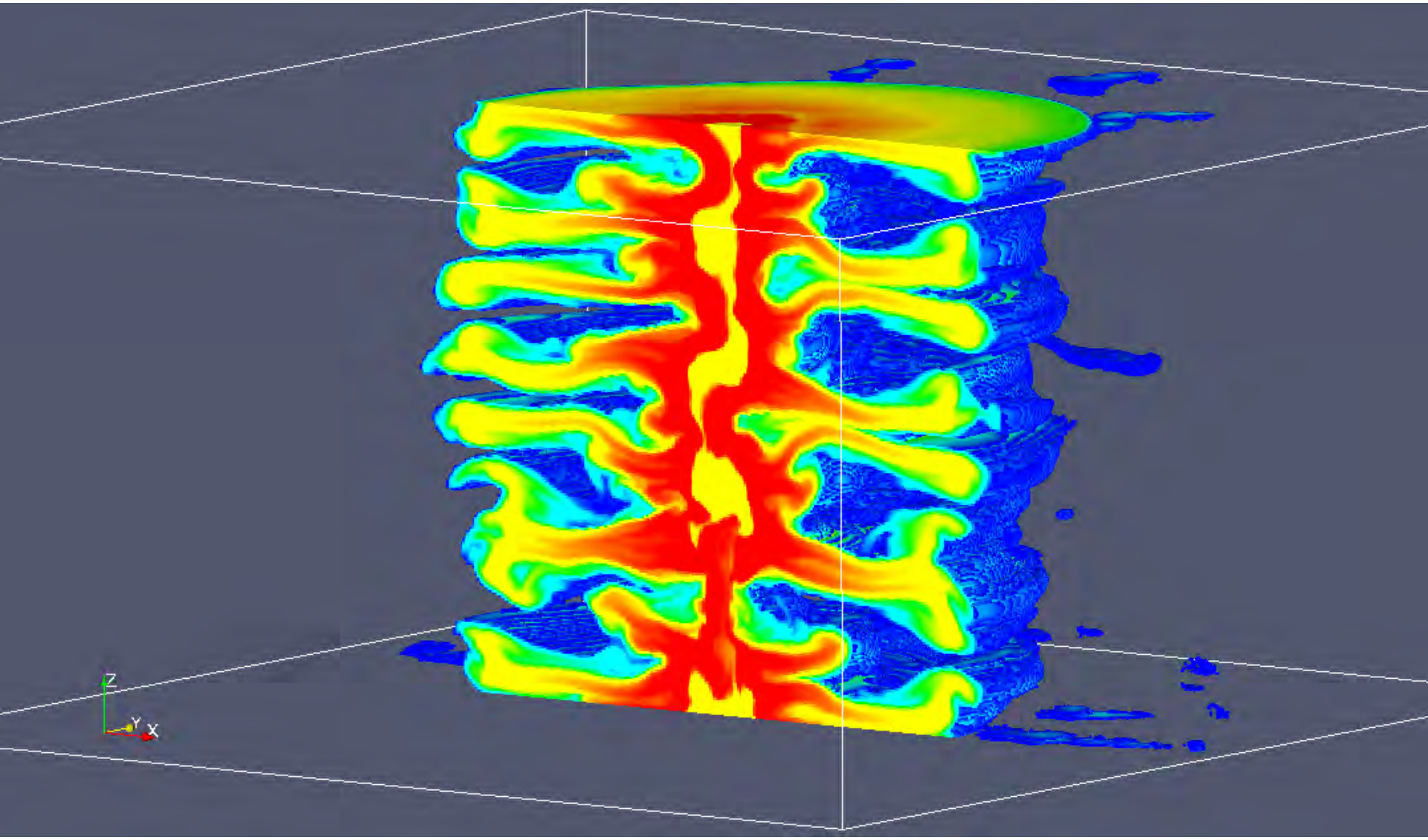
Z
Y
X

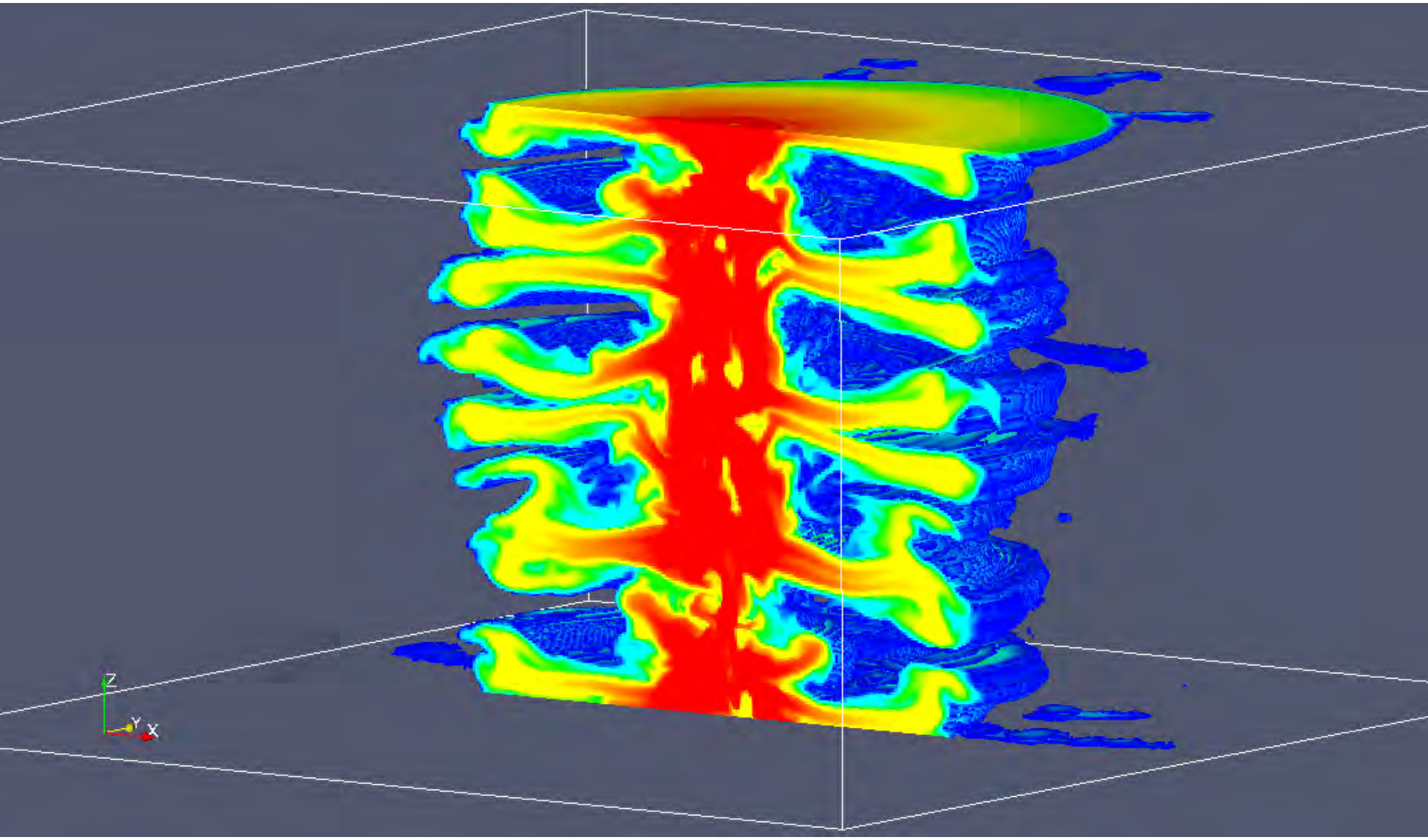
Z
Y
X

Investigating the Effect of Axial Magnetic Field on the MRT Instability

Hollow aluminium liner imploded by 20MA driving current
MRT seeded by 400μm sinusoidal perturbation as in Sinars et al
but without central tungsten rod and with the addition of an initial B_z of 30T

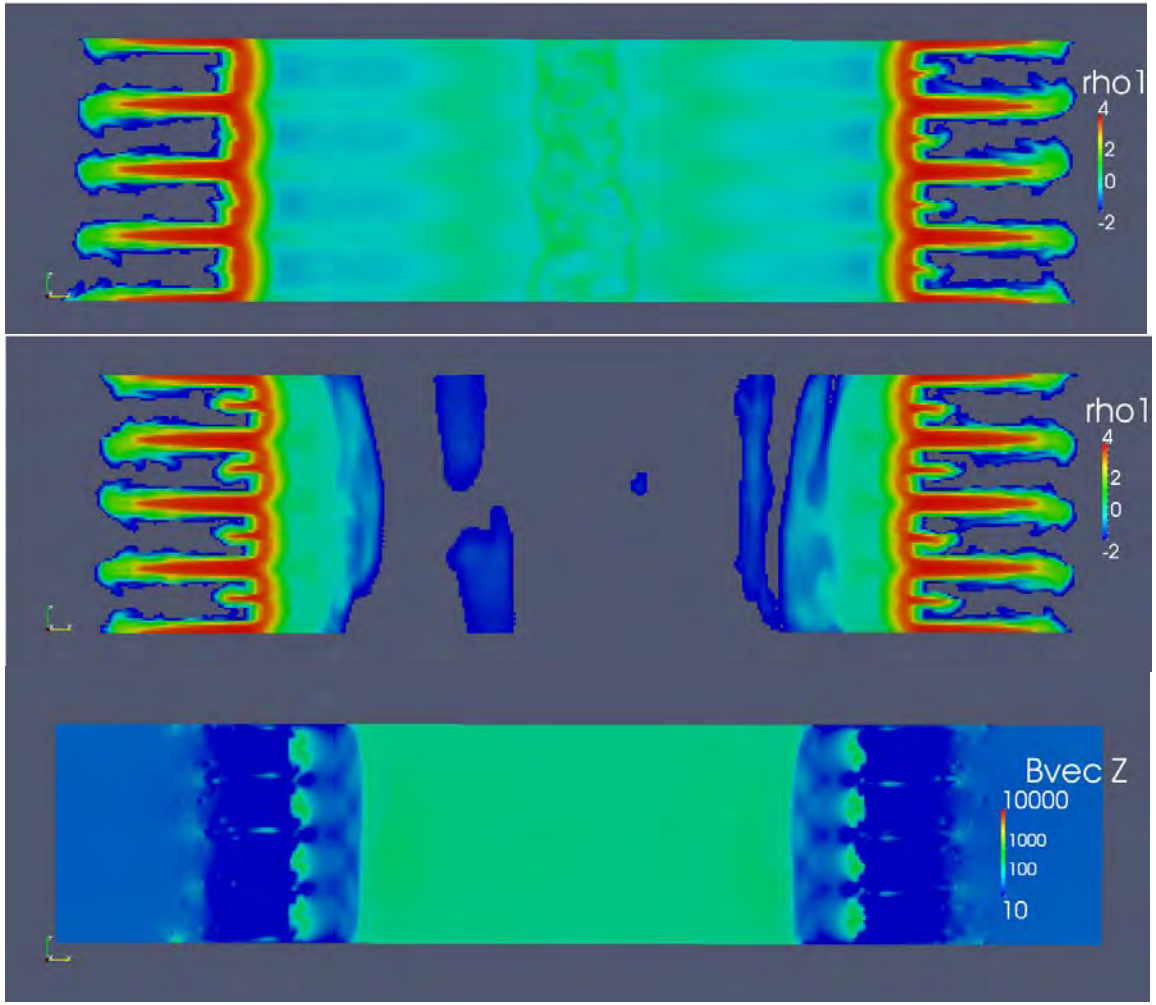

Provides a degree of stabilisation but only at stagnation

Investigating the Effect of Axial Magnetic Field on the MRT Instability

Hollow aluminium liner imploded by 20MA driving current
MRT seeded by 400μm sinusoidal perturbation as in Sinars et al
but without central tungsten rod and with the addition of an initial B_z of 30T

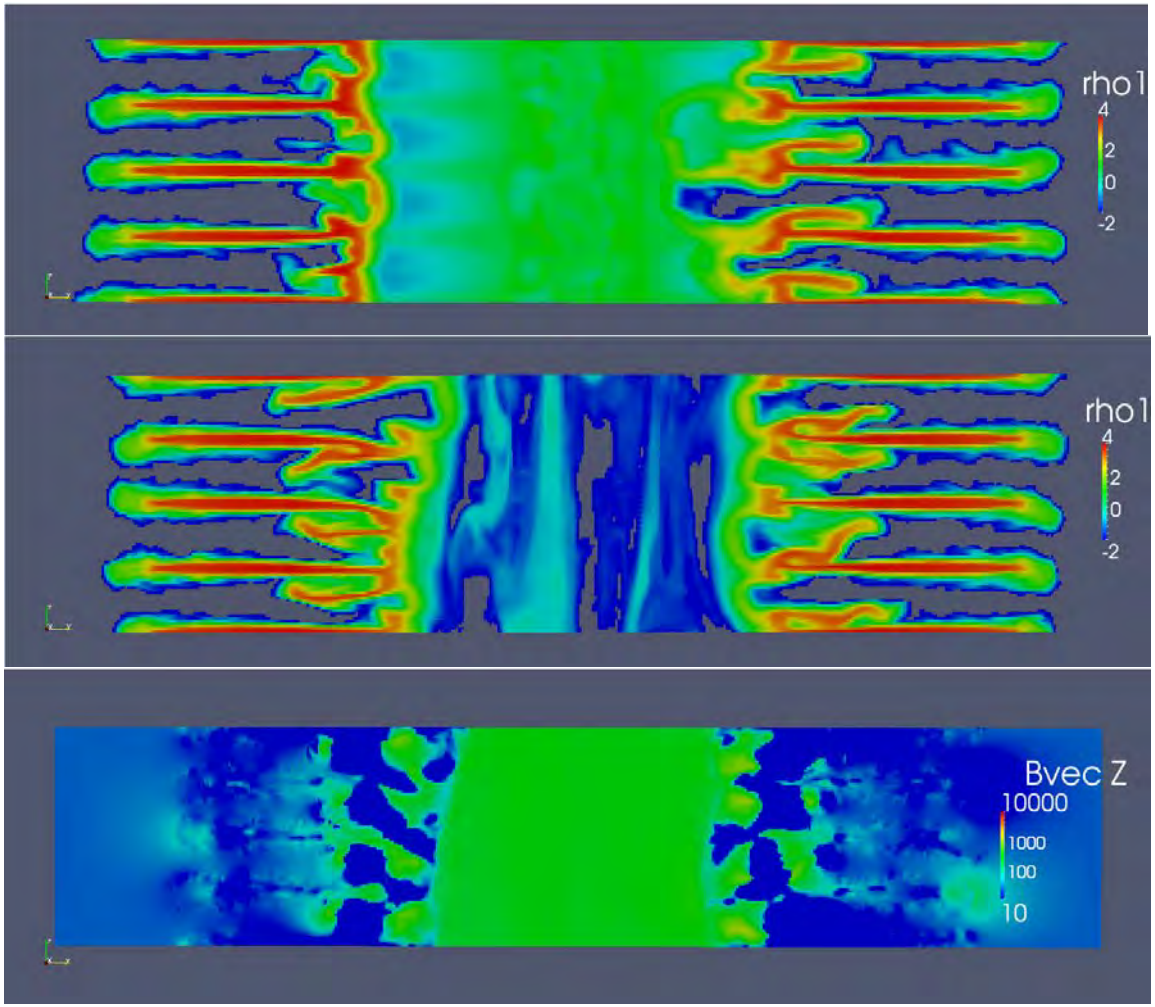

Provides a degree of stabilisation but only at stagnation

Investigating the Effect of Axial Magnetic Field on the MRT Instability

Hollow aluminium liner imploded by 20MA driving current
MRT seeded by 400μm sinusoidal perturbation as in Sinars et al
but without central tungsten rod and with the addition of an initial B_z of 30T

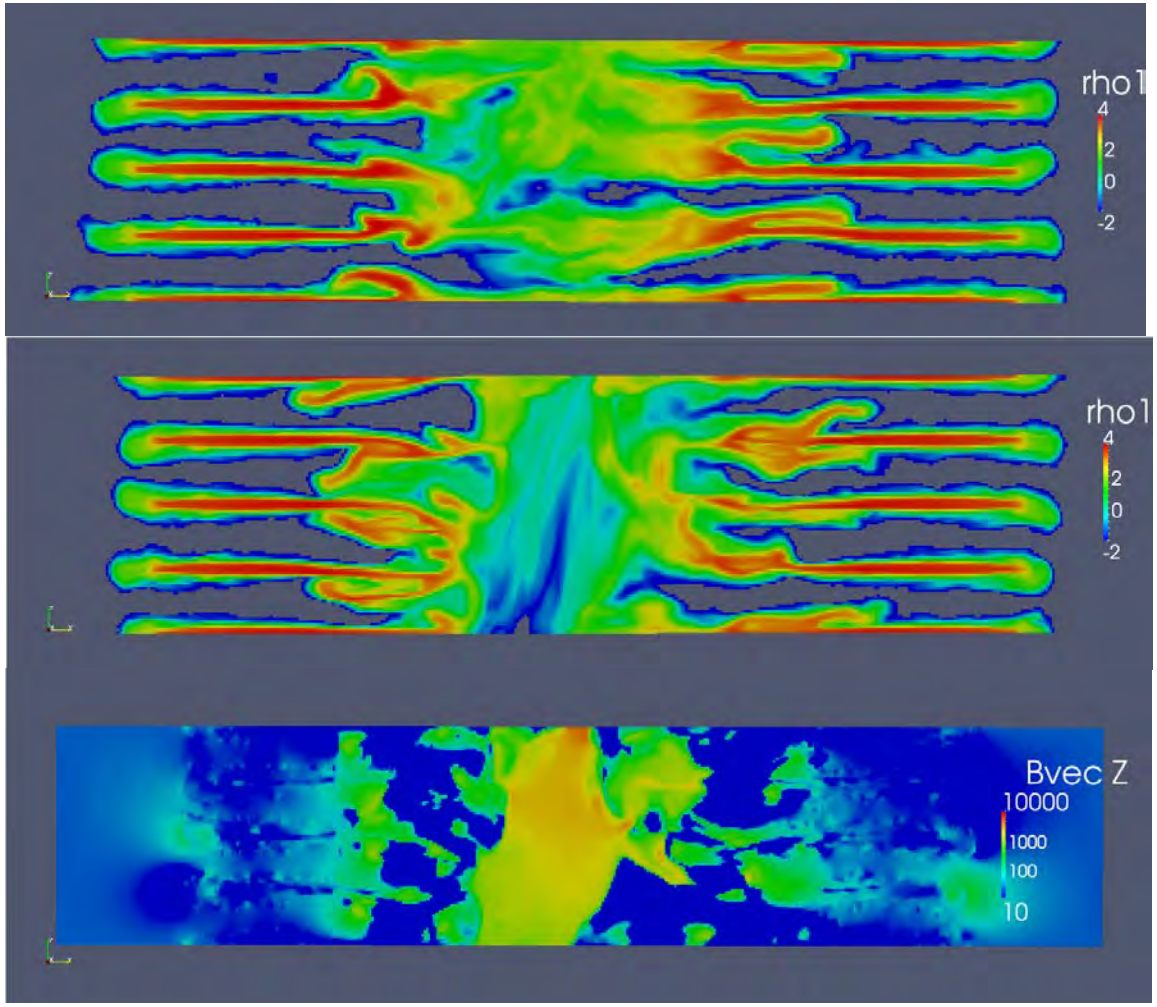

Provides a degree of stabilisation but only at stagnation

Investigating the Effect of Axial Magnetic Field on the MRT Instability

Hollow aluminium liner imploded by 20MA driving current
MRT seeded by 400μm sinusoidal perturbation as in Sinars et al
but without central tungsten rod and with the addition of an initial B_z of 30T

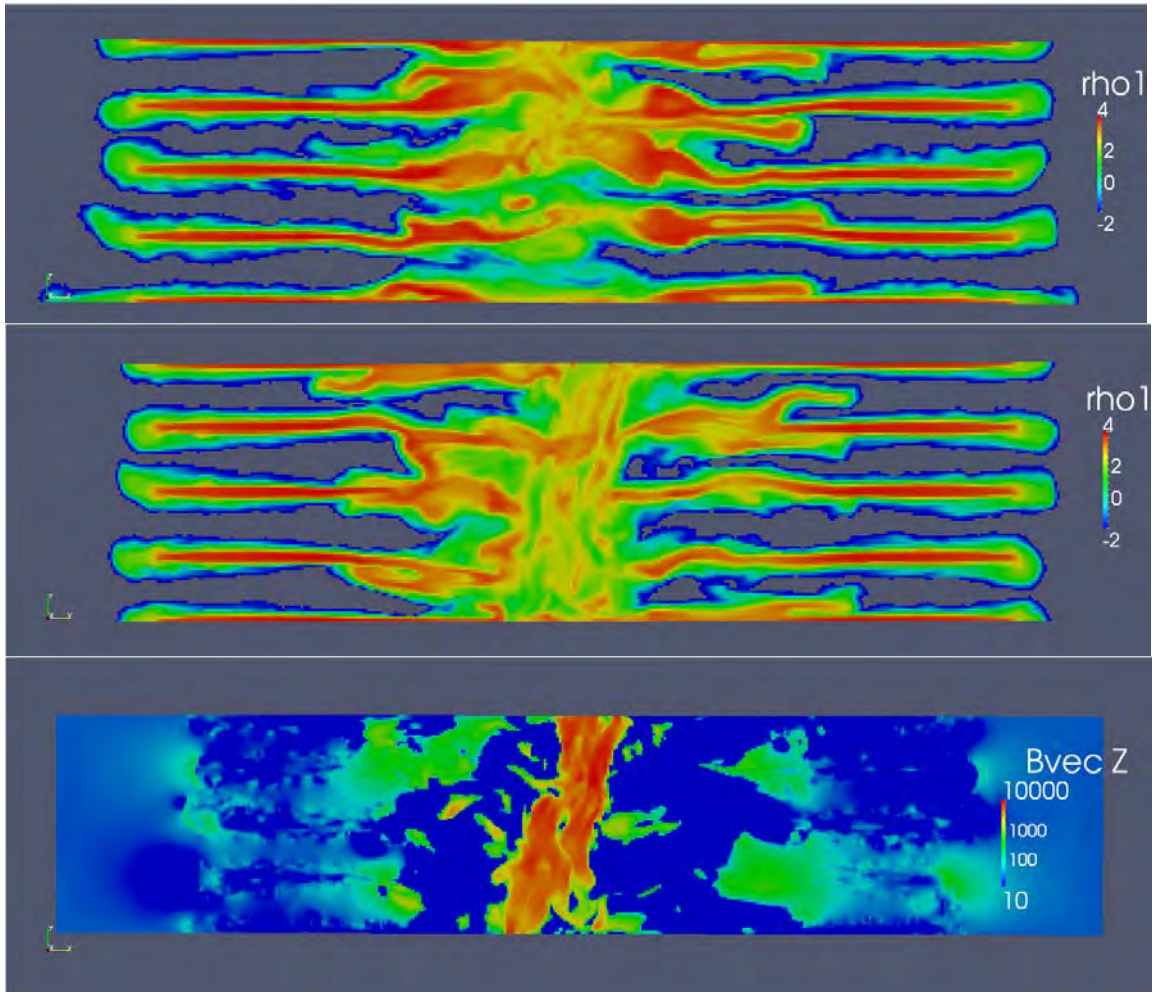

Provides a degree of stabilisation but only at stagnation

2nd generation MagLIF, Be liner, DT gas & ice , 69MA, B_z 11T

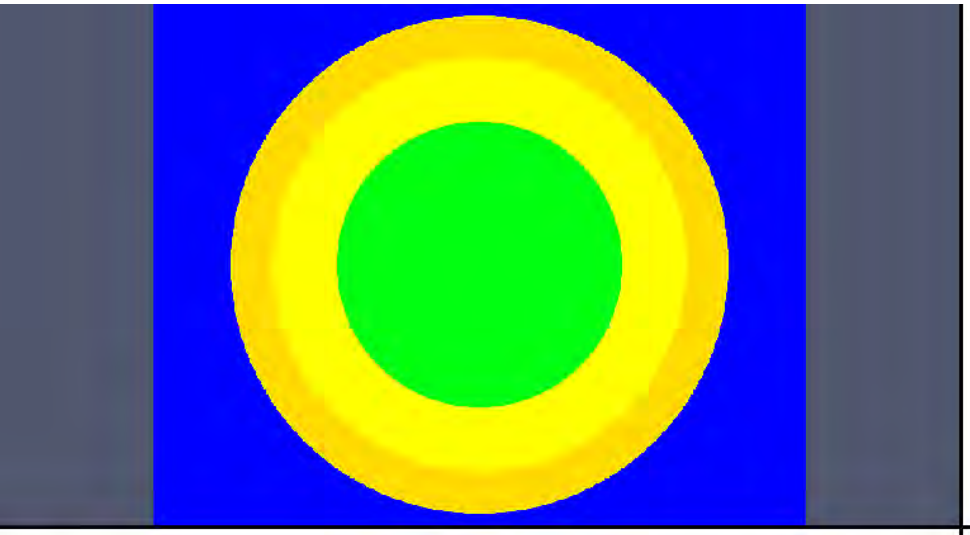

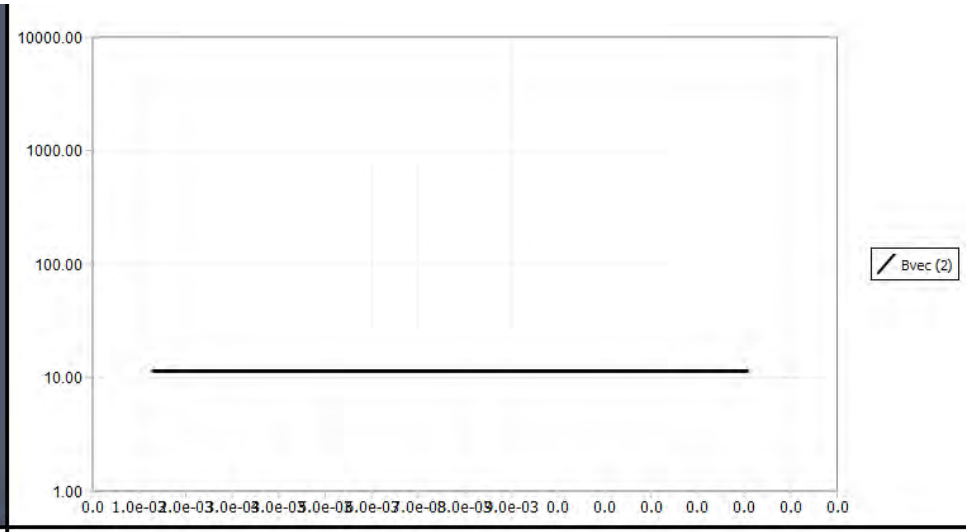

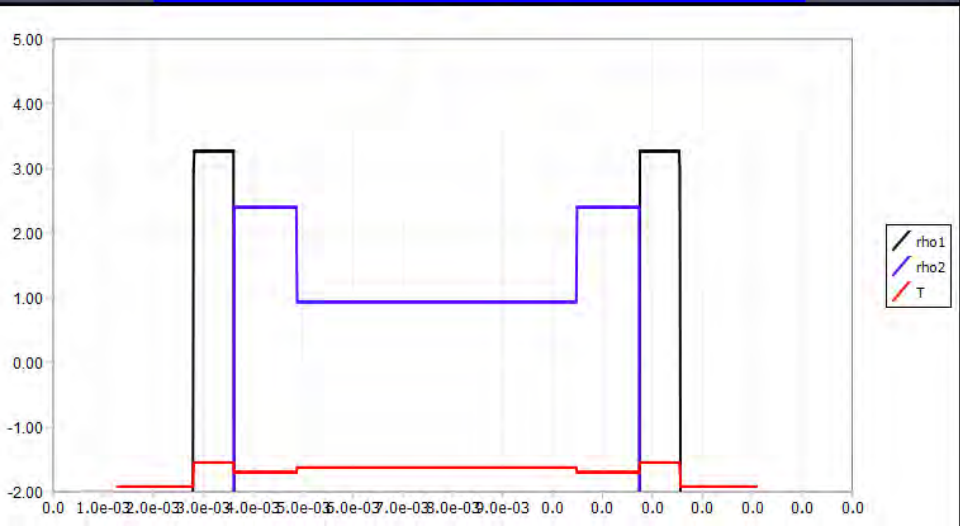

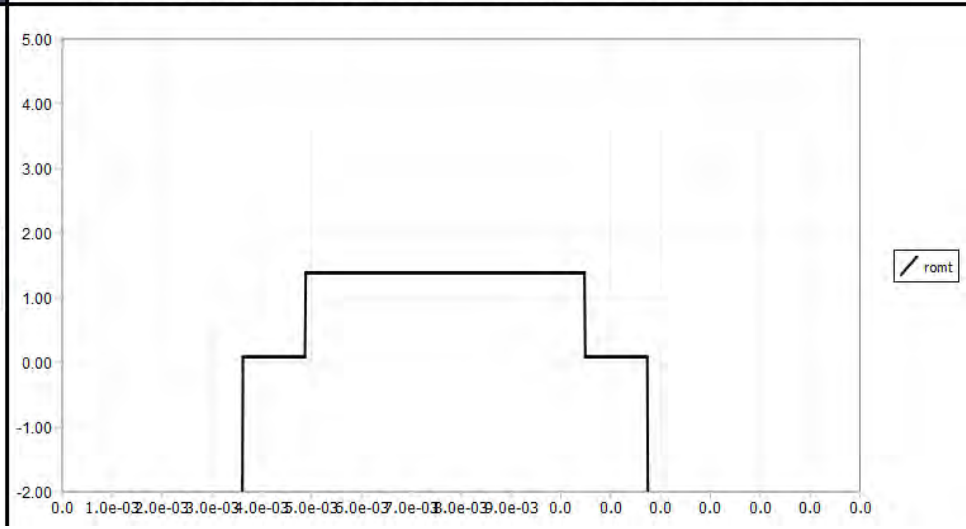

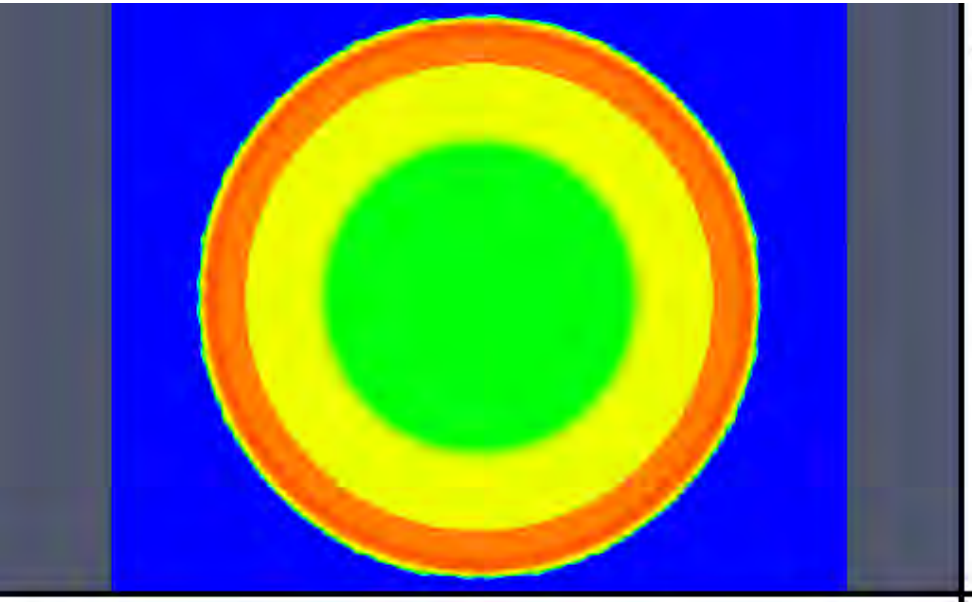

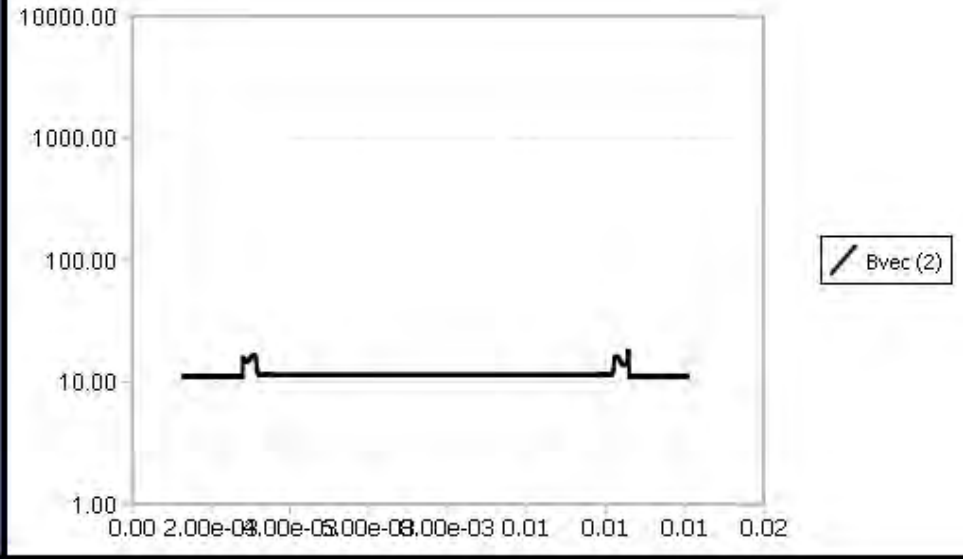
10000.00
1000.00
100.00
10.00
1.00
0.00 2.00e-03 4.00e-03 6.00e-03 8.00e-03 0.01 0.01 0.01 0.02
Bvec (2)

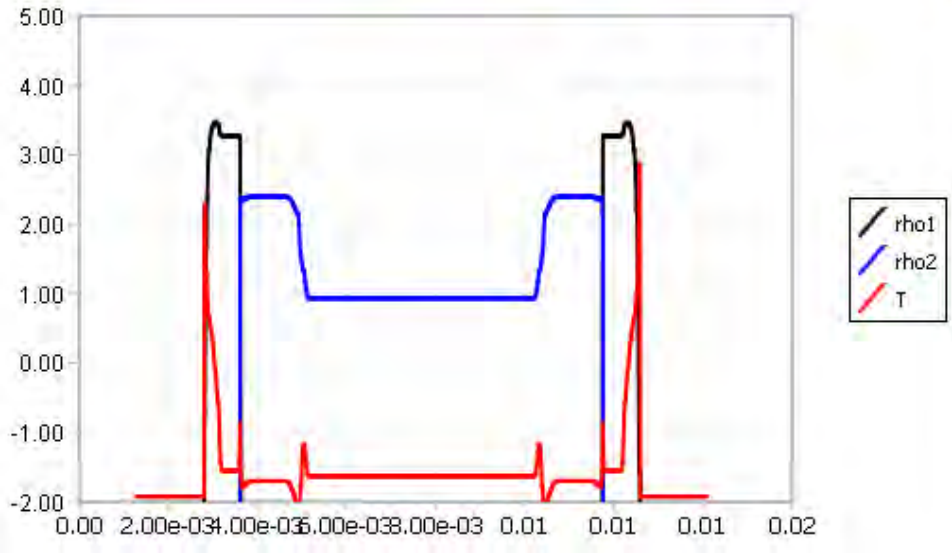
5.00
4.00
3.00
2.00
1.00
0.00
-1.00
-2.00
0.00 2.00e-03 4.00e-03 6.00e-03 8.00e-03 0.01 0.01 0.01 0.02
rho1
rho2
T

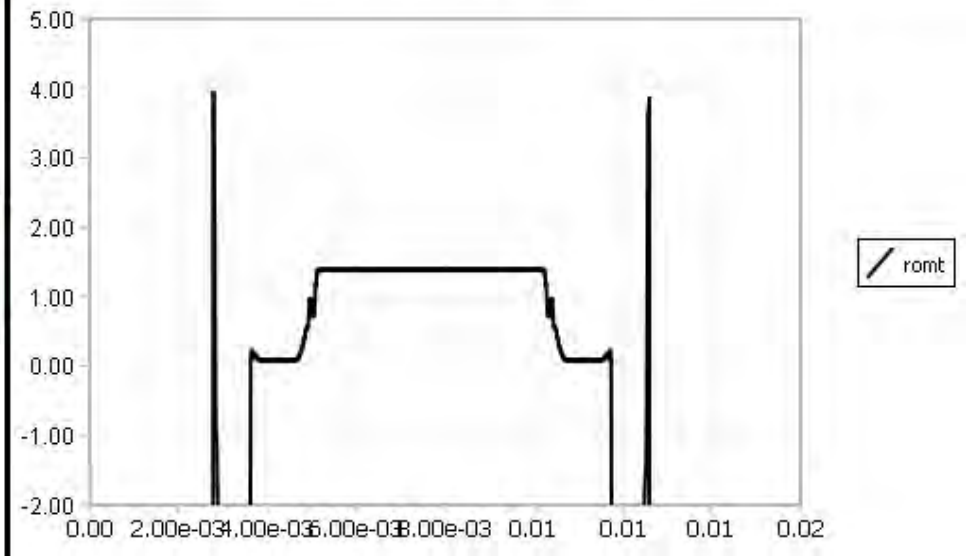
5.00
4.00
3.00
2.00
1.00
0.00
-1.00
-2.00
0.00 2.00e-03 4.00e-03 6.00e-03 8.00e-03 0.01 0.01 0.01 0.02
romt

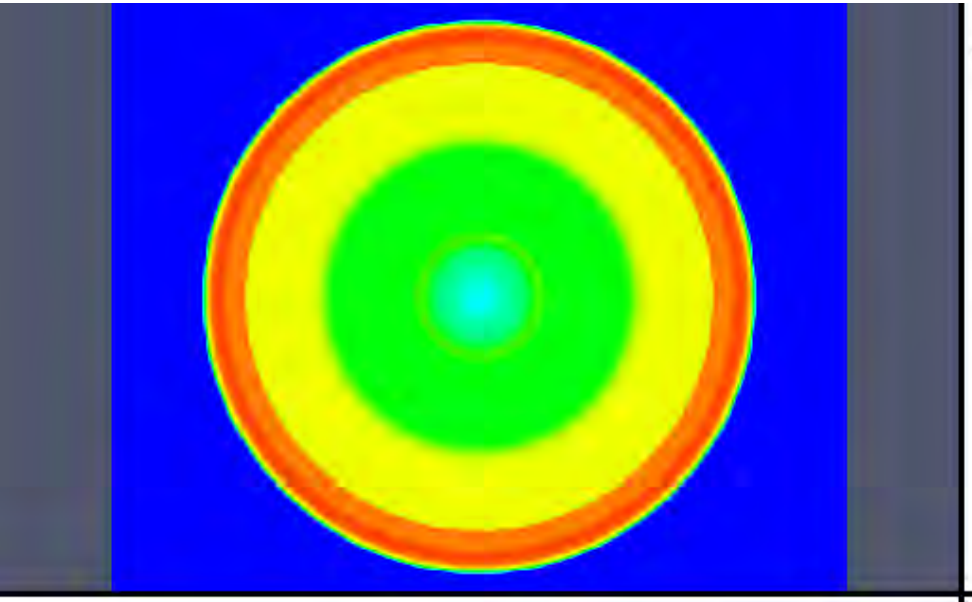

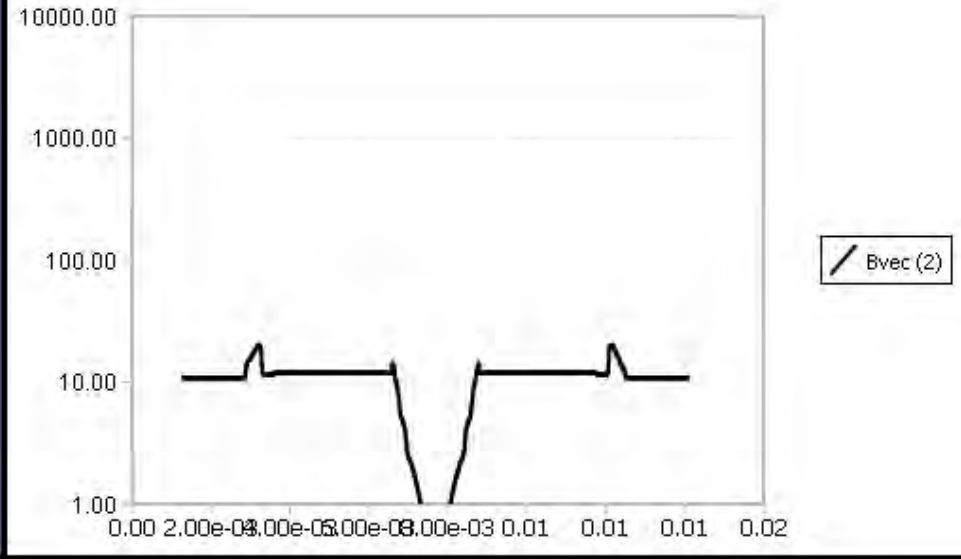
10000.00
1000.00
100.00
10.00
1.00
0.00 2.00e-03 4.00e-03 6.00e-03 8.00e-03 0.01 0.01 0.01 0.02
Bvec (2)

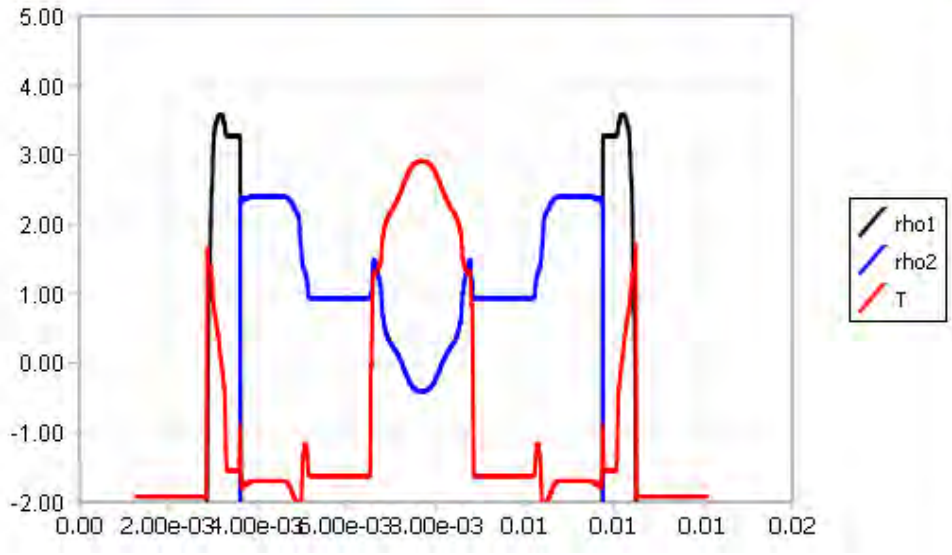
5.00
4.00
3.00
2.00
1.00
0.00
-1.00
-2.00
0.00 2.00e-03 4.00e-03 6.00e-03 8.00e-03 0.01 0.01 0.01 0.02
rho1
rho2
T

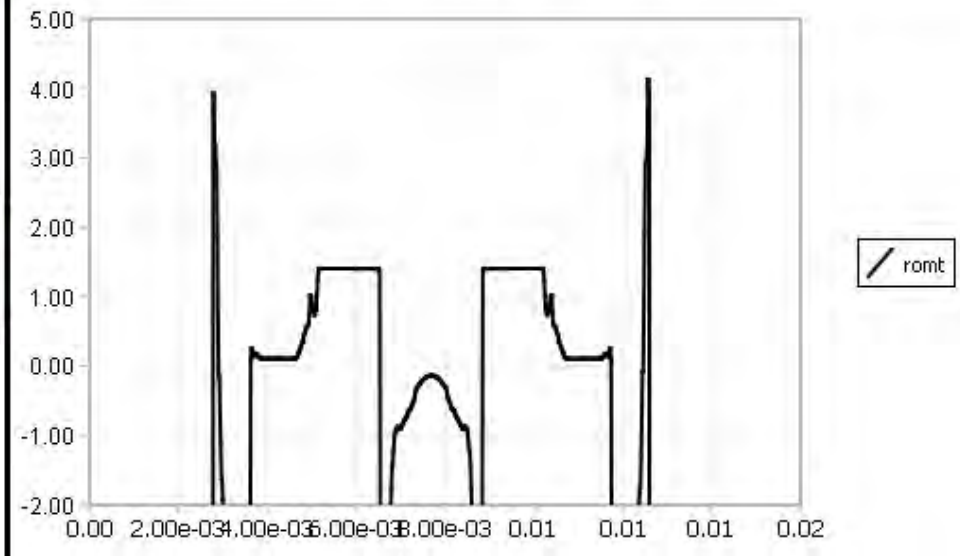
5.00
4.00
3.00
2.00
1.00
0.00
-1.00
-2.00
0.00 2.00e-03 4.00e-03 6.00e-03 8.00e-03 0.01 0.01 0.01 0.02
romt

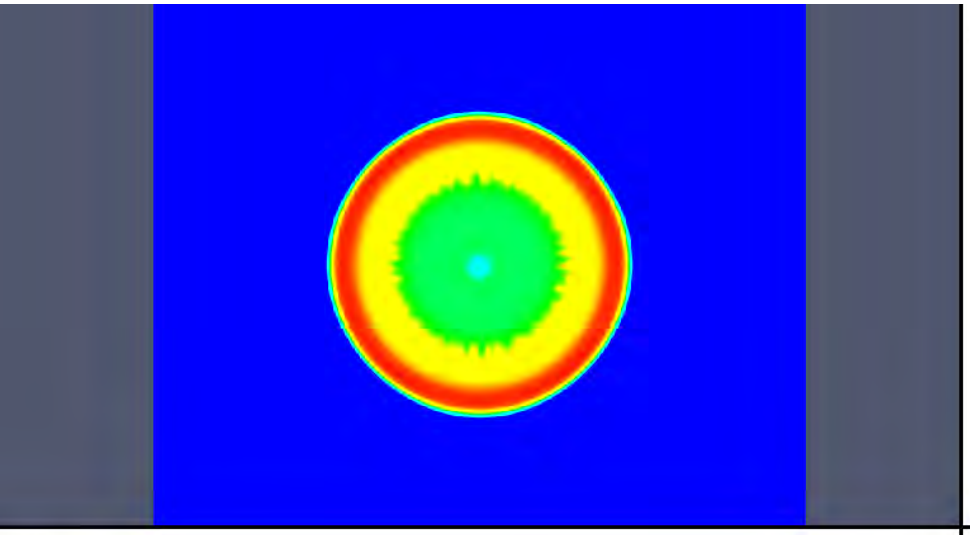

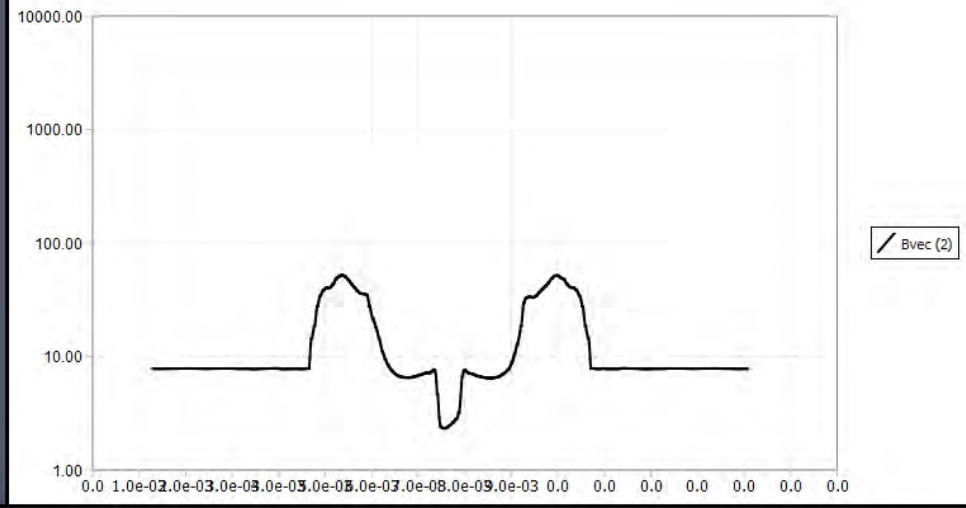
10000.00
1000.00
100.00
10.00
1.00
0.0 1.0e-03 2.0e-03 3.0e-03 4.0e-03 5.0e-03 6.0e-03 7.0e-03 8.0e-03 9.0e-03 0.0 0.0 0.0 0.0 0.0 0.0 0.0
Bvec (2)

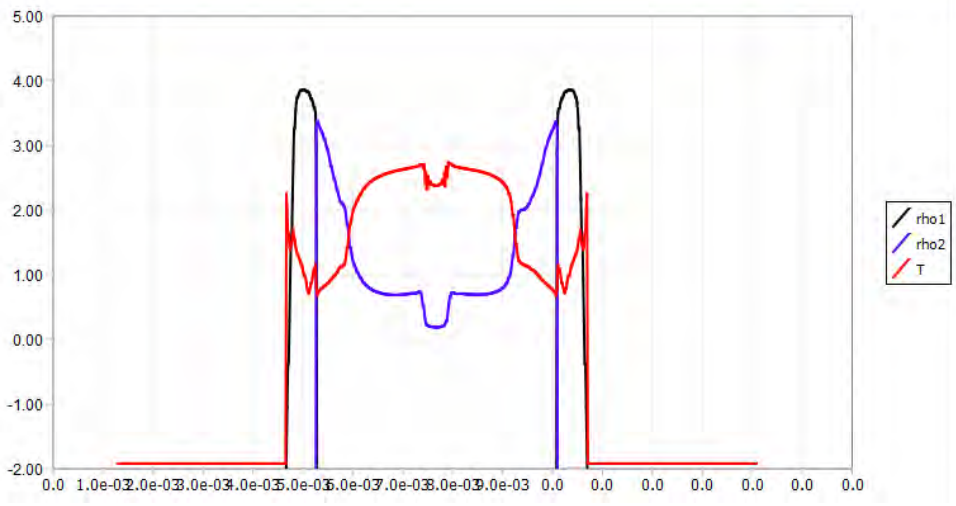
5.00
4.00
3.00
2.00
1.00
0.00
-1.00
-2.00
0.0 1.0e-03 2.0e-03 3.0e-03 4.0e-03 5.0e-03 6.0e-03 7.0e-03 8.0e-03 9.0e-03 0.0 0.0 0.0 0.0 0.0 0.0 0.0
rho1
rho2
T

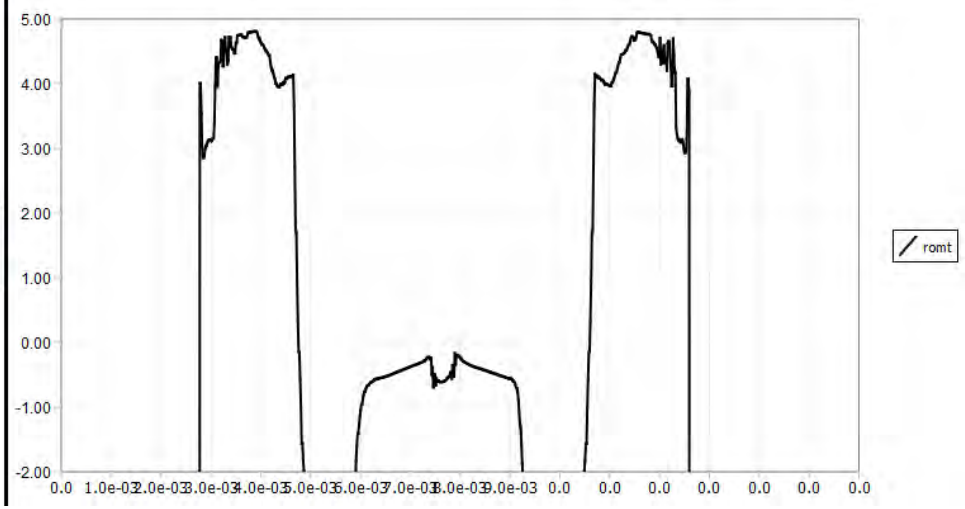
5.00
4.00
3.00
2.00
1.00
0.00
-1.00
-2.00
0.0 1.0e-03 2.0e-03 3.0e-03 4.0e-03 5.0e-03 6.0e-03 7.0e-03 8.0e-03 9.0e-03 0.0 0.0 0.0 0.0 0.0 0.0 0.0
romt

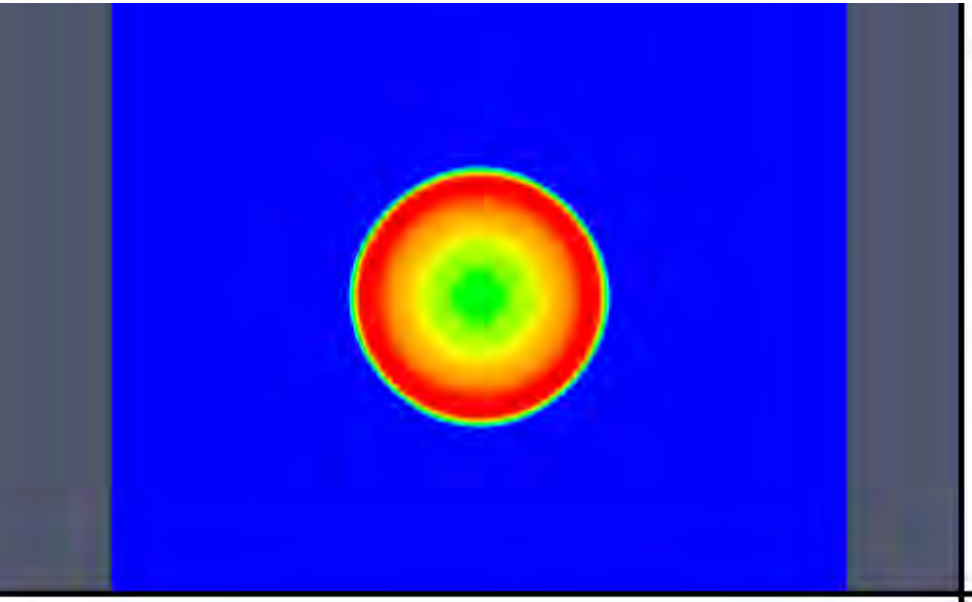

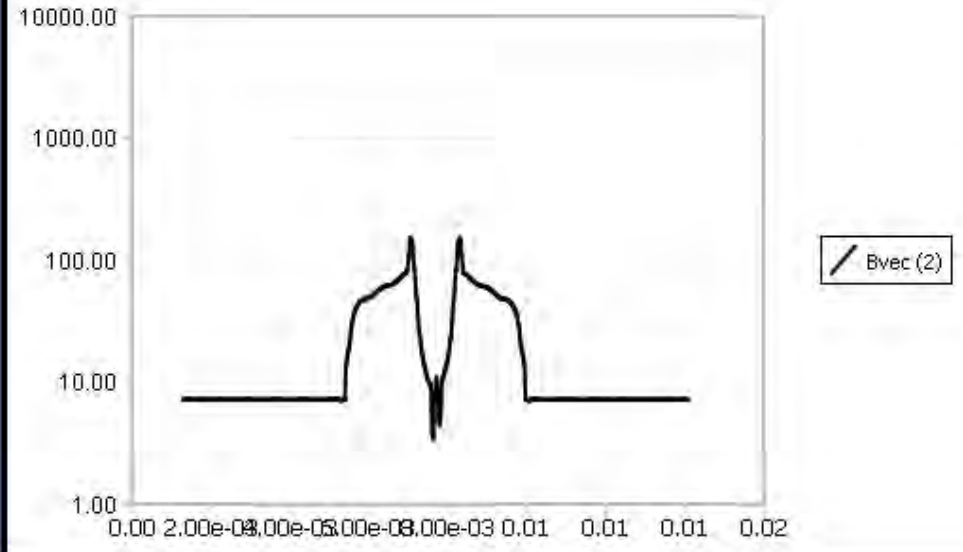
10000.00
1000.00
100.00
10.00
1.00
0.00 2.00e-03 4.00e-03 6.00e-03 8.00e-03 0.01 0.01 0.01 0.02
Bvec (2)

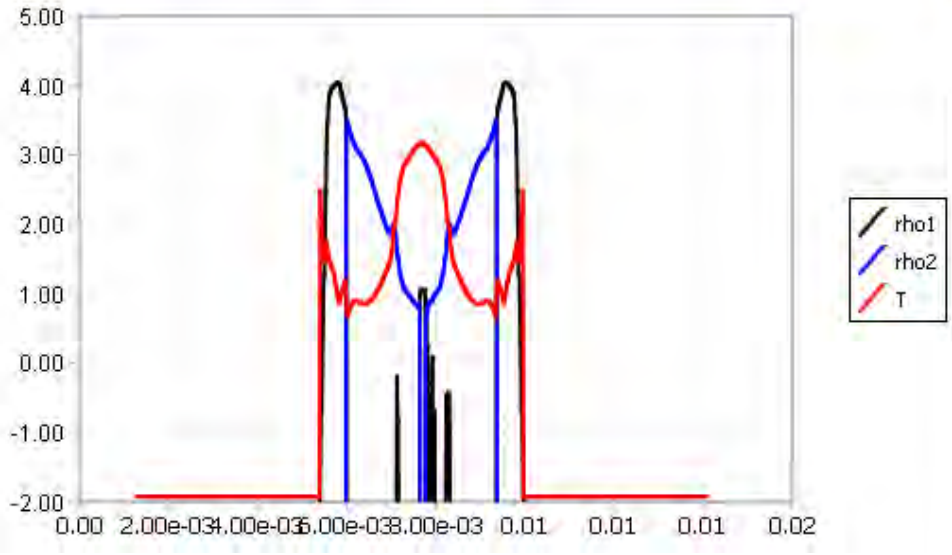
5.00
4.00
3.00
2.00
1.00
0.00
-1.00
-2.00
0.00 2.00e-03 4.00e-03 6.00e-03 8.00e-03 0.01 0.01 0.01 0.02
rho1
rho2
T

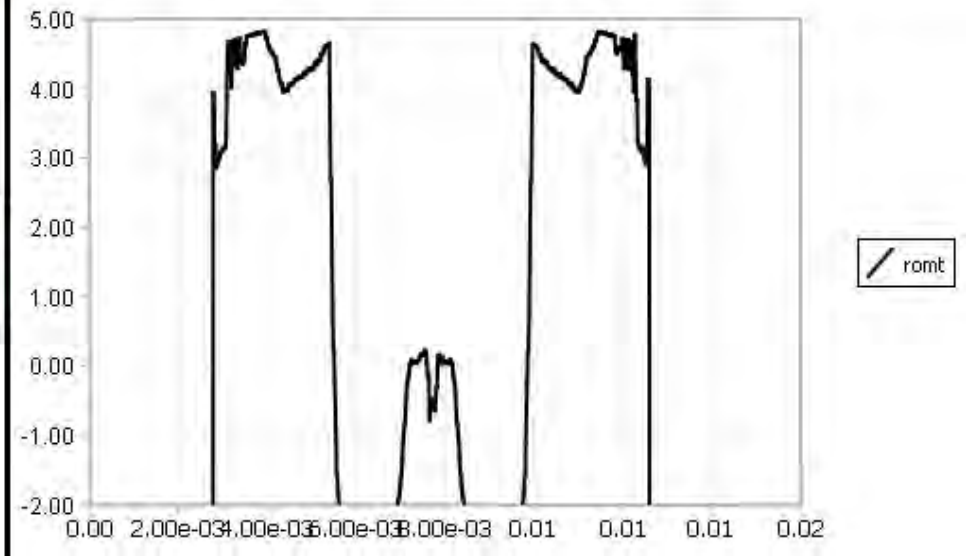
5.00
4.00
3.00
2.00
1.00
0.00
-1.00
-2.00
0.00 2.00e-03 4.00e-03 6.00e-03 8.00e-03 0.01 0.01 0.01 0.02
romt

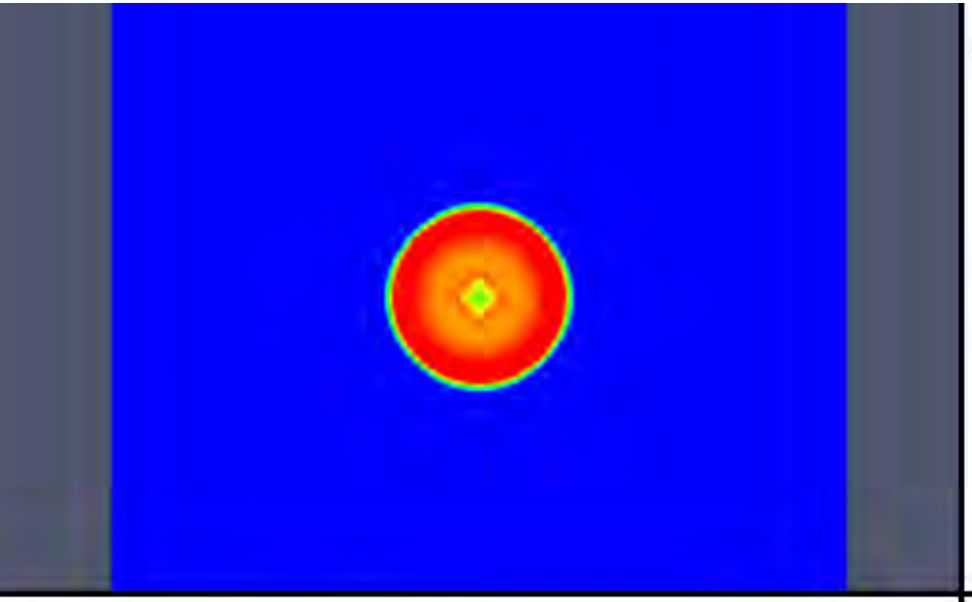

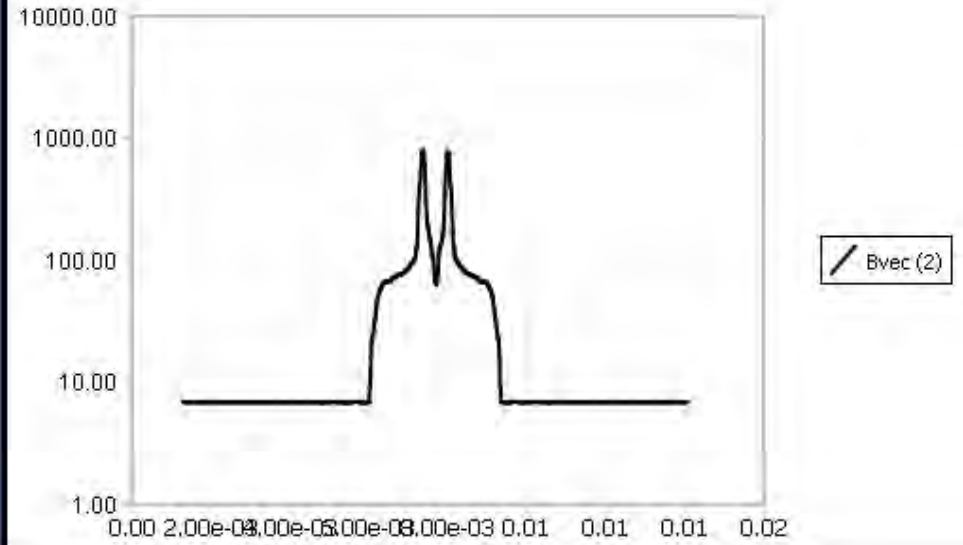
10000.00
1000.00
100.00
10.00
1.00
0.00
2.00e-03
4.00e-03
6.00e-03
8.00e-03
0.01
0.01
0.01
0.02
Bvec (2)

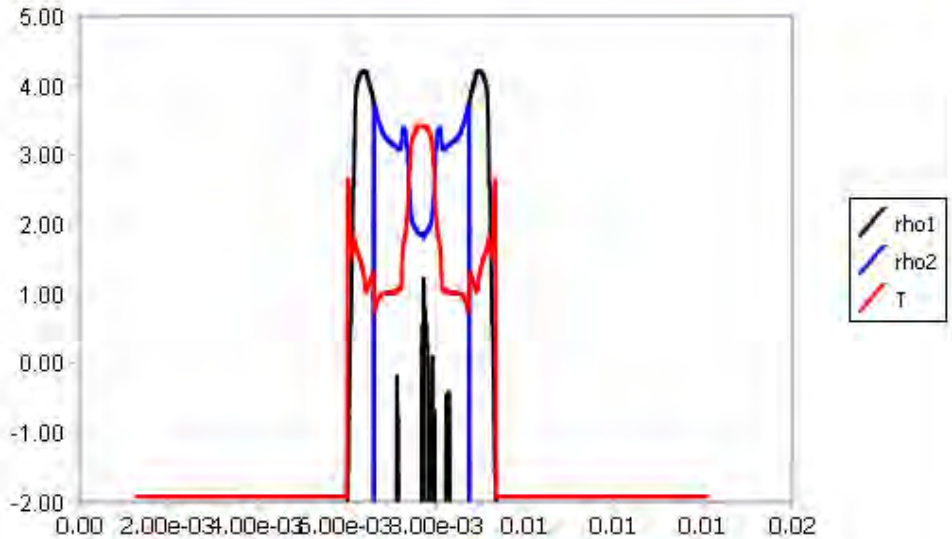
5.00
4.00
3.00
2.00
1.00
0.00
-1.00
-2.00
0.00
2.00e-03
4.00e-03
6.00e-03
8.00e-03
0.01
0.01
0.01
0.02
rho1
rho2
T

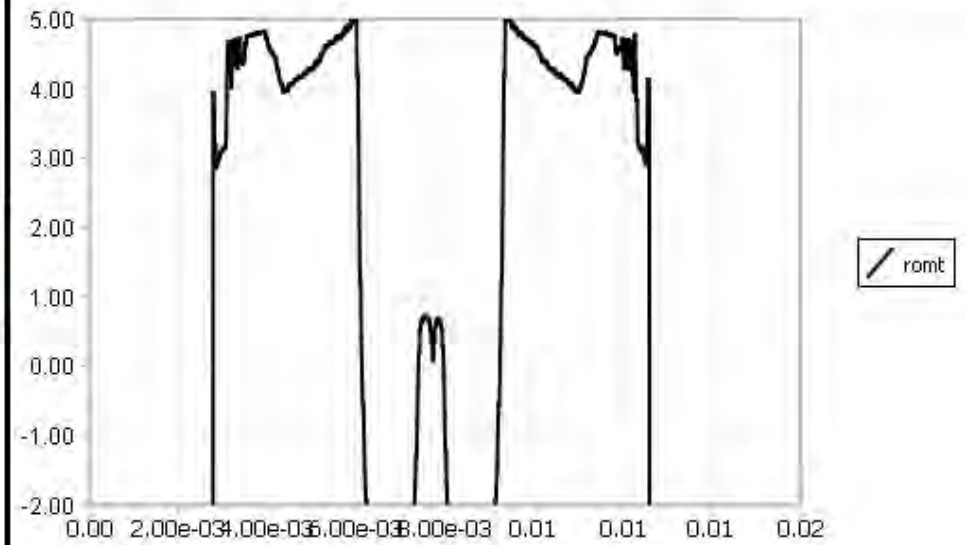
5.00
4.00
3.00
2.00
1.00
0.00
-1.00
-2.00
0.00
2.00e-03
4.00e-03
6.00e-03
8.00e-03
0.01
0.01
0.01
0.02
romt

Alpha particle trajectories in igniting Bennett pinches

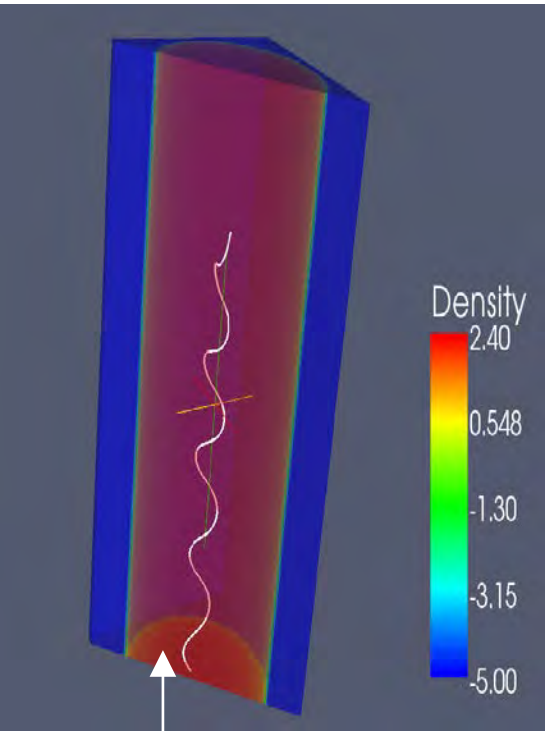

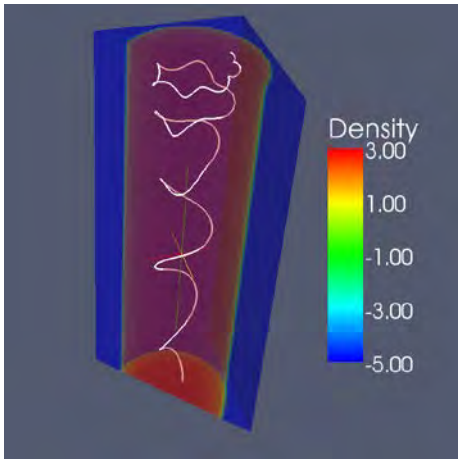

B field profile in a Z-pinch allows significant nonlocal alpha transport

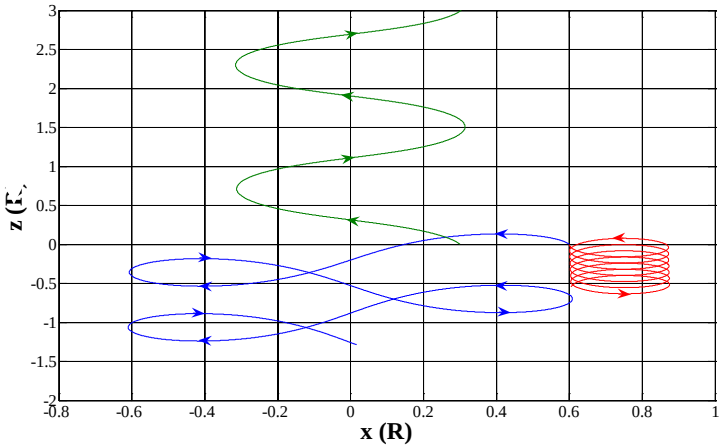

Alpha particles have both off-axis magnetised trajectories and singular orbits.

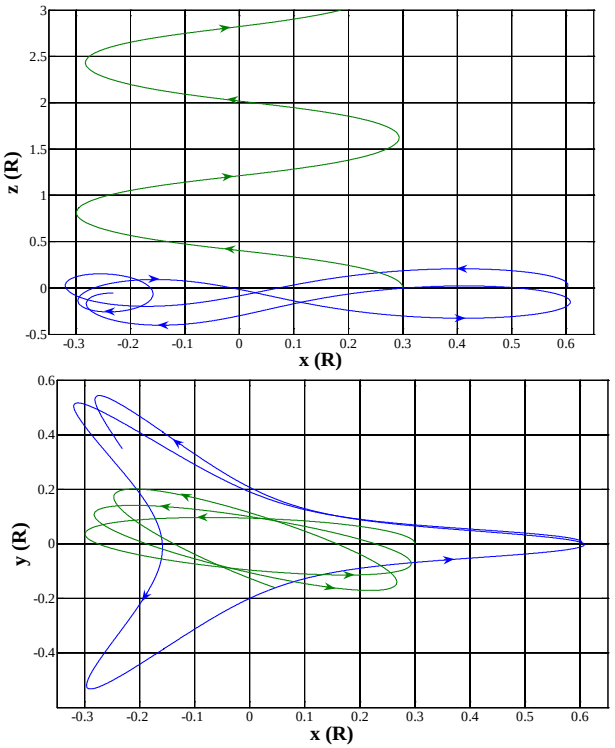

Particles produced near axis can undergo large axial displacement due to singular orbits (axial fields can enhance this effect)

Large densities in high-gain MagLiF reduce the effects of nonlocal transport.

From MHD simulations fuel radius at stagnation ~ 0.5mm.

Mean free paths decrease with R, B fields less important for confinement.

Dense DT edge prevents alpha particles from penetrating liner.

Yield for kinetic model and local heating model are similar (~2 MJ/cm).

mfp ~ 200μm

mfp ~ 100μm

mfp ~ 10μm

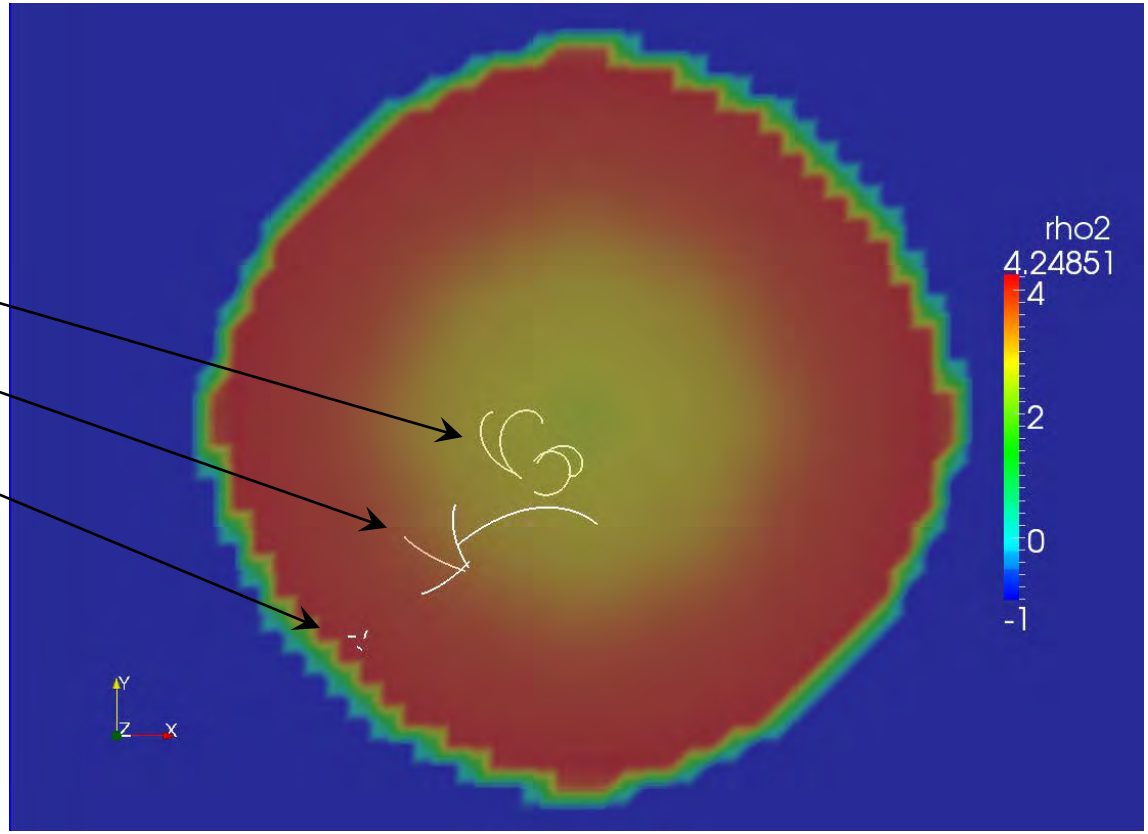

Goal: homogeneous isentropic compression of a uniform ideal gas	Kidder's spherical compression	Cylindrical compression
Lagrangian volume change	$d^3x = h^3[t]\, d^3x_0$	$d^2x = h^2[t]\, d^2x_0$
Mass conservation	$dm = \rho\, r^2 dr = \rho_0\, r_0{}^2\, dr_0$	$dm = \rho\, r\, dr = \rho_0\, r_0 dr_0$
Equation of motion	$\dot{u} = -\, r^2\, (dp/dm)$	$\dot{u} = -\, r\, (dp/dm)$
Ideal gas isentrope	$p(r_0,t) = c\, \rho^\gamma = p_0\, (r_0)/h^{3\gamma}$	$p(r_0,t) = p_0\, (r_0)/h^{2\gamma}$
Solve ODE	$h^{3\gamma-2}\ddot{h} = h^3\ \ddot{h} = c$	$h^{2\gamma-1}\ddot{h} = h^{7/3}\ \ddot{h} = c$
Result	$\boldsymbol{h_3 = \sqrt{1-(t/t_0)^2}}$	**Numerical solution gives:** $\boldsymbol{h_2 = h[\frac{t}{t_0}]}$
Boundary pressure	$\boldsymbol{P_3(t) = P(0)/(1-(t/t_0)^2)^{5/2}}$	$\boldsymbol{P_2(t) = P(0)\ /h^{2\gamma}}$

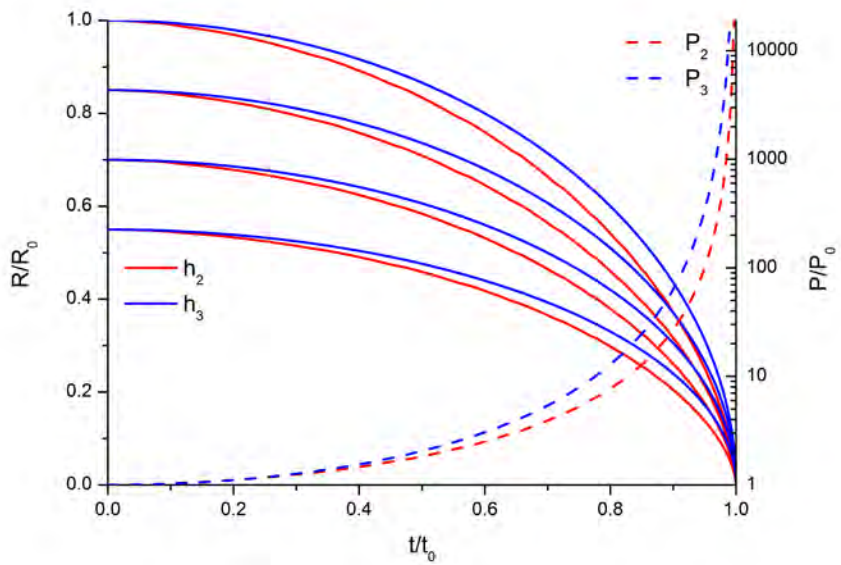

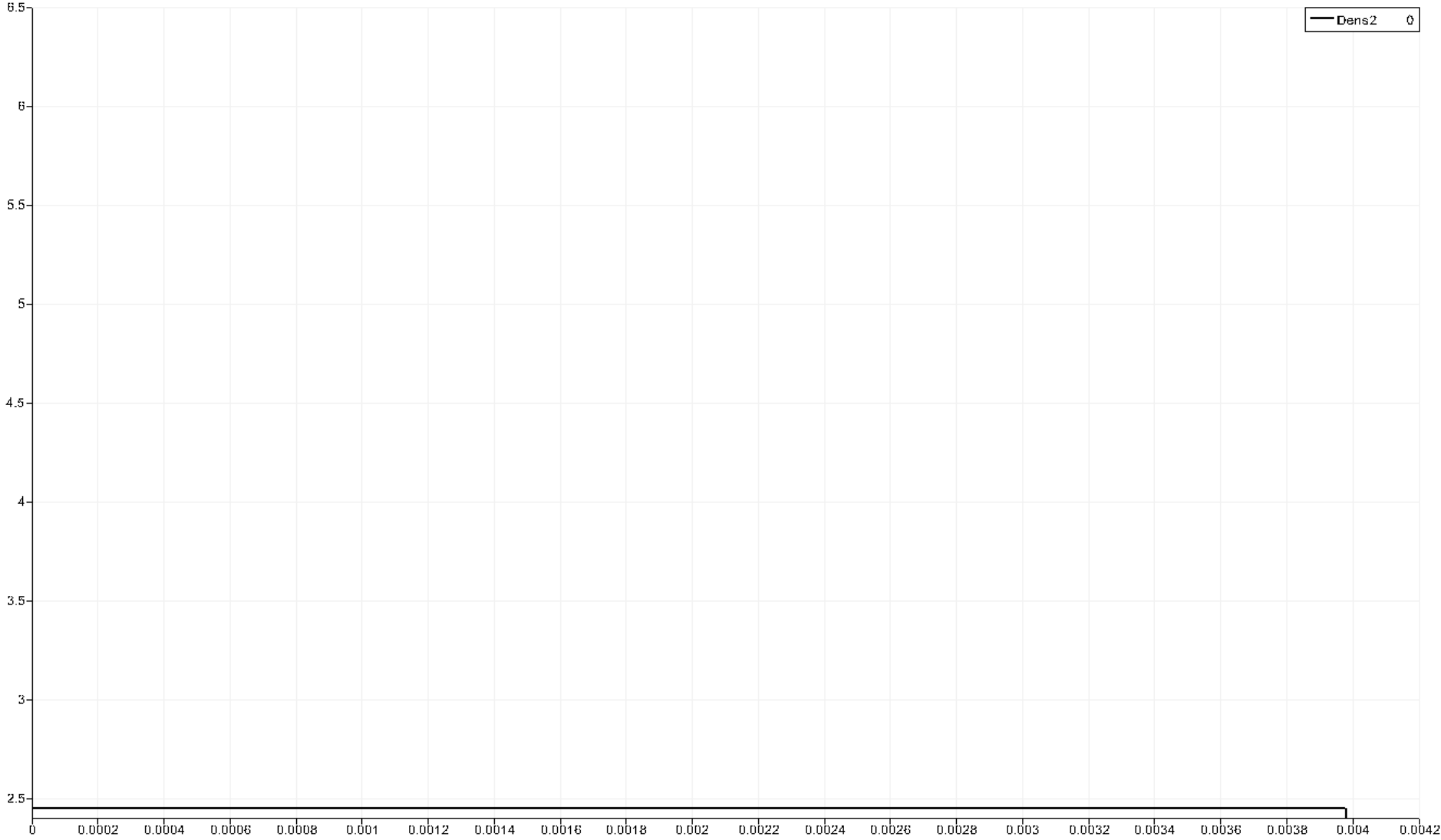
Dens2 0
6.5
6
5.5
5
4.5
4
3.5
3
2.5
0
0.0002
0.0004
0.0006
0.0008
0.001
0.0012
0.0014
0.0016
0.0018
0.002
0.0022
0.0024
0.0026
0.0028
0.003
0.0032
0.0034
0.0036
0.0038
0.004
0.0042

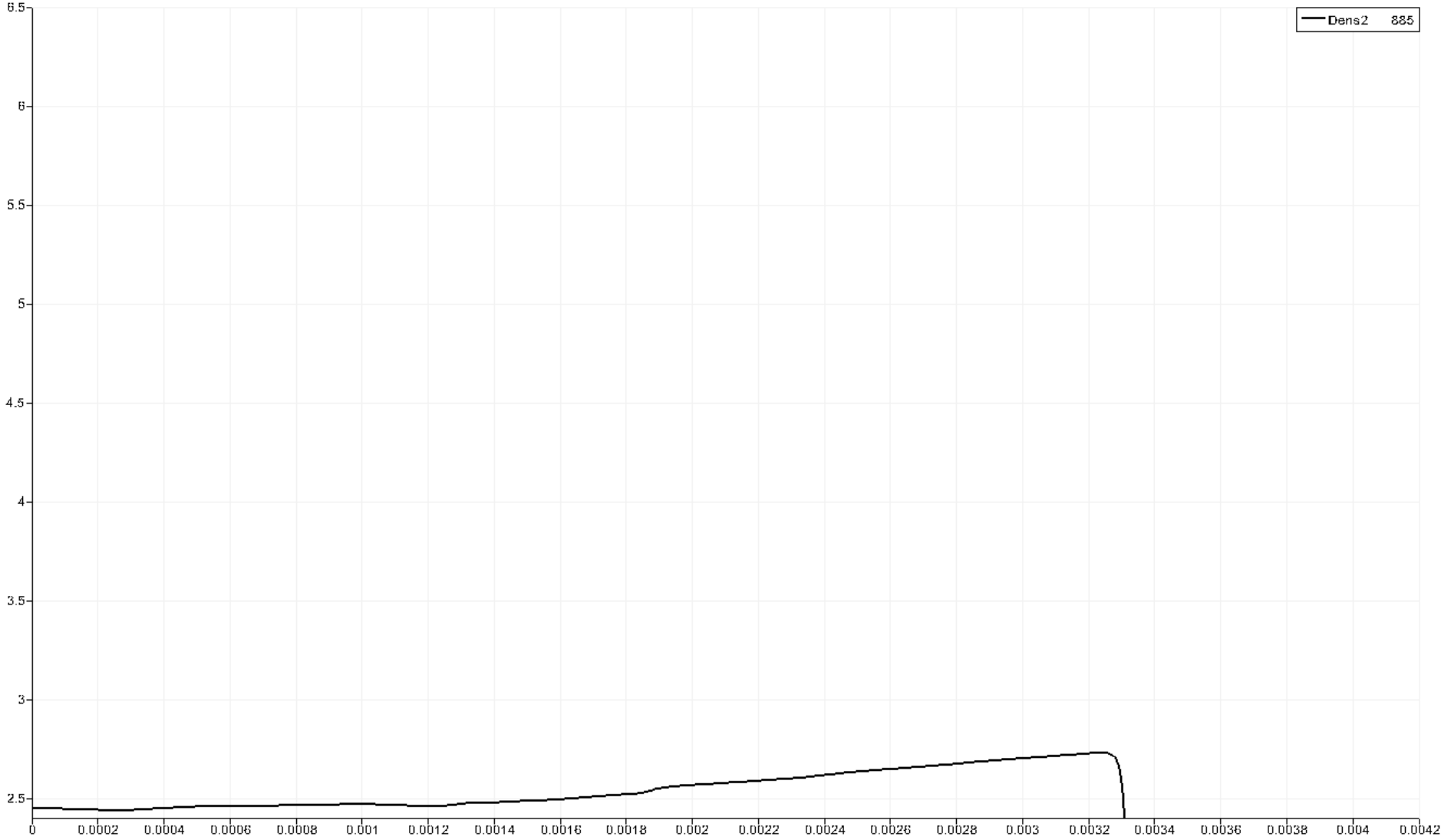
Dens2 885
6.5
6
5.5
5
4.5
4
3.5
3
2.5
0
0.0002
0.0004
0.0006
0.0008
0.001
0.0012
0.0014
0.0016
0.0018
0.002
0.0022
0.0024
0.0026
0.0028
0.003
0.0032
0.0034
0.0036
0.0038
0.004
0.0042

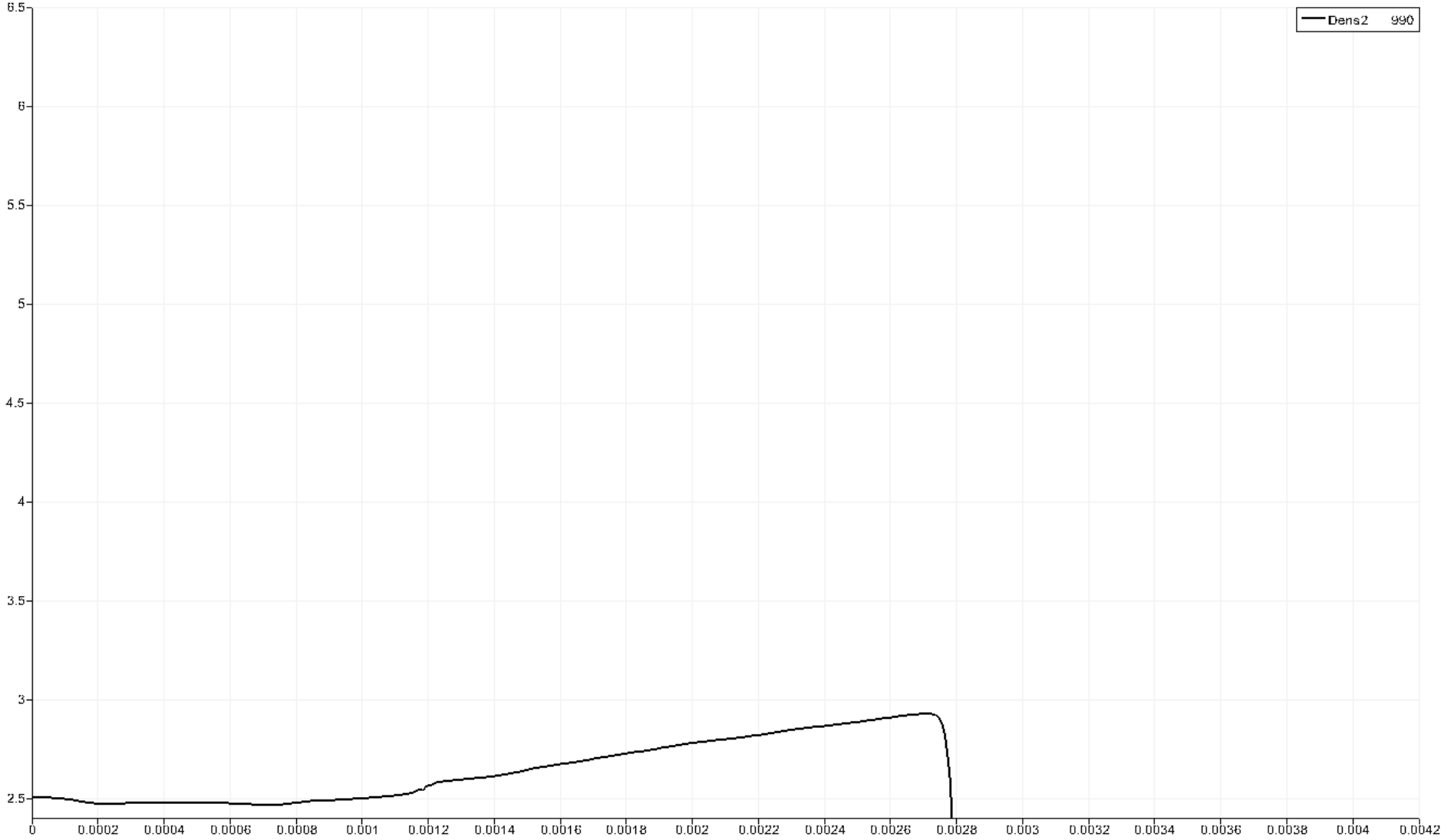
Dens2 990
6.5
6
5.5
5
4.5
4
3.5
3
2.5
0
0.0002
0.0004
0.0006
0.0008
0.001
0.0012
0.0014
0.0016
0.0018
0.002
0.0022
0.0024
0.0026
0.0028
0.003
0.0032
0.0034
0.0036
0.0038
0.004
0.0042

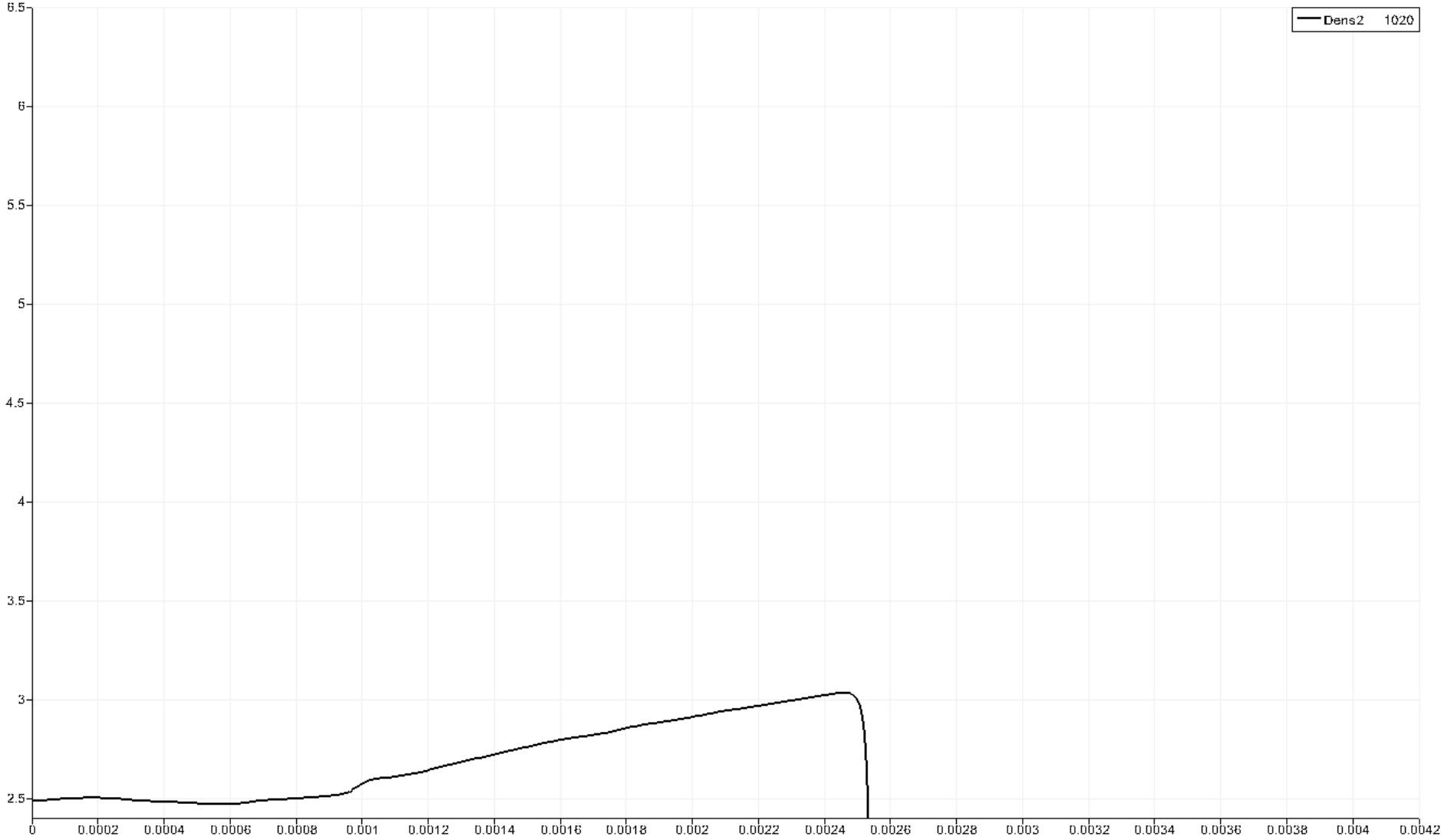
Dens2 1020
6.5
6
5.5
5
4.5
4
3.5
3
2.5
0
0.0002
0.0004
0.0006
0.0008
0.001
0.0012
0.0014
0.0016
0.0018
0.002
0.0022
0.0024
0.0026
0.0028
0.003
0.0032
0.0034
0.0036
0.0038
0.004
0.0042

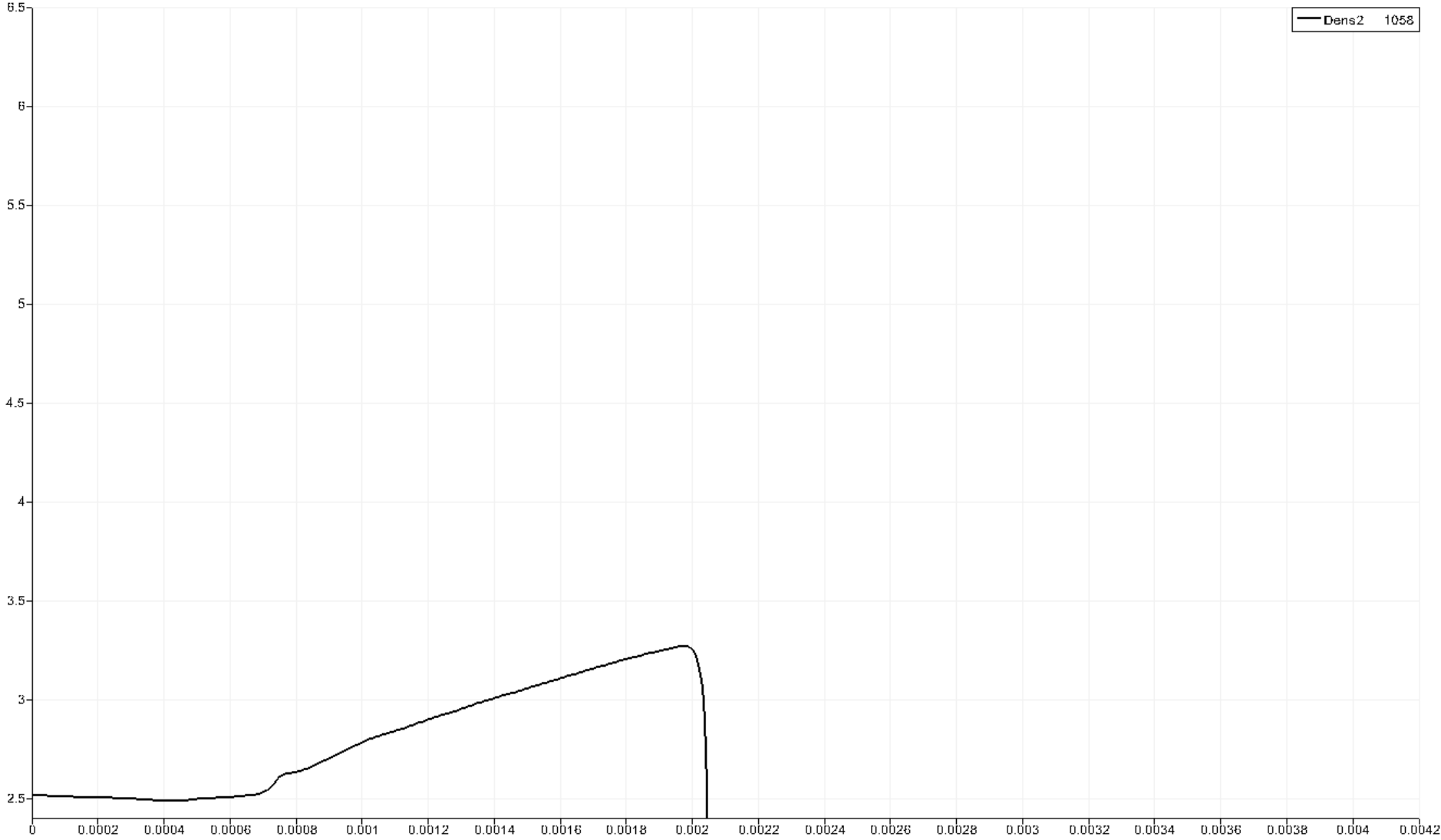
Dens2 1058
6.5
6
5.5
5
4.5
4
3.5
3
2.5
0
0.0002
0.0004
0.0006
0.0008
0.001
0.0012
0.0014
0.0016
0.0018
0.002
0.0022
0.0024
0.0026
0.0028
0.003
0.0032
0.0034
0.0036
0.0038
0.004
0.0042

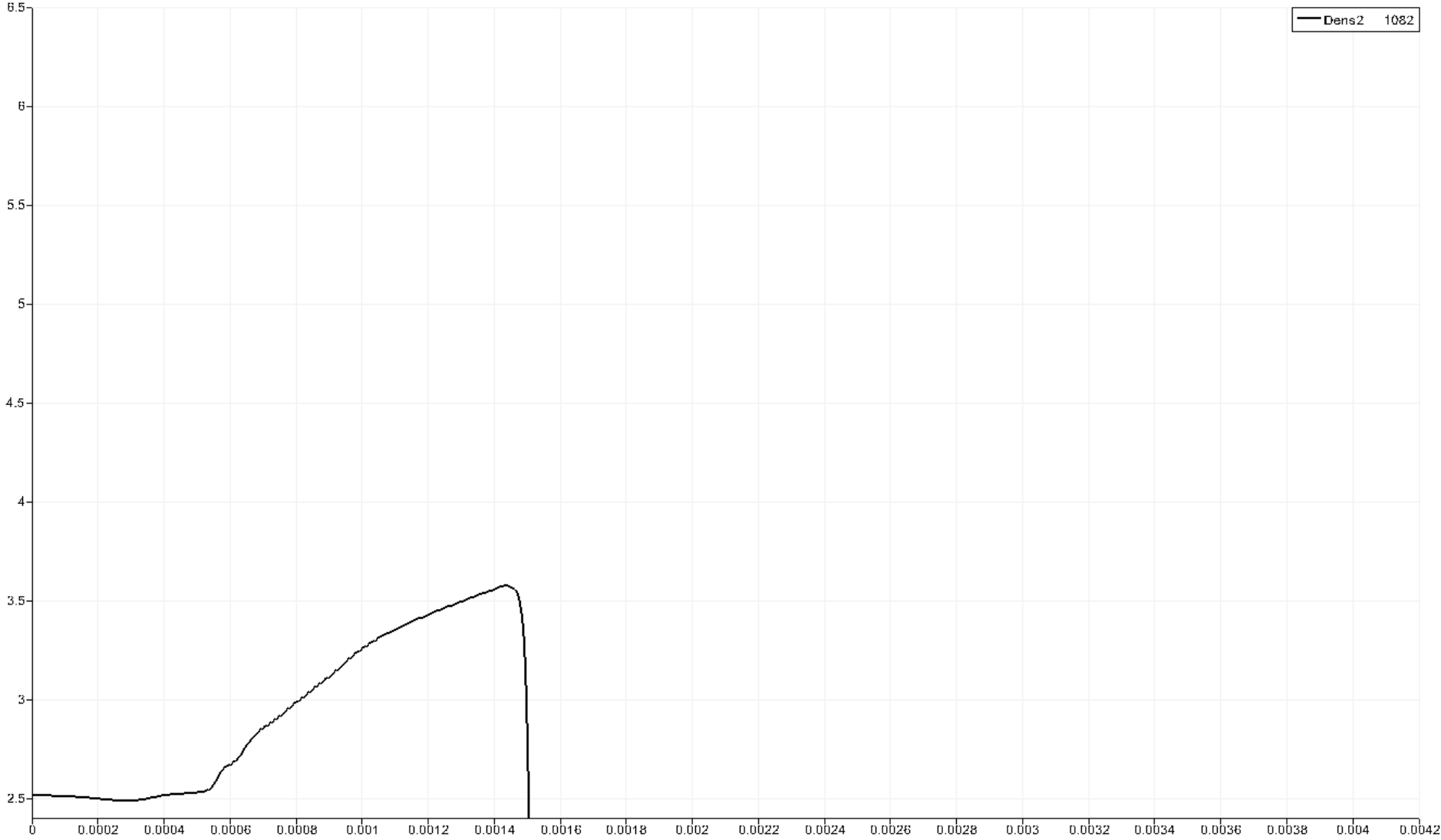
Dens2 1082
6.5
6
5.5
5
4.5
4
3.5
3
2.5
0
0.0002
0.0004
0.0006
0.0008
0.001
0.0012
0.0014
0.0016
0.0018
0.002
0.0022
0.0024
0.0026
0.0028
0.003
0.0032
0.0034
0.0036
0.0038
0.004
0.0042

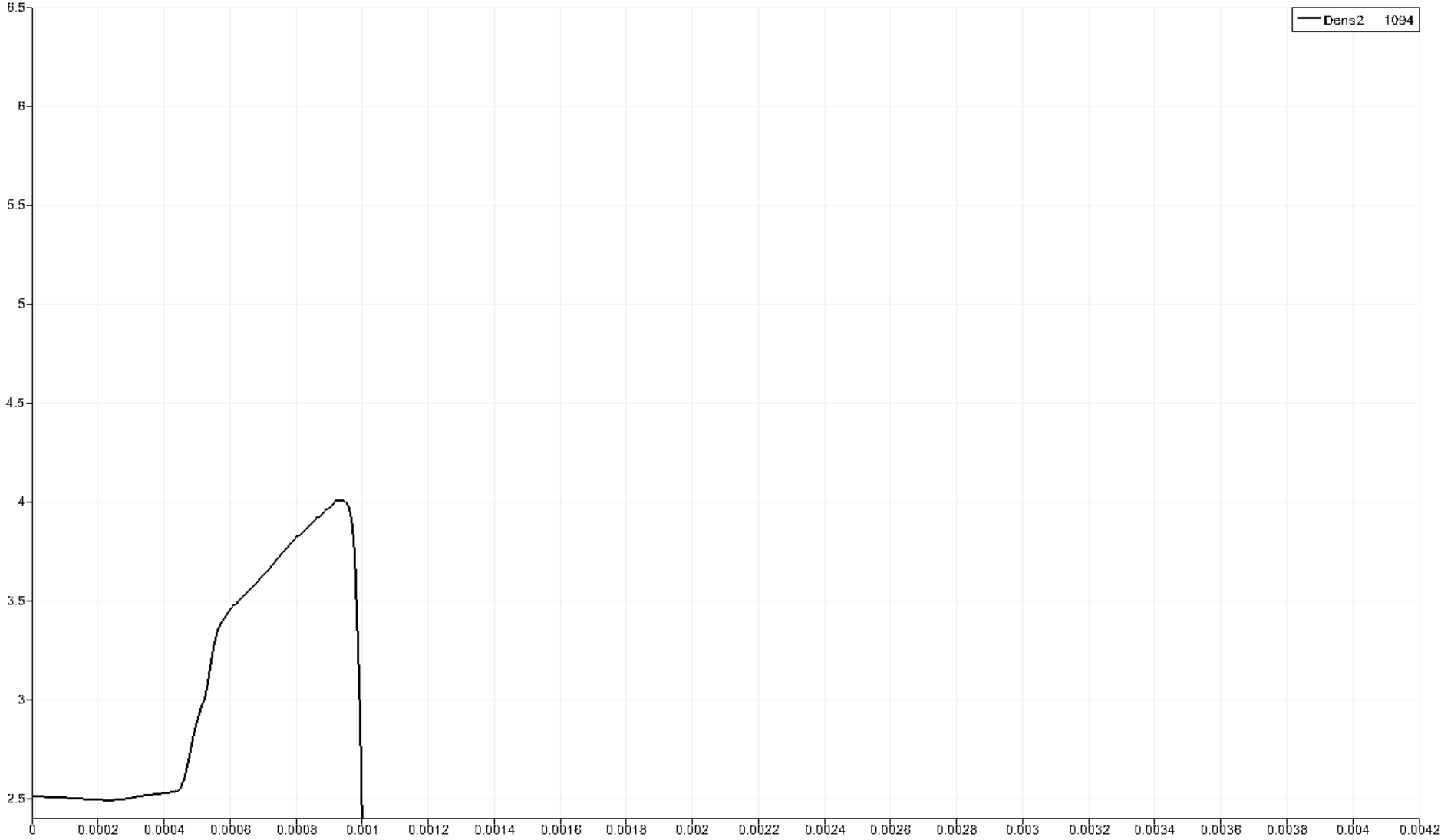
Dens2 1094
6.5
6
5.5
5
4.5
4
3.5
3
2.5
0
0.0002
0.0004
0.0006
0.0008
0.001
0.0012
0.0014
0.0016
0.0018
0.002
0.0022
0.0024
0.0026
0.0028
0.003
0.0032
0.0034
0.0036
0.0038
0.004
0.0042

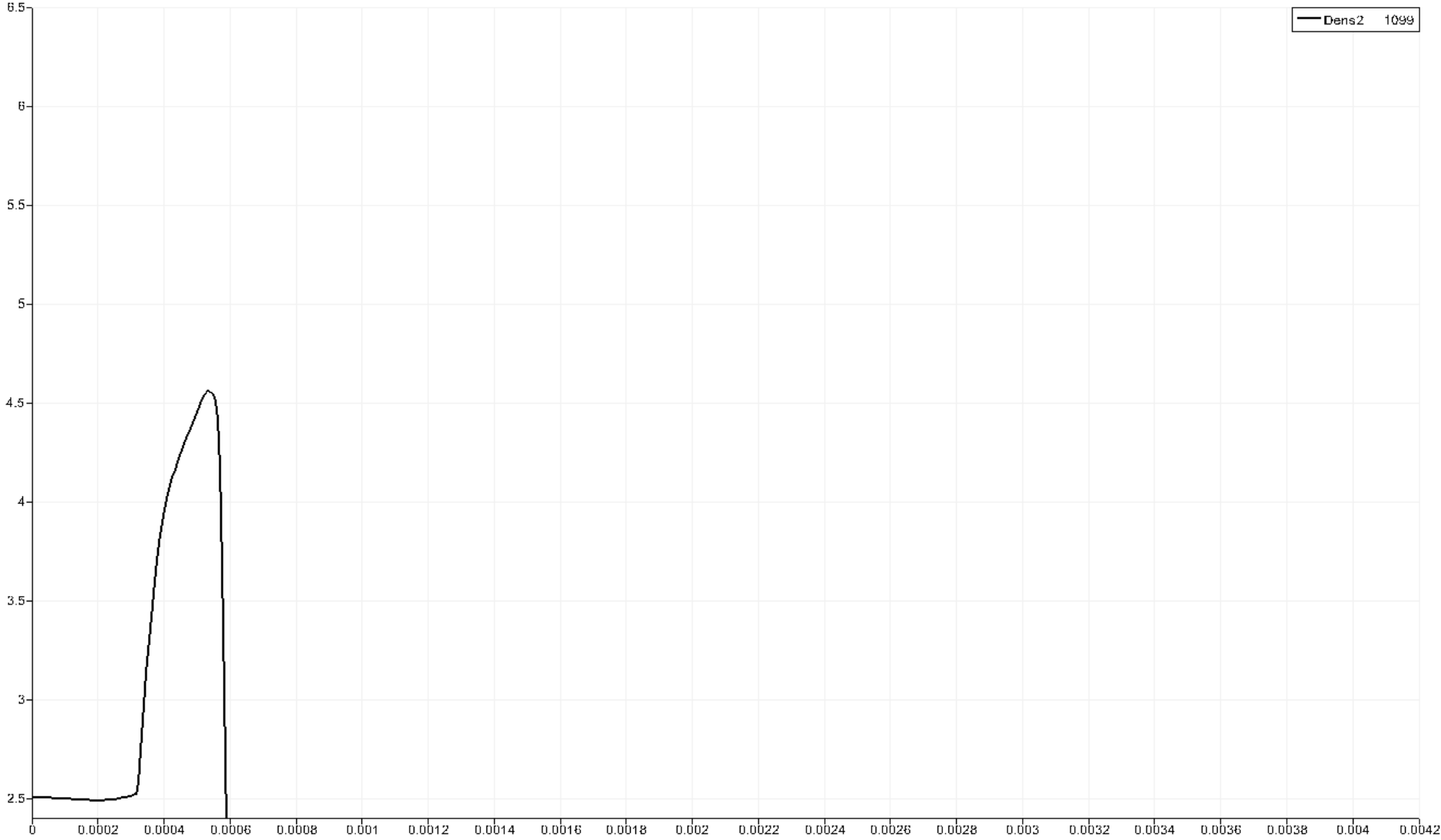
Dens2 1099
6.5
6
5.5
5
4.5
4
3.5
3
2.5
0
0.0002
0.0004
0.0006
0.0008
0.001
0.0012
0.0014
0.0016
0.0018
0.002
0.0022
0.0024
0.0026
0.0028
0.003
0.0032
0.0034
0.0036
0.0038
0.004
0.0042

Application to pulsed power machines

The solution of the cylindrical isentropic compression gives the trajectory of the boundary r_b and the boundary pressure profile P_b	$r_b = r_0\ h[t/t_0]$	$P_b(t) = P(0)\ /h^{2\gamma}$
We obtain the current profile, which could be supplied by a pulsed power machine, from the outer radius and the boundary pressure of the fluid	$I = \pi\ r_b\sqrt{8P_b/\mu_0}$	$I = \pi\ r_0\sqrt{8P_0/\mu_0}\ h^{1-\gamma} = I_0\ /\ h^{\gamma-1}$
• Note that I_0 *is the current, which holds the fluid initially at rest.* • $1\ /\ h^2$ is the compression ratio c_R, at h=0.1 corresponds to ρ/ρ_0 = 100		
We obtain the initial current for a given maximum current I_m and desired compression ratio. The higher the final compression the lower the initial current is. If we want to achieve higher compression, we have to start from a lower entropy state.	$I_0 = I_m\ /\ c_R^{(\gamma-1)/2} = I_m\ /\ c_R^{1/3}$	c_R=400 $h = 0.05$ I_m= 25 MA $\rightarrow I_0 \approx$ 3.4 MA
Starting from lower initial currents seems favorable. However, the maximum $\frac{dI}{dt}$ is limited. Note that h=$h\left[\frac{t}{t_0}\right]$. Therefore, we obtain:	$\frac{dI}{dt} = \frac{(1-\gamma)\ h'\ I_0}{t_0\ h^{\gamma}} \approx \frac{940\ \ I_0}{t_0}$	$\frac{dI}{dt}$= 0.5 MA/ns $\rightarrow t_0 \approx$ 6400 ns $\frac{dI}{dt}$= 2 MA/ns $\rightarrow t_0 \approx 1600$ ns
The first disturbance, which travels through the initially uniform fluid, reaches the center at t=r_0/c_s Where c_s is the speed of sound at t=0, and r_0 is the initial radius of the fluid.	We require all waves to catch up with the first one. Therefore the initial radius of initial radius of the fluid is: $r_0 = c_s\ t_0$	For c_s = 2500 m/s and $t_0 = 1600$ *ns* *we obtain an initial radius of 4mm*

Generalization of Kidder's solution to an arbitrary EOS	Ideal gas	General EOS
Fluid density as a function of time	$\rho = \rho_0/h^2$	$\rho = \rho_0/h^2$
Isentrope	$p(r_0,t) = c\,\rho^\gamma = p_0\,(r_0)/h^{2\gamma}$	$p(r_0,t) = p(\rho)=p(\rho_0/h^2)$
Equation of motion	$\dot{u} = r_0\ddot{h} = -\frac{h}{\rho_0}\frac{dp}{dr_0}$	$\dot{u} = r_0\ddot{h} = -\frac{h}{\rho_0}\frac{dp}{dr_0}$
ODE	$\ddot{h}/h = -\frac{1}{r_0\rho_0}\frac{dp_0}{dr_0}/h^{2\gamma} = -c/h^{2\gamma}$	$\ddot{h}/h = -\frac{1}{r_0\rho_0}\frac{d\,p(\rho_0/h^2)}{dr_0}$
Solve ODE	$h^{2\gamma-1}\ddot{h} = h^{7/3}\,\ddot{h} = c$	$\ddot{h}/h = -c\;p(\rho_0/h^2)$

- We repeat the analysis of the previous section, and obtain a somewhat different result.
- We obtain an initial current I_0 = 1.5 MA from the desired compression ratio and the peak current.
- Since solid that has a much higher speed of sound, the first wave sent into the fuel reaches the center earlier compared to the ideal gas case
- This results in a shorter implosion of 1100 ns, since we are trying to catch up with this initial disturbance
- The current profile is slightly flatter than in the ideal gas case. The peak $\frac{dI}{dt}$ reaches 1.5 MA/ns

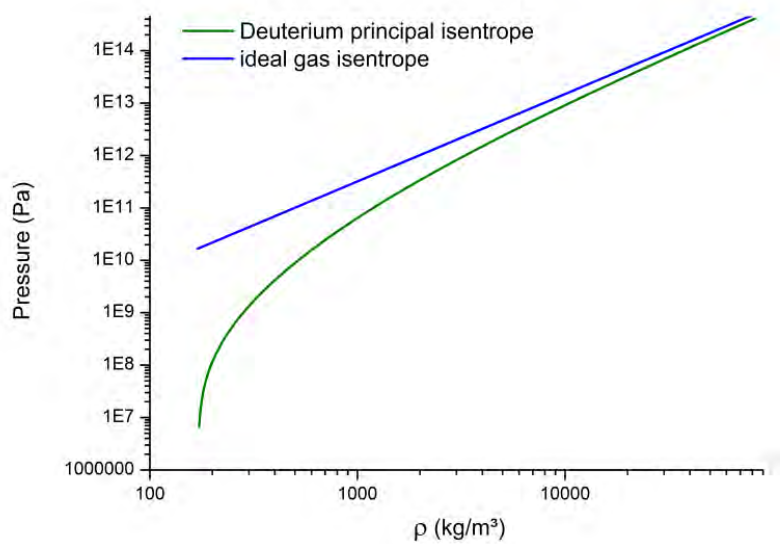

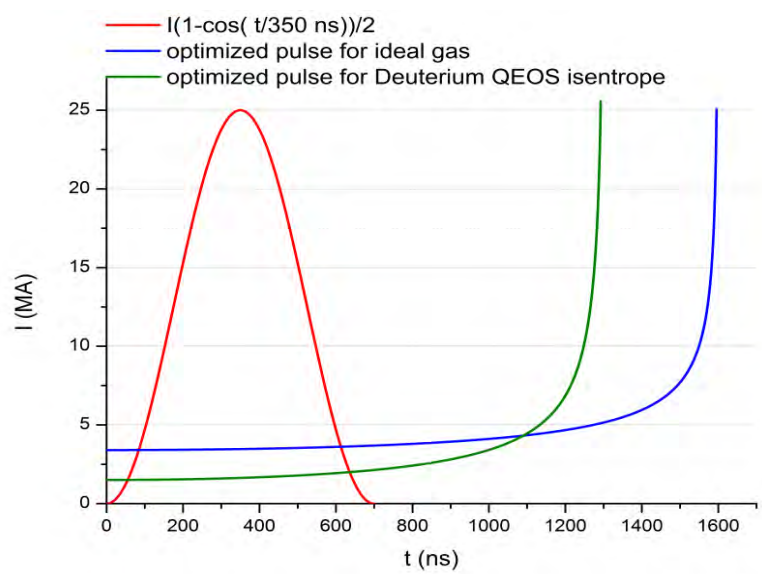

Numerical verification

Kidder's self similar implosion requires the somehow artificial situation of a non-uniform initial pressure profile. Nevertheless, when Kidder's boundary pressure is applied to an initially uniform fluid, the implosion remains closely isentropic.

- the movement of the boundary of the fluid in the simulation differs from the theoretical result
- in Kidder's solution all fluid elements start to move towards the center at t=0
- this is due to a non-uniform initial pressure profile
- therefore the boundary of the fluid in the simulation is lagging behind the theoretical boundary
- In contrary, there is hardly any difference in the current profile between the simulation and the theoretical result
- since the boundary speeds up slowly at early times, the increase in current is due to an increase in pressure.
- At the final stages of the implosion, the boundary in the simulation catches up with the theoretical result. The fluid in the simulation is starting to move self similarly.

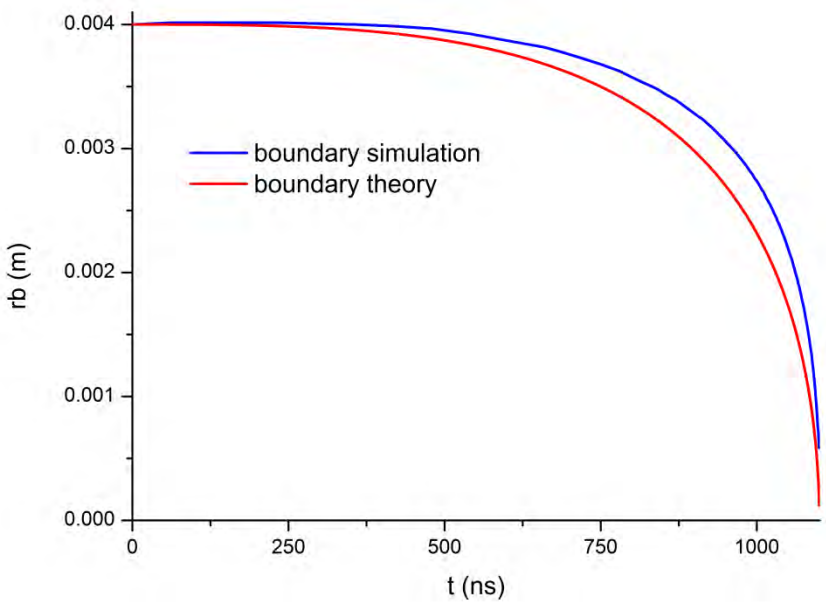

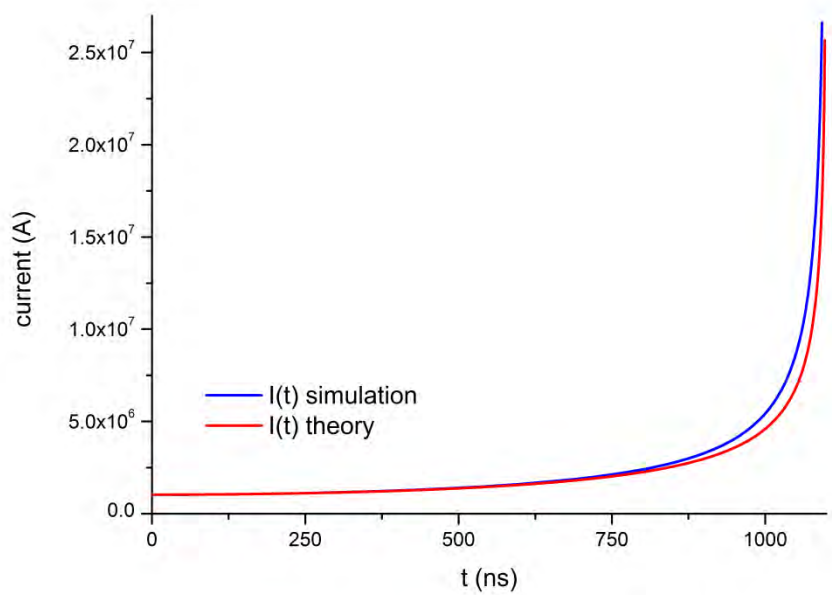

Dens2 0
Dens1 0
4.8
4.6
4.4
4.2
4
3.8
3.6
3.4
3.2
3
2.8
2.6
2.4
2.2
0
0.0002
0.0004
0.0006
0.0008
0.001
0.0012
0.0014
0.0016
0.0018
0.002
0.0022
0.0024
0.0026
0.0028
0.003
0.0032
0.0034
0.0036
0.0038
0.004
0.0042
0.0044

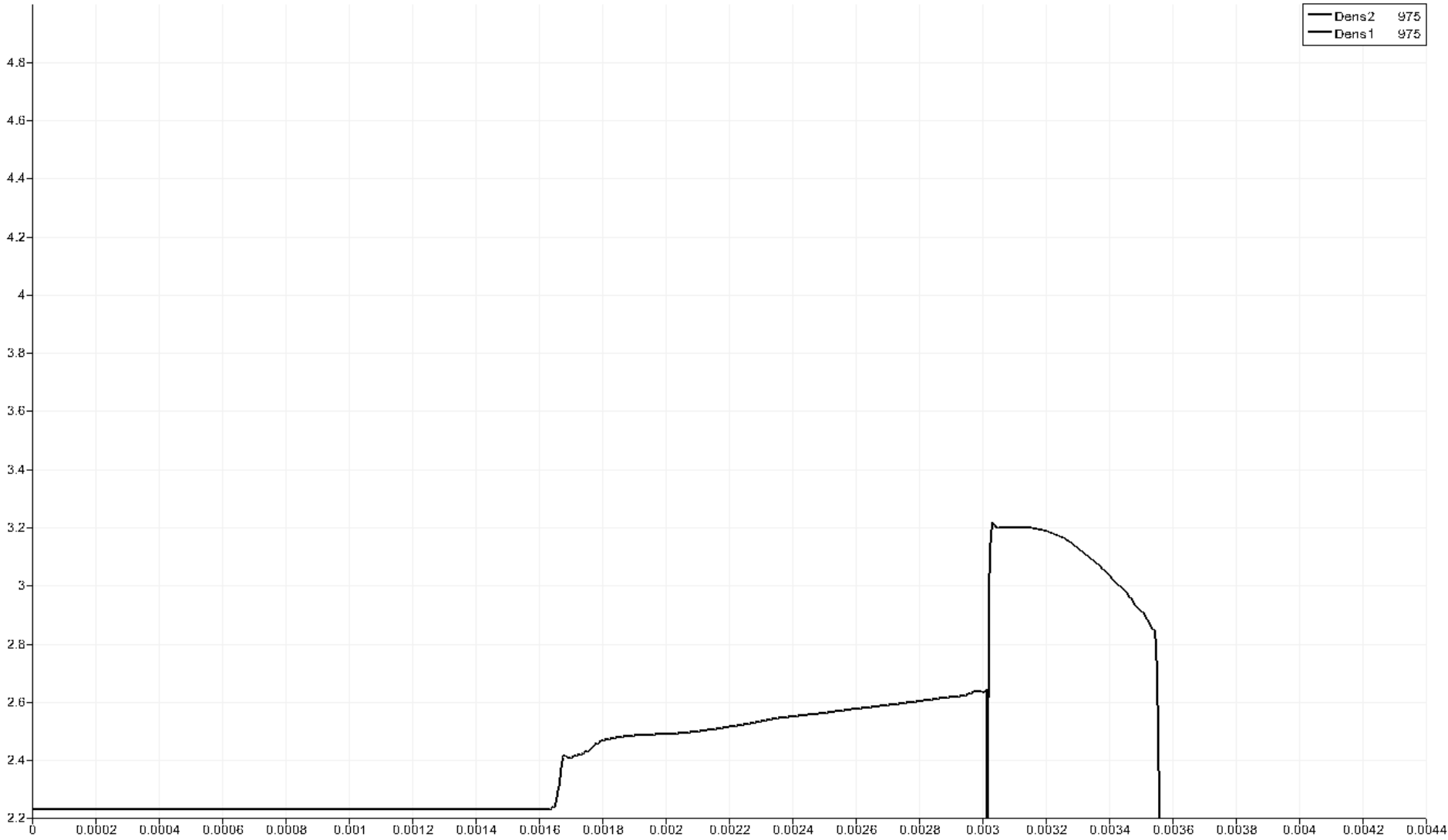
Dens2 975
Dens1 975
4.8
4.6
4.4
4.2
4
3.8
3.6
3.4
3.2
3
2.8
2.6
2.4
2.2
0
0.0002
0.0004
0.0006
0.0008
0.001
0.0012
0.0014
0.0016
0.0018
0.002
0.0022
0.0024
0.0026
0.0028
0.003
0.0032
0.0034
0.0036
0.0038
0.004
0.0042
0.0044

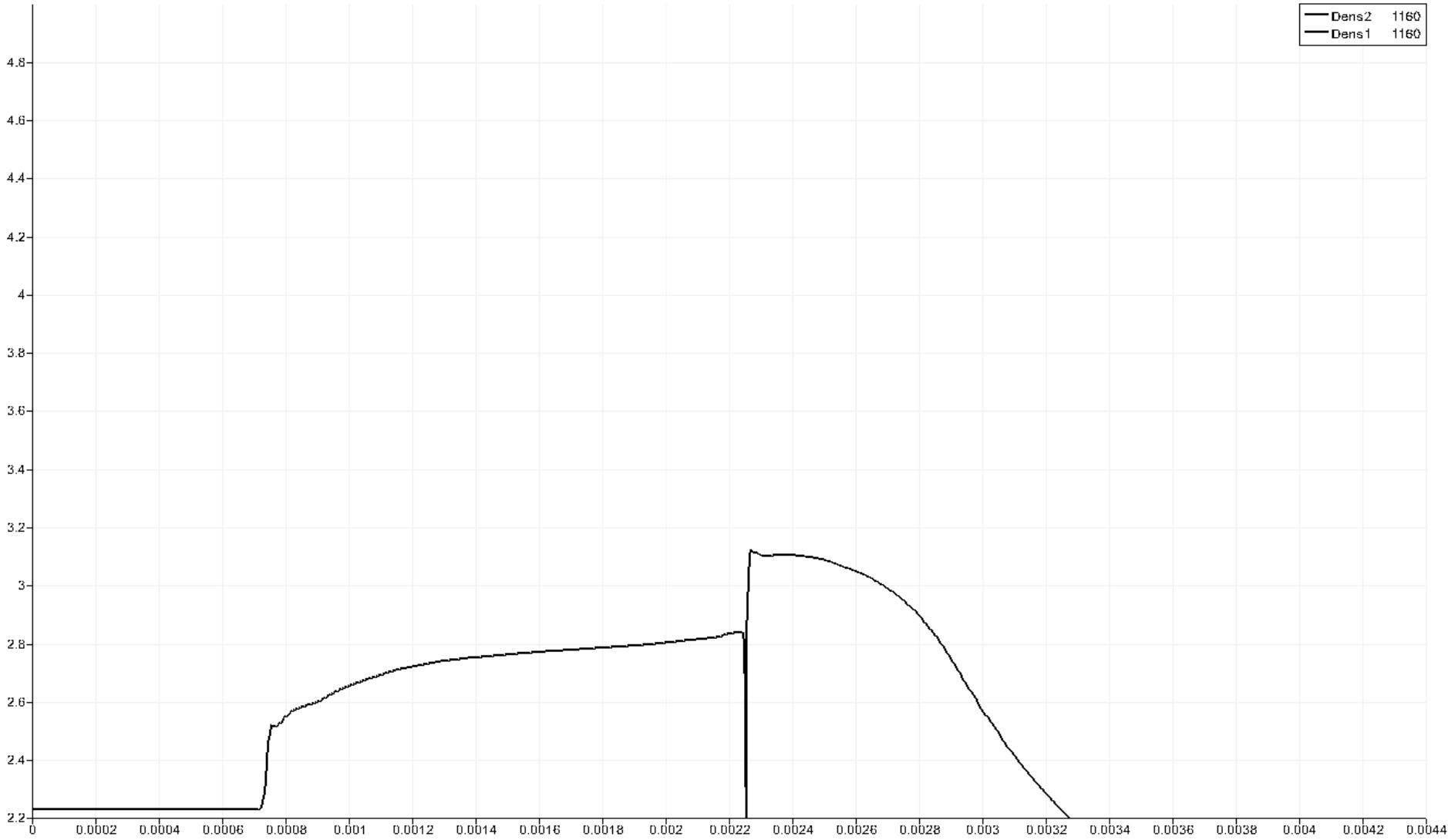
Dens2 1160
Dens1 1160
4.8
4.6
4.4
4.2
4
3.8
3.6
3.4
3.2
3
2.8
2.6
2.4
2.2
0
0.0002
0.0004
0.0006
0.0008
0.001
0.0012
0.0014
0.0016
0.0018
0.002
0.0022
0.0024
0.0026
0.0028
0.003
0.0032
0.0034
0.0036
0.0038
0.004
0.0042
0.0044

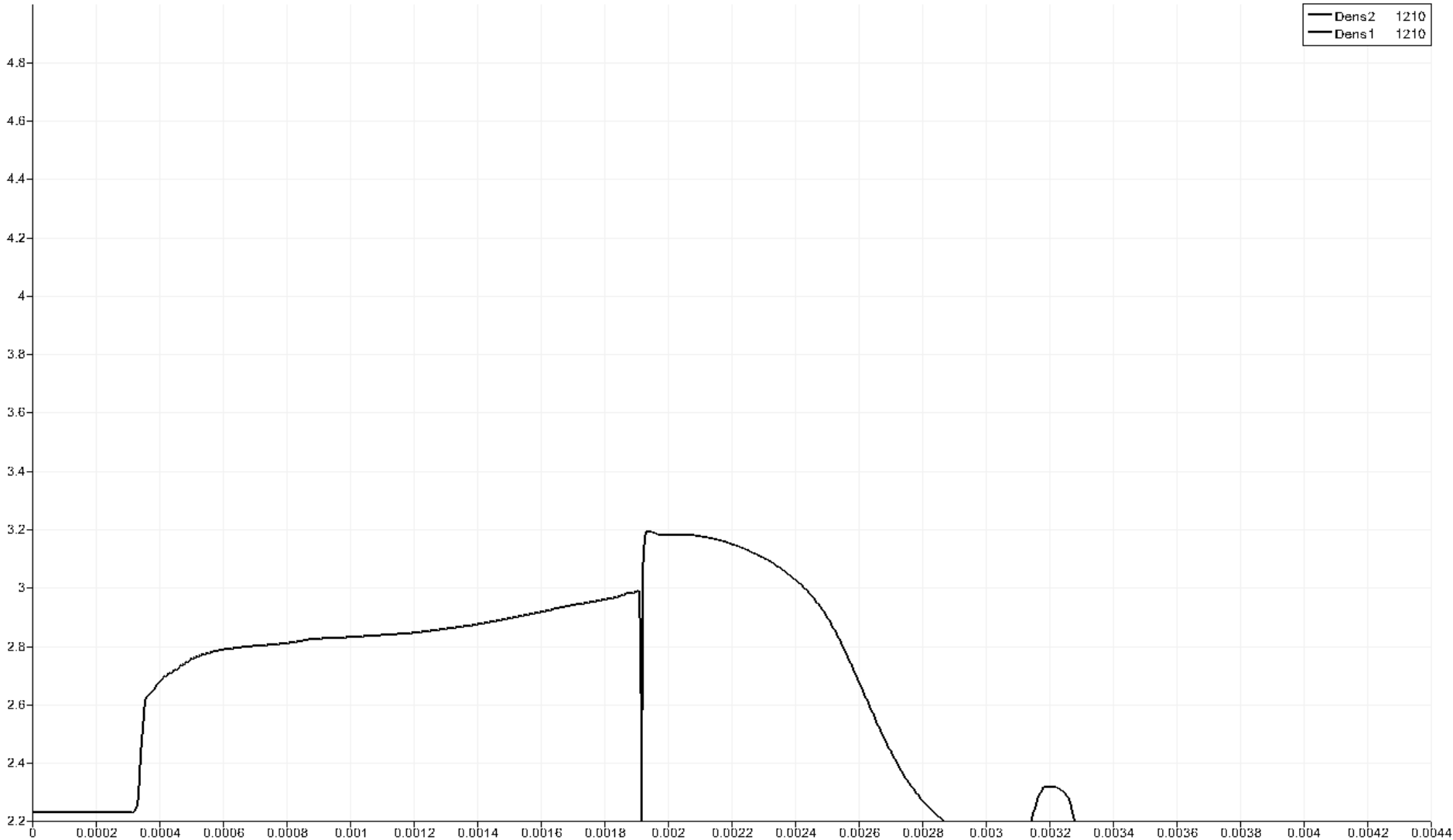
Dens2 1210
Dens1 1210
4.8
4.6
4.4
4.2
4
3.8
3.6
3.4
3.2
3
2.8
2.6
2.4
2.2
0
0.0002
0.0004
0.0006
0.0008
0.001
0.0012
0.0014
0.0016
0.0018
0.002
0.0022
0.0024
0.0026
0.0028
0.003
0.0032
0.0034
0.0036
0.0038
0.004
0.0042
0.0044

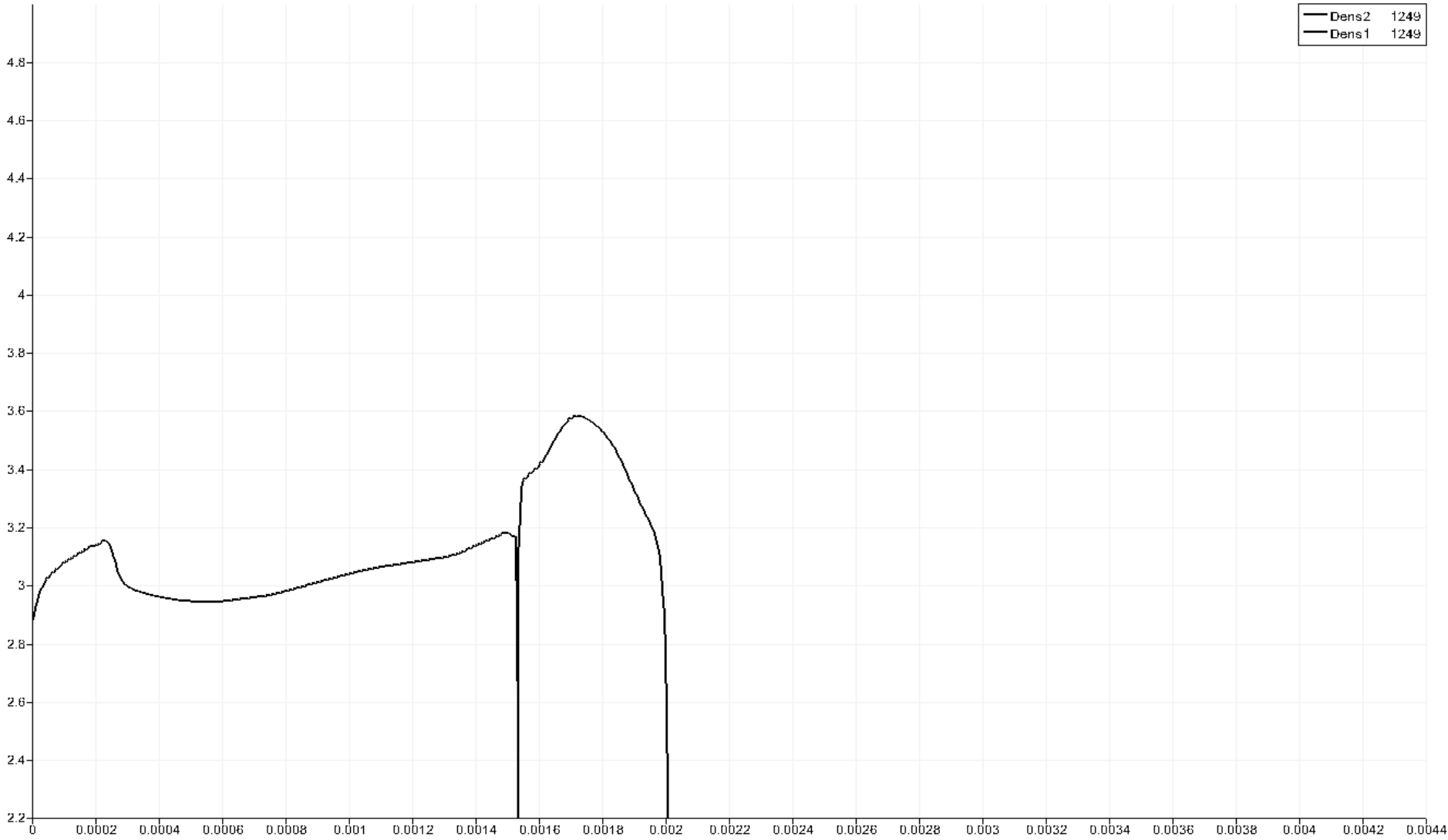
Dens2 1249
Dens1 1249
4.8
4.6
4.4
4.2
4
3.8
3.6
3.4
3.2
3
2.8
2.6
2.4
2.2
0
0.0002
0.0004
0.0006
0.0008
0.001
0.0012
0.0014
0.0016
0.0018
0.002
0.0022
0.0024
0.0026
0.0028
0.003
0.0032
0.0034
0.0036
0.0038
0.004
0.0042
0.0044

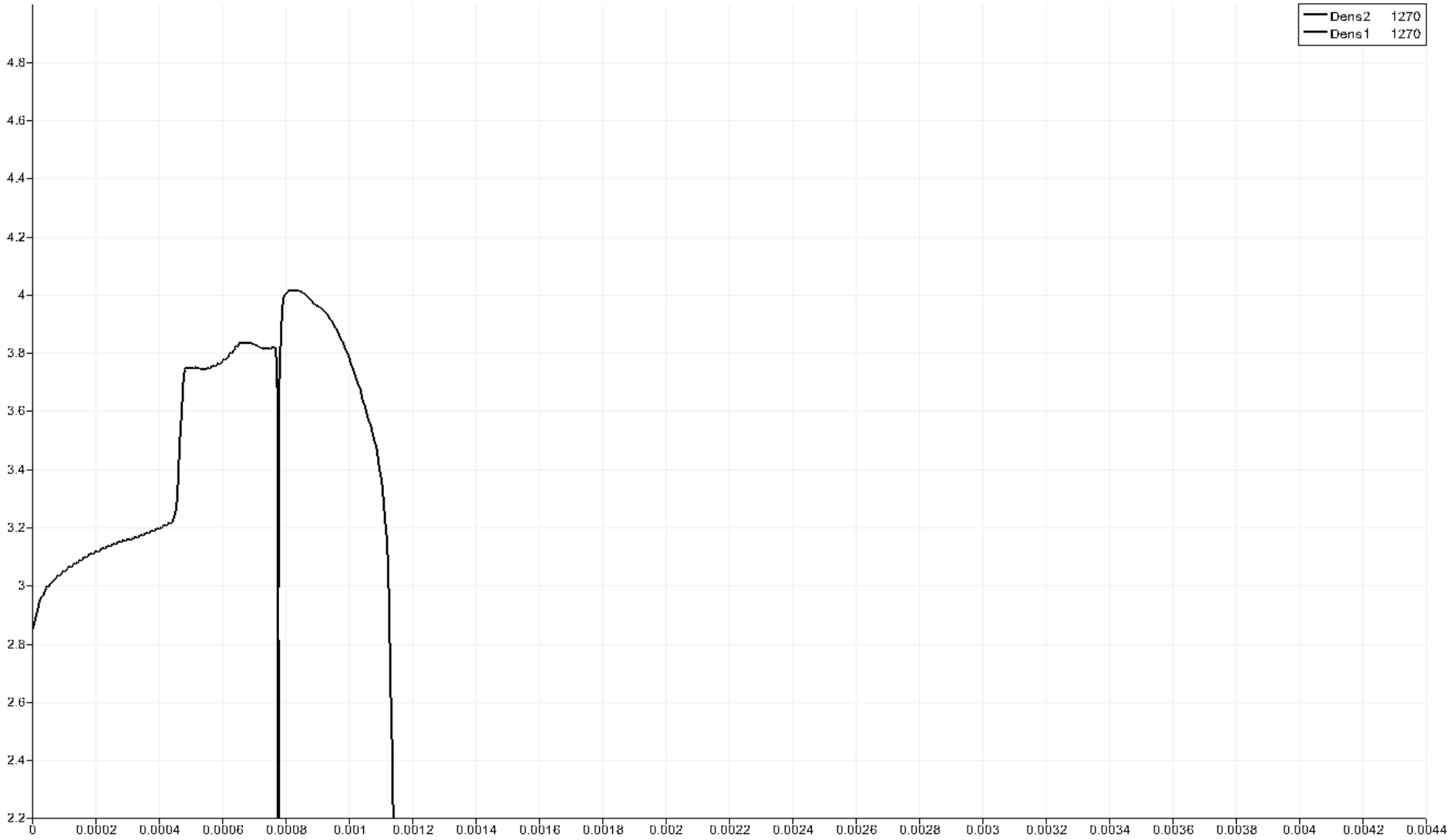
Dens2 1270
Dens1 1270
4.8
4.6
4.4
4.2
4
3.8
3.6
3.4
3.2
3
2.8
2.6
2.4
2.2
0
0.0002
0.0004
0.0006
0.0008
0.001
0.0012
0.0014
0.0016
0.0018
0.002
0.0022
0.0024
0.0026
0.0028
0.003
0.0032
0.0034
0.0036
0.0038
0.004
0.0042
0.0044

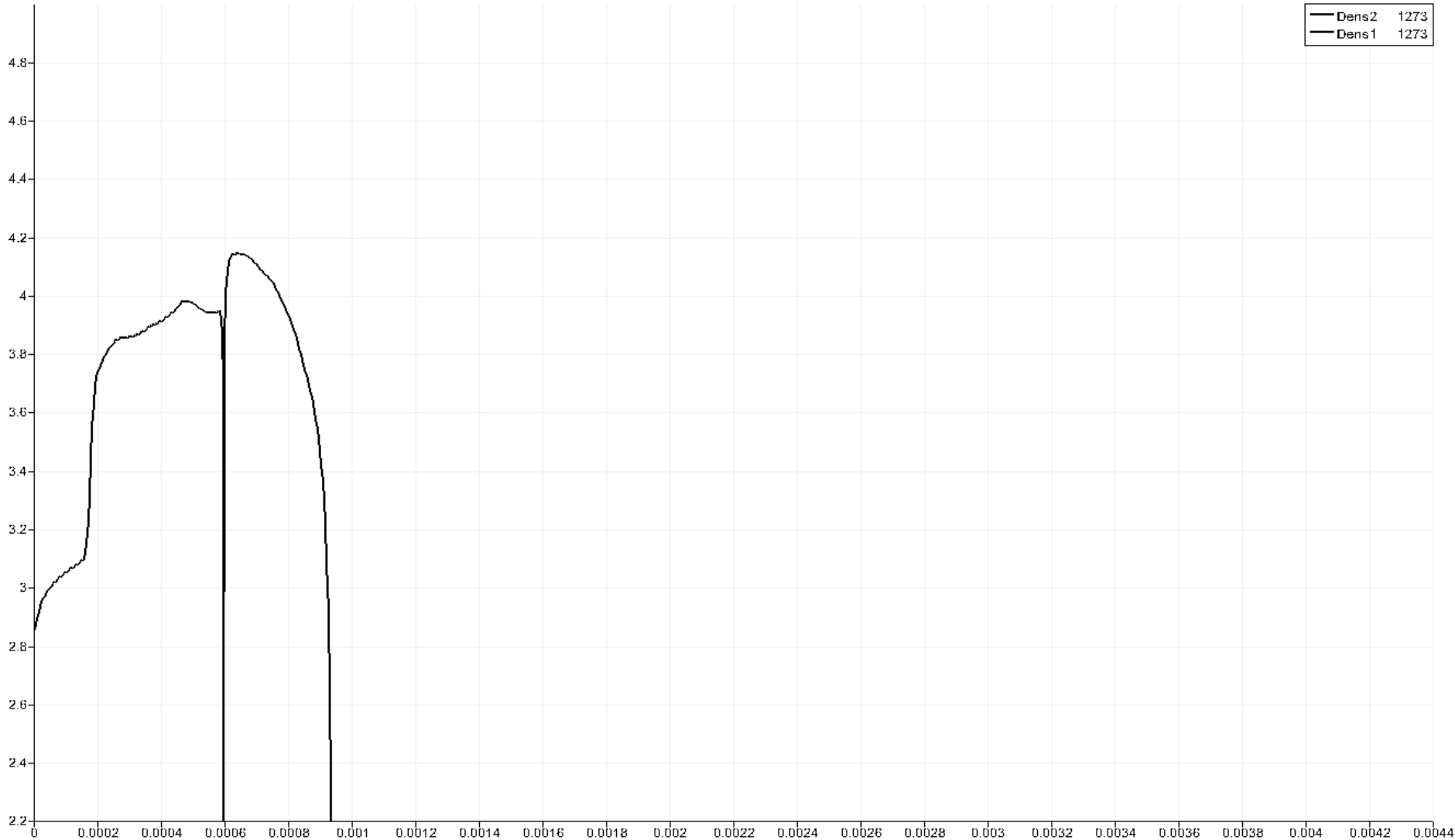
Dens2 1273
Dens1 1273
4.8
4.6
4.4
4.2
4
3.8
3.6
3.4
3.2
3
2.8
2.6
2.4
2.2
0
0.0002
0.0004
0.0006
0.0008
0.001
0.0012
0.0014
0.0016
0.0018
0.002
0.0022
0.0024
0.0026
0.0028
0.003
0.0032
0.0034
0.0036
0.0038
0.004
0.0042
0.0044

MagLIF simulations with Gorgon

Dynamics
Preheat
Perturbation
Instability
Stagnation
Ignition
Pulse Shaping

Liner workshop, Albuquerque Feb. 2012

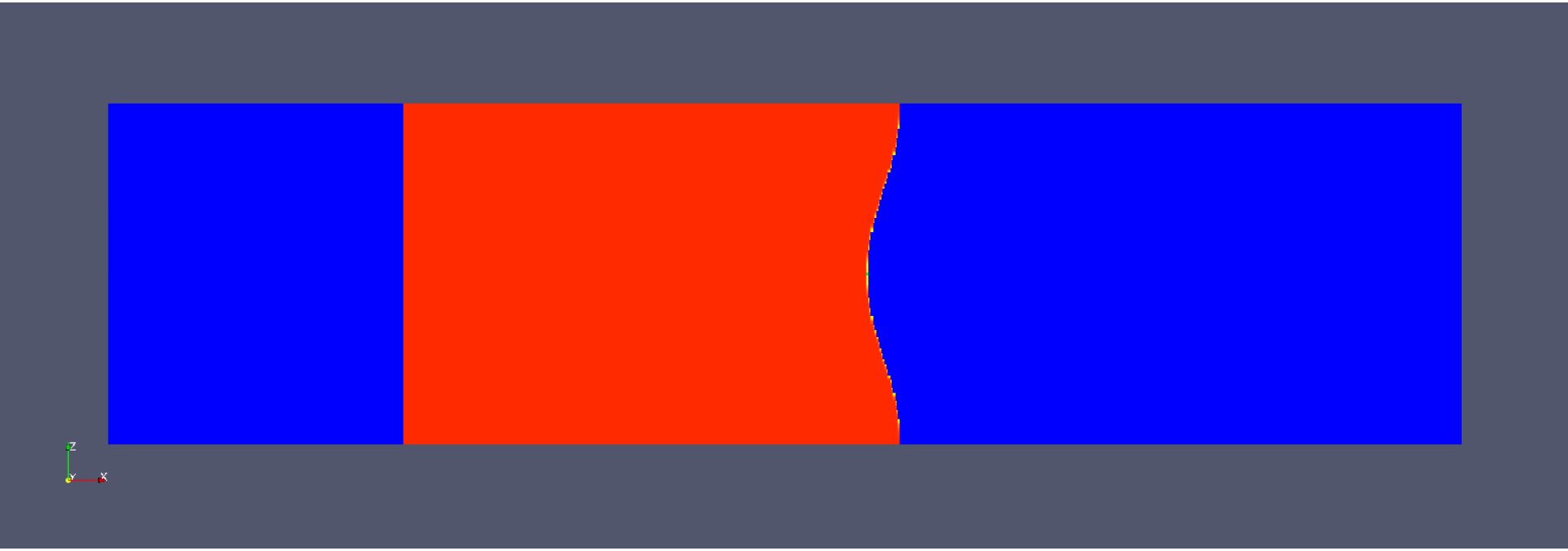
Z
Y
X

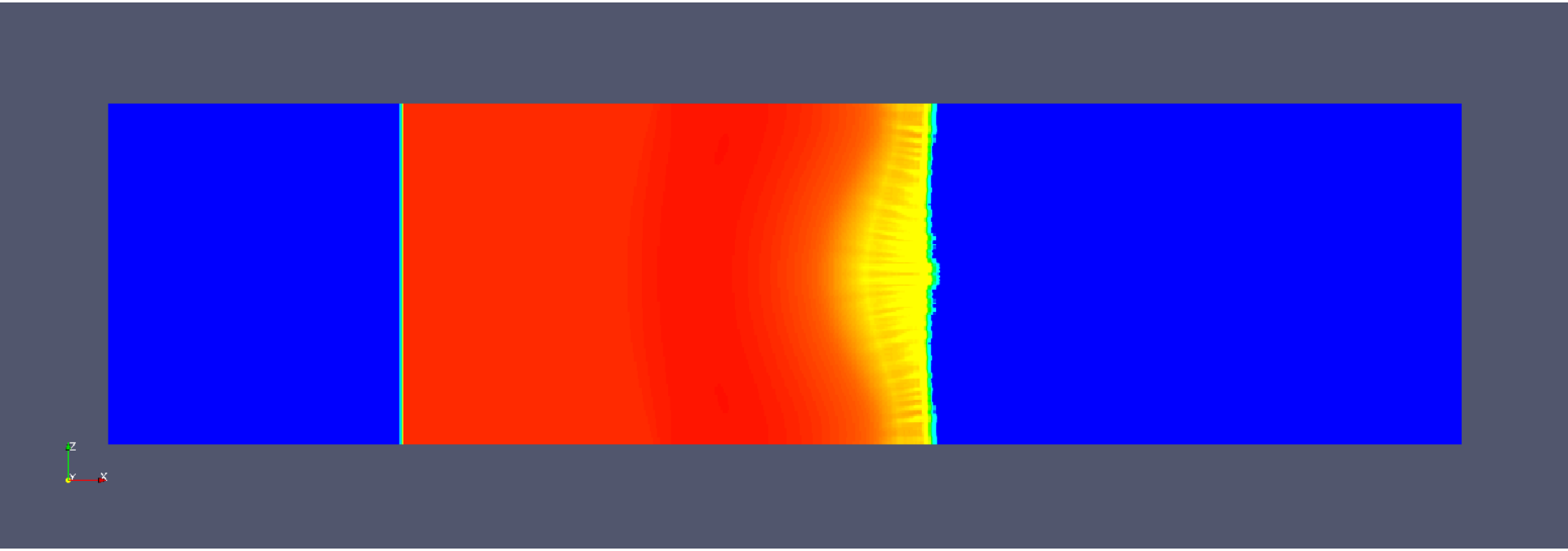
Z
Y
X

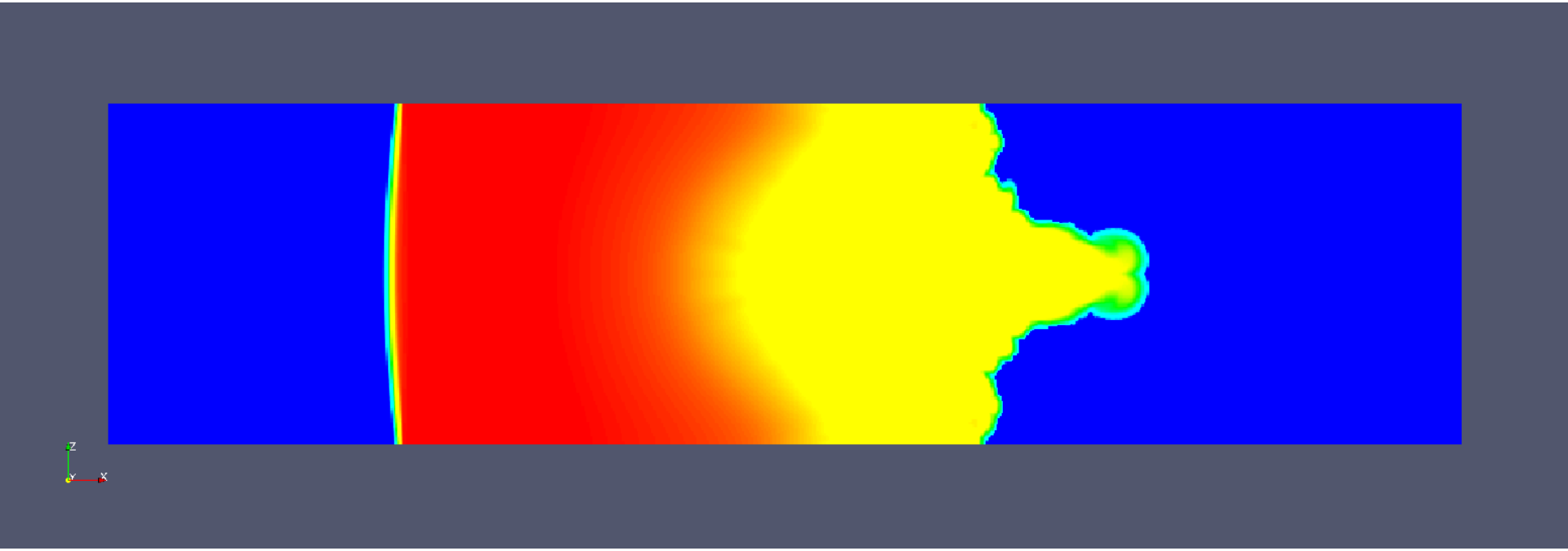
Z
Y
X

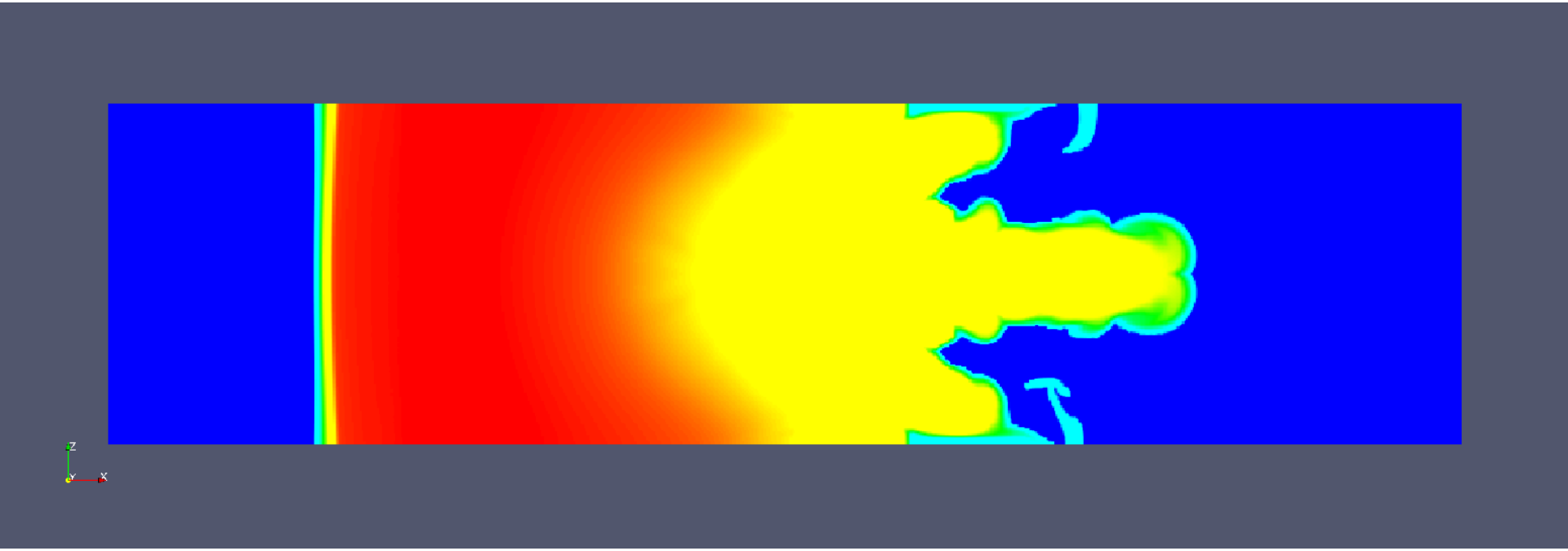
Z
Y
X

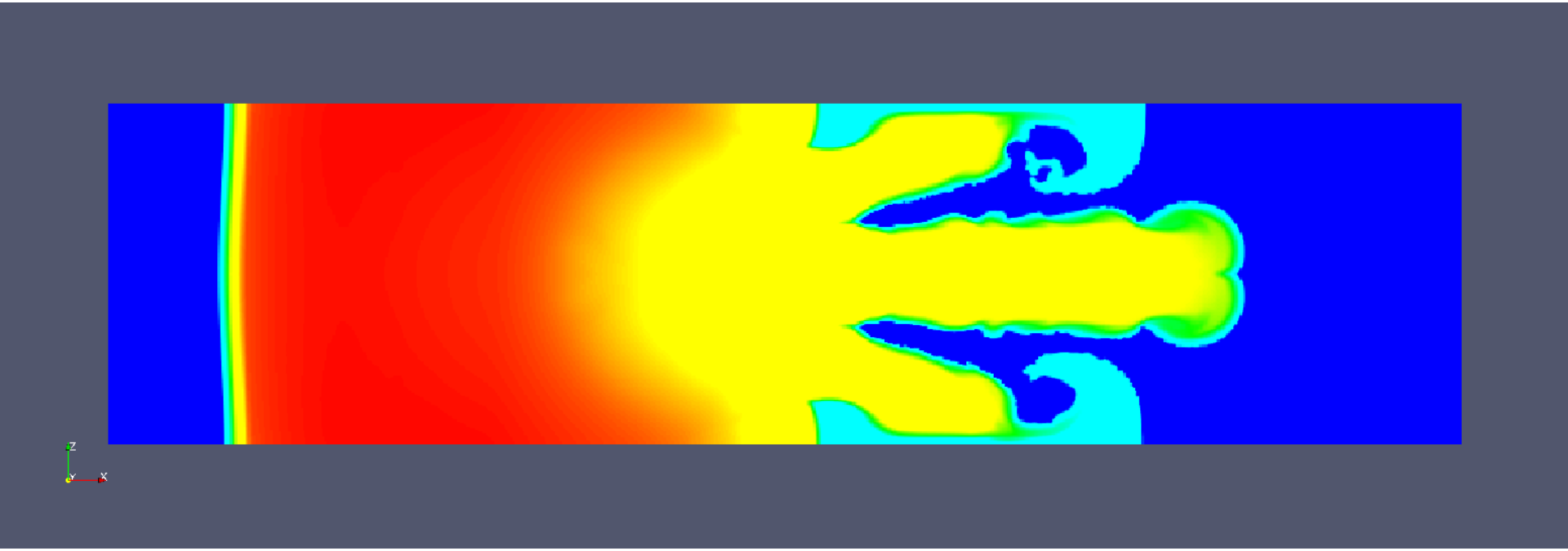
Z
Y
X

2nd generation MagLIF, Be liner, DT gas & ice , 69MA, B_z 11T

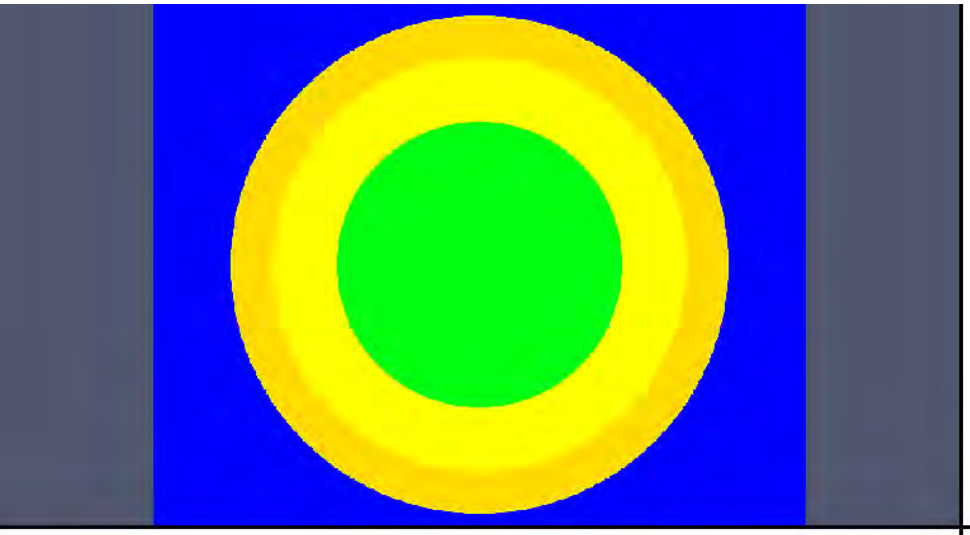

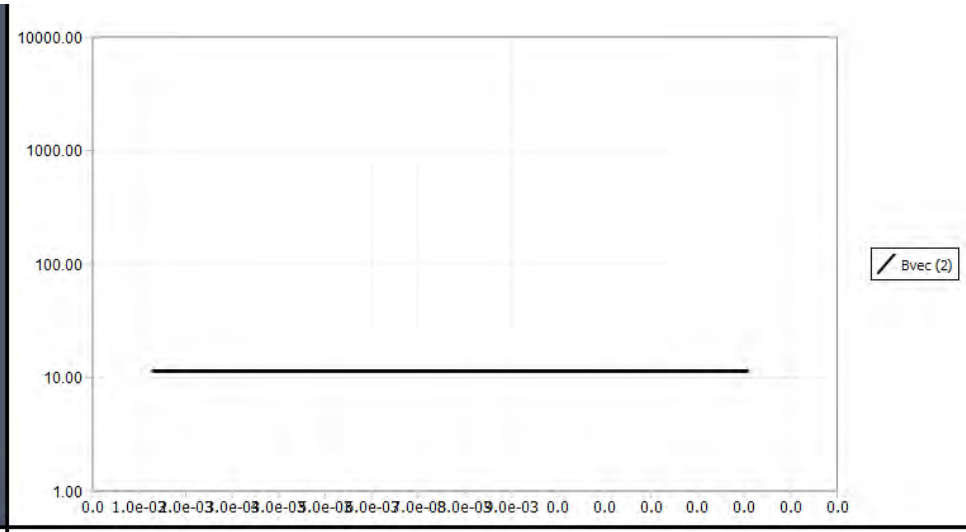

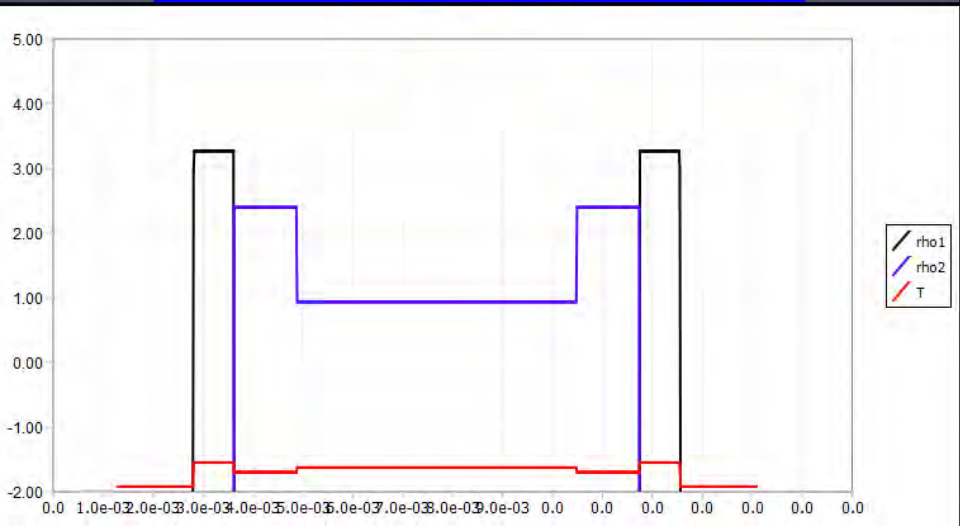

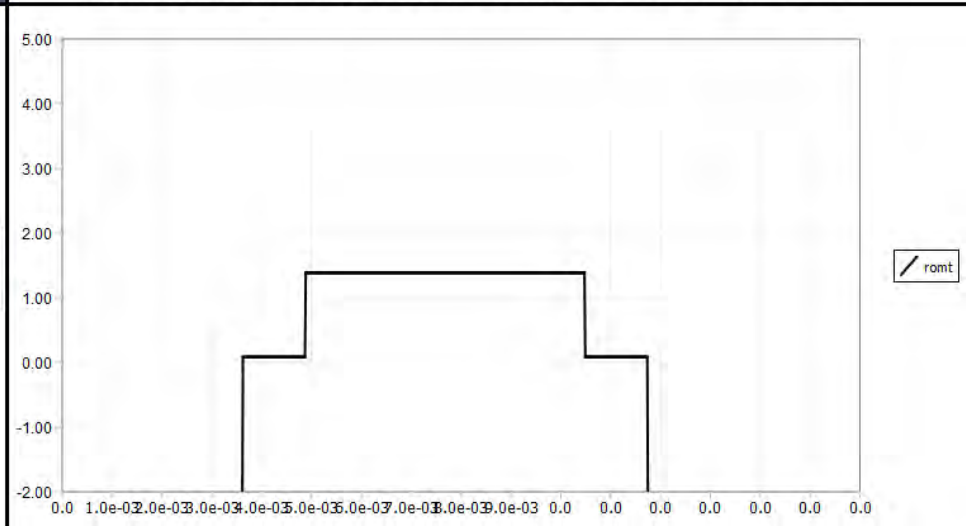

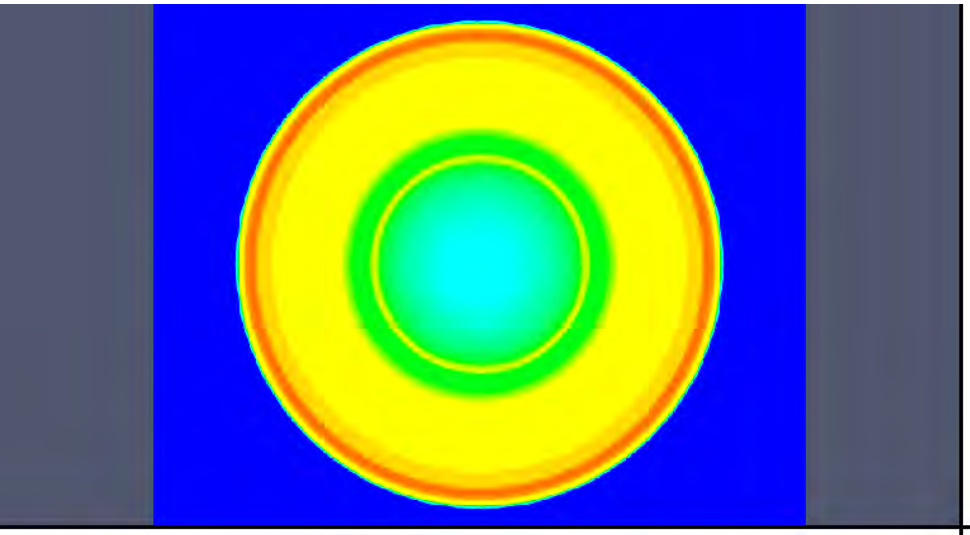

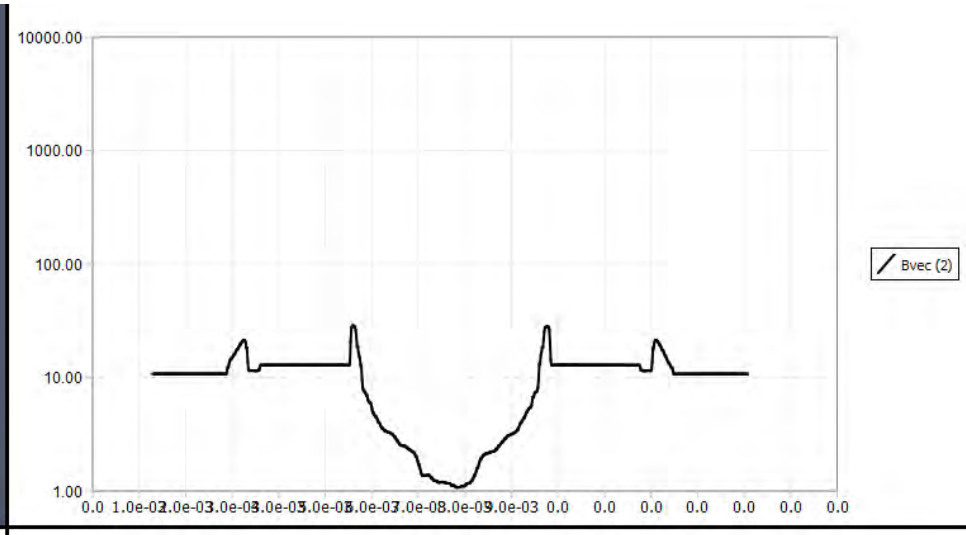
10000.00
1000.00
100.00
10.00
1.00
0.0 1.0e-03 2.0e-03 3.0e-03 4.0e-03 5.0e-03 6.0e-03 7.0e-03 8.0e-03 9.0e-03 0.0 0.0 0.0 0.0 0.0 0.0 0.0
Bvec (2)

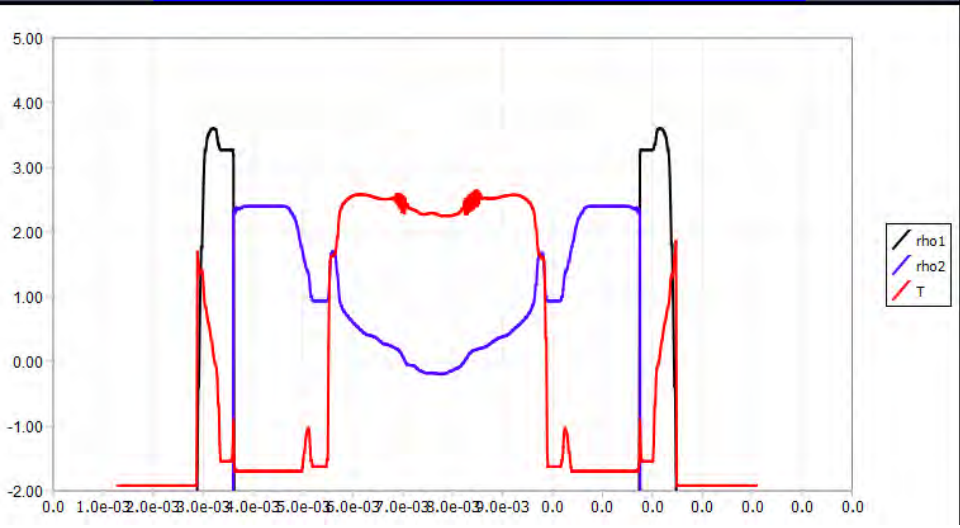
5.00
4.00
3.00
2.00
1.00
0.00
-1.00
-2.00
0.0 1.0e-03 2.0e-03 3.0e-03 4.0e-03 5.0e-03 6.0e-03 7.0e-03 8.0e-03 9.0e-03 0.0 0.0 0.0 0.0 0.0 0.0 0.0
rho1
rho2
T

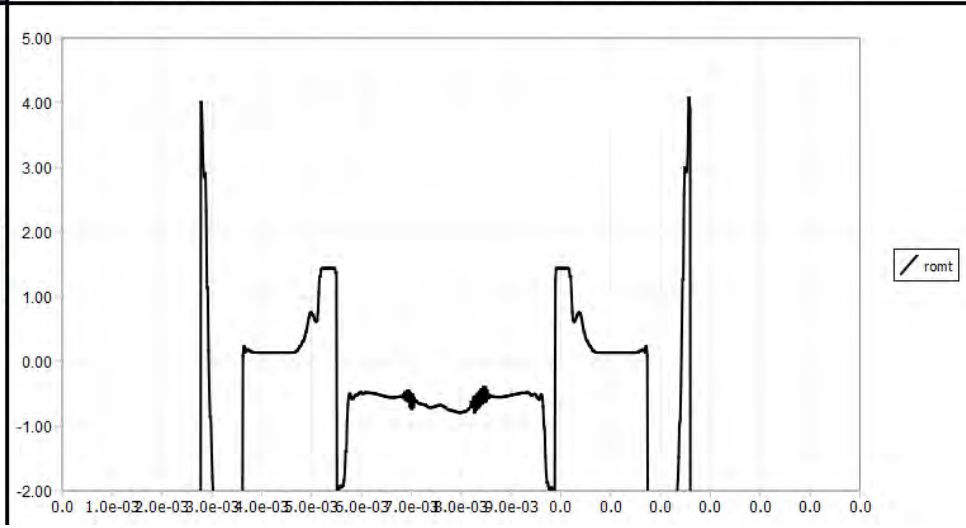
5.00
4.00
3.00
2.00
1.00
0.00
-1.00
-2.00
0.0 1.0e-03 2.0e-03 3.0e-03 4.0e-03 5.0e-03 6.0e-03 7.0e-03 8.0e-03 9.0e-03 0.0 0.0 0.0 0.0 0.0 0.0 0.0
romt

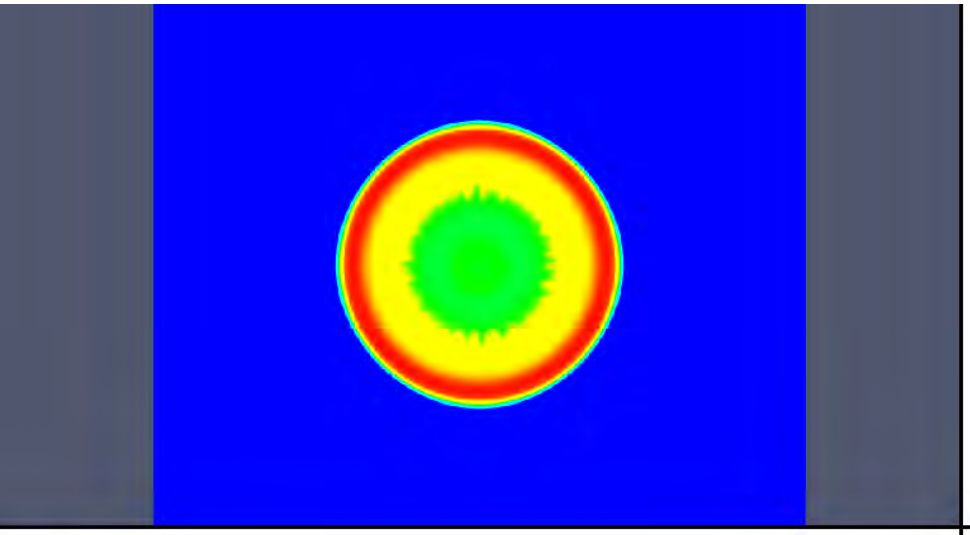

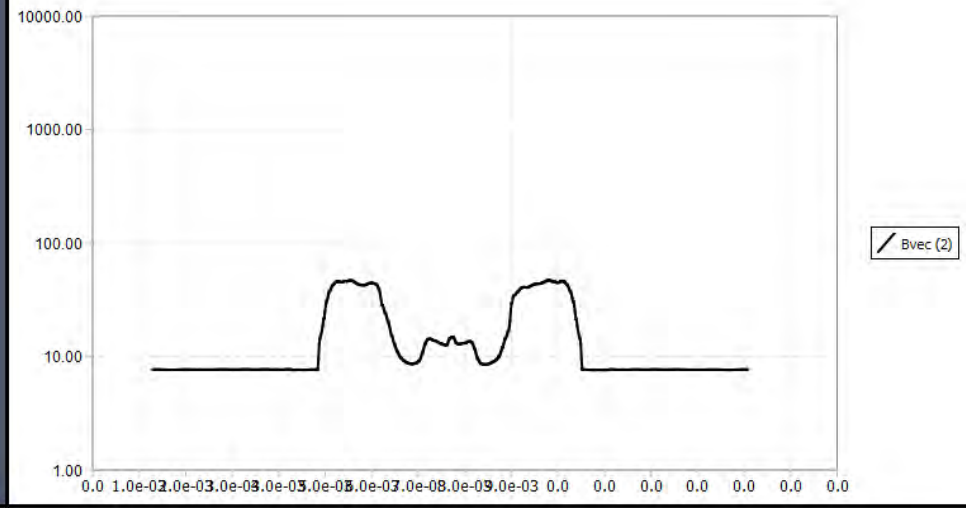
10000.00
1000.00
100.00
10.00
1.00
0.0 1.0e-02 2.0e-03 3.0e-03 4.0e-03 5.0e-03 6.0e-03 7.0e-03 8.0e-03 9.0e-03 0.0 0.0 0.0 0.0 0.0 0.0 0.0
Bvec (2)

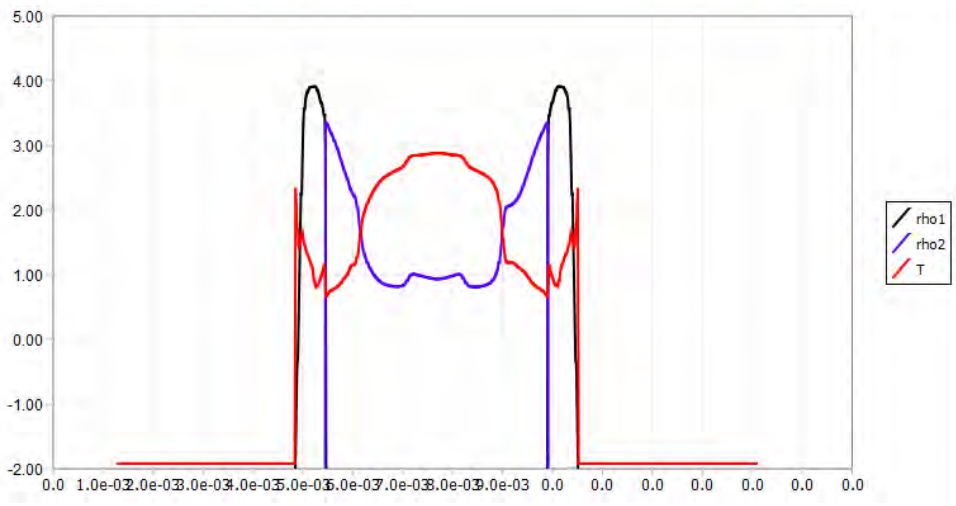
5.00
4.00
3.00
2.00
1.00
0.00
-1.00
-2.00
0.0 1.0e-02 2.0e-03 3.0e-03 4.0e-03 5.0e-03 6.0e-03 7.0e-03 8.0e-03 9.0e-03 0.0 0.0 0.0 0.0 0.0 0.0 0.0
rho1
rho2
T

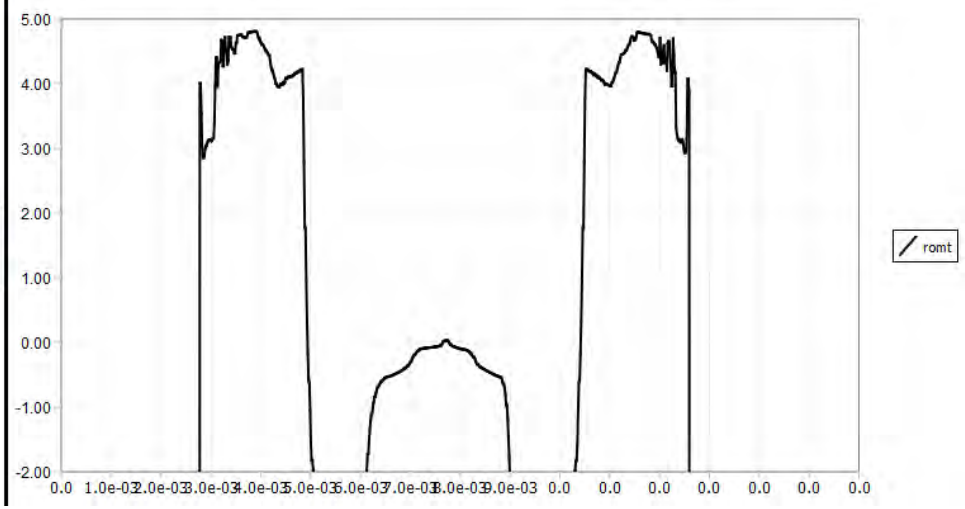
5.00
4.00
3.00
2.00
1.00
0.00
-1.00
-2.00
0.0 1.0e-02 2.0e-03 3.0e-03 4.0e-03 5.0e-03 6.0e-03 7.0e-03 8.0e-03 9.0e-03 0.0 0.0 0.0 0.0 0.0 0.0 0.0
romt

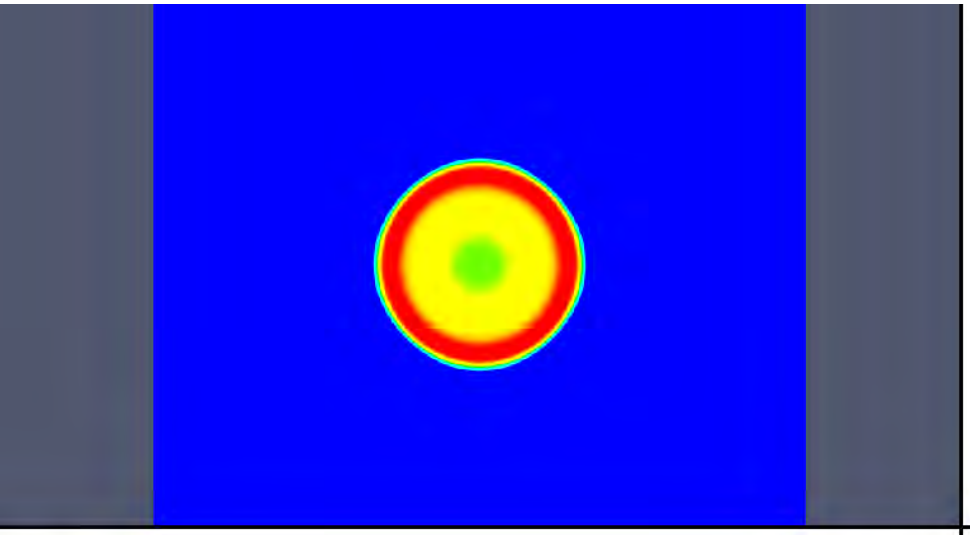

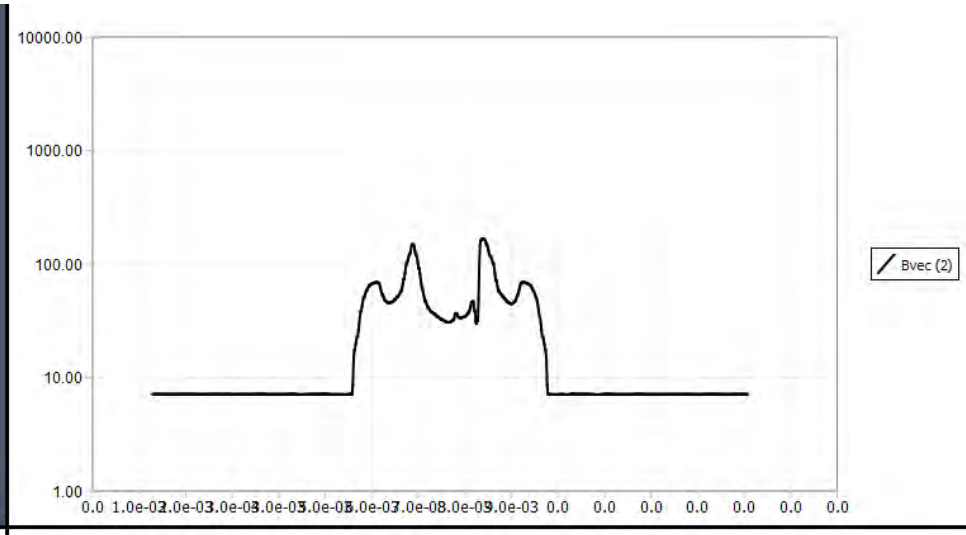
10000.00
1000.00
100.00
10.00
1.00
0.0 1.0e-03 2.0e-03 3.0e-03 4.0e-03 5.0e-03 6.0e-03 7.0e-03 8.0e-03 9.0e-03 0.0 0.0 0.0 0.0 0.0 0.0 0.0
Bvec (2)

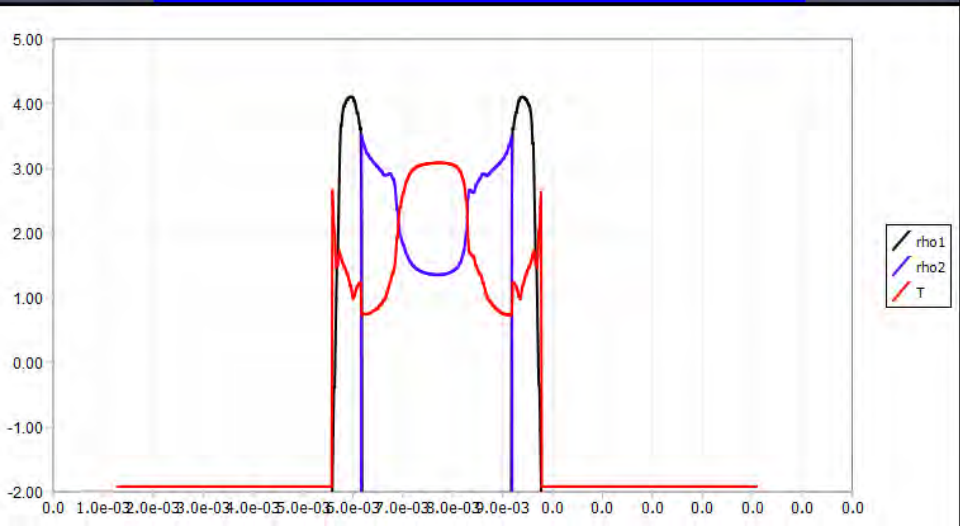
5.00
4.00
3.00
2.00
1.00
0.00
-1.00
-2.00
0.0 1.0e-03 2.0e-03 3.0e-03 4.0e-03 5.0e-03 6.0e-03 7.0e-03 8.0e-03 9.0e-03 0.0 0.0 0.0 0.0 0.0 0.0 0.0
rho1
rho2
T

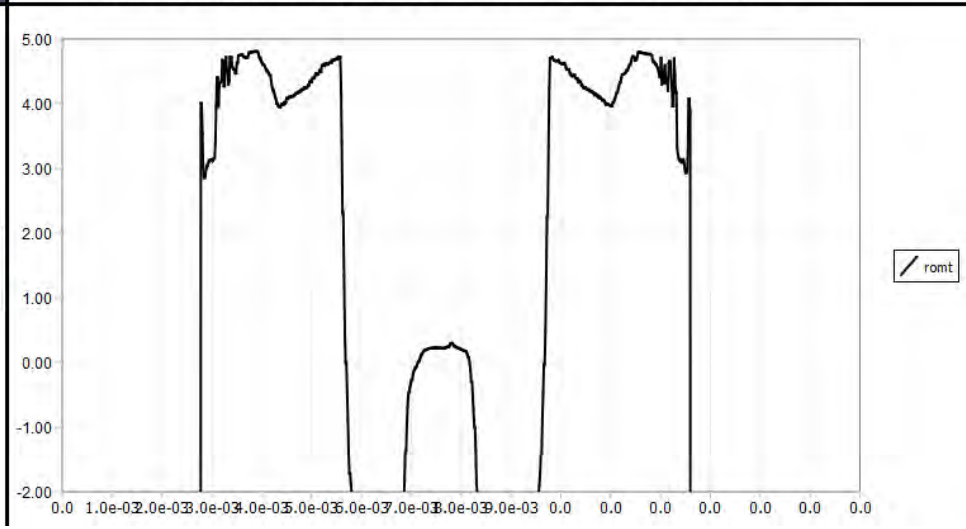
5.00
4.00
3.00
2.00
1.00
0.00
-1.00
-2.00
0.0 1.0e-03 2.0e-03 3.0e-03 4.0e-03 5.0e-03 6.0e-03 7.0e-03 8.0e-03 9.0e-03 0.0 0.0 0.0 0.0 0.0 0.0 0.0
romt

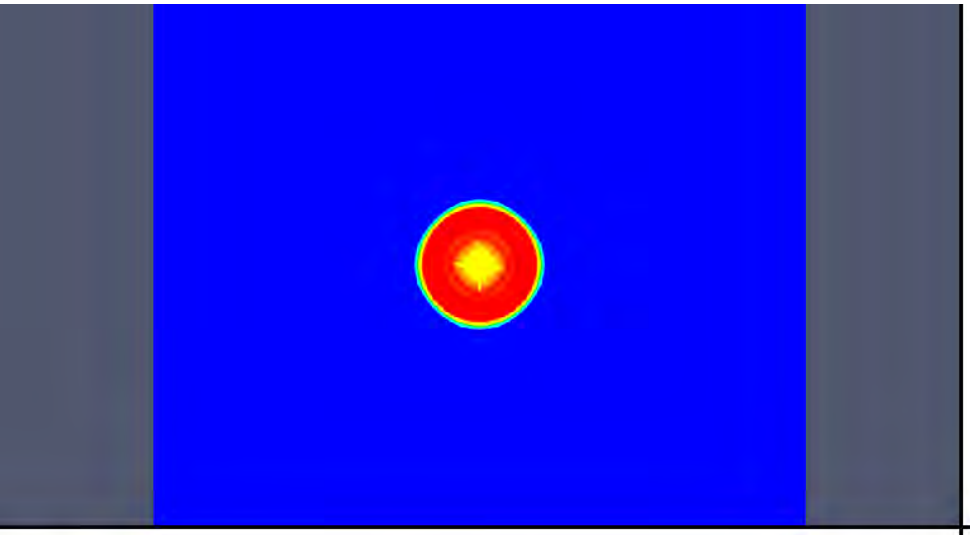

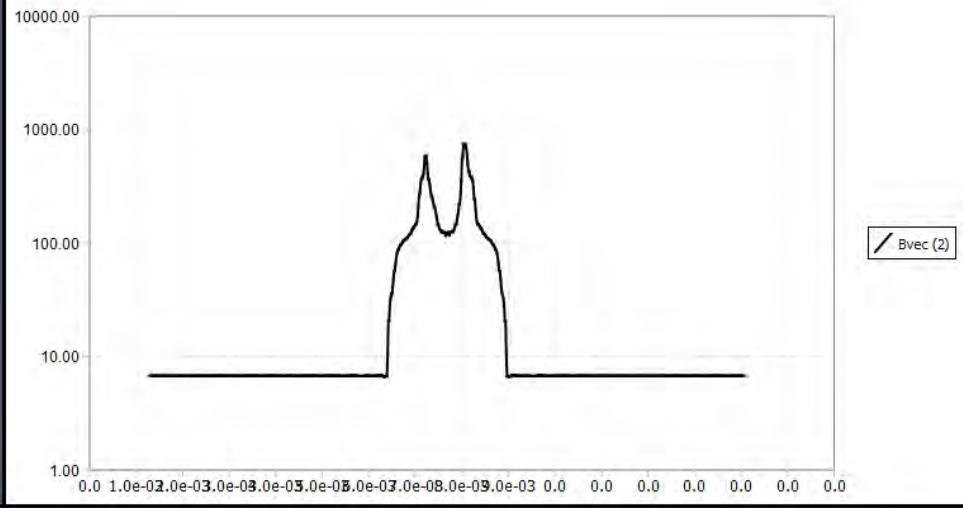
10000.00
1000.00
100.00
10.00
1.00
0.0 1.0e-03 2.0e-03 3.0e-03 4.0e-03 5.0e-03 6.0e-03 7.0e-03 8.0e-03 9.0e-03 0.0 0.0 0.0 0.0 0.0 0.0 0.0
Bvec (2)

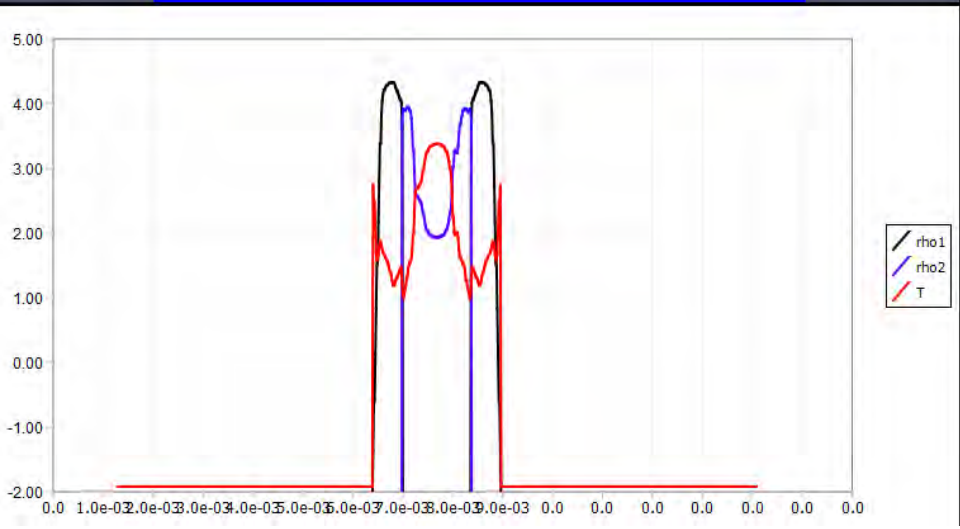
5.00
4.00
3.00
2.00
1.00
0.00
-1.00
-2.00
0.0 1.0e-03 2.0e-03 3.0e-03 4.0e-03 5.0e-03 6.0e-03 7.0e-03 8.0e-03 9.0e-03 0.0 0.0 0.0 0.0 0.0 0.0 0.0
rho1
rho2
T

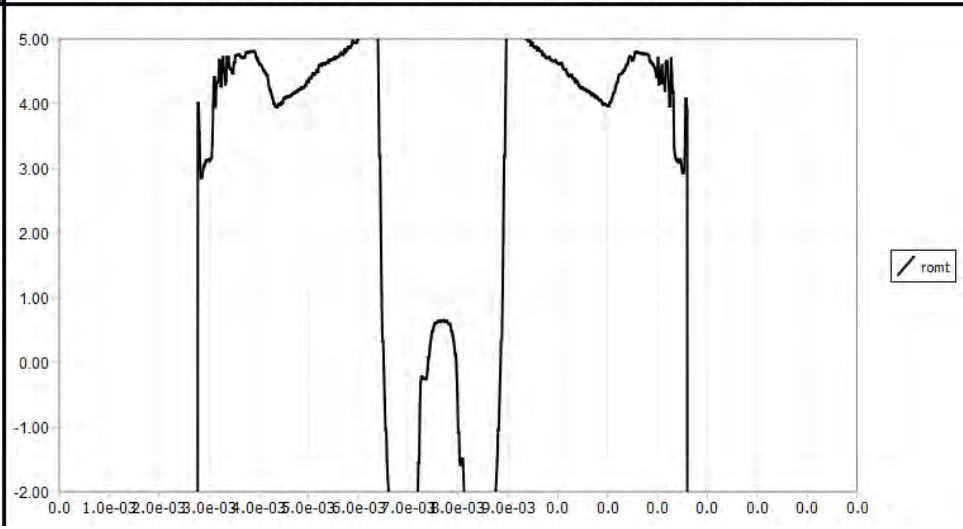
5.00
4.00
3.00
2.00
1.00
0.00
-1.00
-2.00
0.0 1.0e-03 2.0e-03 3.0e-03 4.0e-03 5.0e-03 6.0e-03 7.0e-03 8.0e-03 9.0e-03 0.0 0.0 0.0 0.0 0.0 0.0 0.0
romt